UNIVERSITY OF CALIFORNIA, SAN DIEGO

Molecular Insights into the Function and Regulation of Diatom Silicon Transporters

A Dissertation submitted in partial satisfaction of the requirements for the degree

Doctor of Philosophy

in

Marine Biology

by

Kimberlee Thamatrakoln

Committee in charge:

Michael I. Latz, Chair
Mark A. Brzezinski
Mark Hildebrand
Brian Palenik
Julian I. Schroeder
Victor D. Vacquier

2006

The Dissertation of Kimberlee Thamatrakoln is approved, and it is acceptable in quality and form for publication on microfilm:

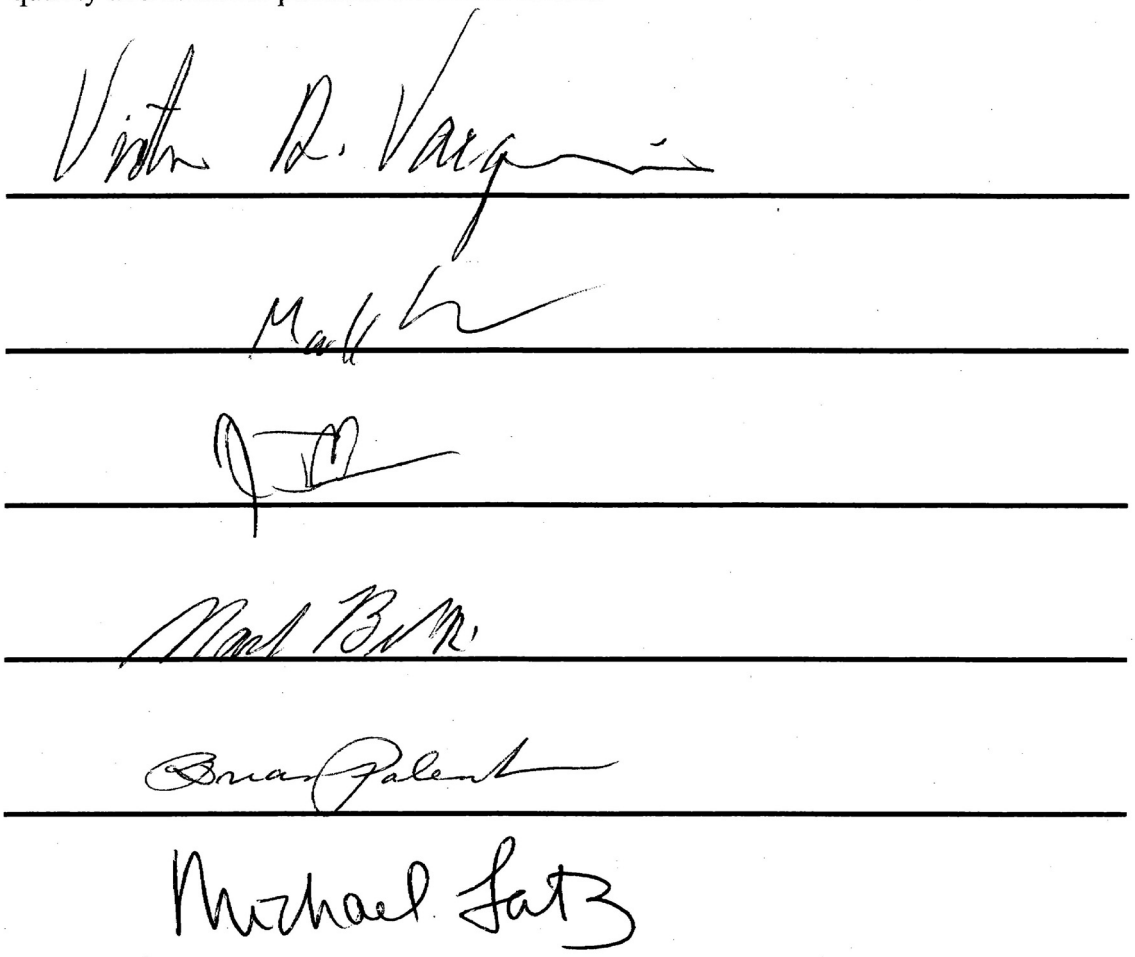

Chair

University of California, San Diego

2006

DEDICATION

To my parents, Wit and Juri,
who have always supported everything I've ever wanted to do.

To Sage,
who always reminds me to get outside

To Jackson,
my biggest accomplishment,
who teaches me something new everyday

To Kalani,
there are no words
For your love and support, I dedicate this to you

TABLE OF CONTENTS

LIST OF ABBREVIATIONS

SIT	silicon transporter
ASW	artificial seawater
FWT	freshwater tryptone
RACE	rapid amplification of cDNA ends
QPCR	quantitative PCR
SDV	silica deposition vesicle
TMS	transmembrane segment
$Si(OH)_4$	silicic acid
TpEL4	*Thalassiosira pseudonana* extracellular loop 4

LIST OF FIGURES

LIST OF TABLES

ACKNOWLEDGEMENTS

Although I am the author of this dissertation, the work involved in this undertaking would not have been possible without the support of numerous others who need to be acknowledged. I'll start by thanking my advisor, Michael Latz. Mike brought me into graduate school to work on differential gene expression in dinoflagellates. I spent my first 2 ½ years at SIO working on this and writing grants, unfortunately to no avail. Instead of kicking me out, or worse, making me work on a project I wasn't interested in, Mike allowed me the freedom to look for alternative projects and when I decided to work on diatoms, he was fully supportive. He graciously stayed on as my advisor and allowed me the use of lab space and equipment. Mike has been instrumental in teaching me the basic skills of science writing and presentation, skills equally important to a successful career as learning how to do the science. The confidence I have in my ability to write grants and manuscripts, and to present my research in a clear and concise manner, I owe to him.

I would also like to acknowledge other members of my committee, Mark Brzezinski, for insightful discussions about silicon uptake kinetics, Brian Palenik, for always helping me see the 'big' picture and allowing me use of lab equipment and supplies, Julian Schroeder, for advice and encouragement, and Victor Vacquier for help with anything protein. I have thoroughly enjoyed each and every one of my committee meetings.

I cannot describe the immense amount of knowledge I have gained from the most critical member of my committee, Mark Hildebrand. As everyone in Hubbs Hall

knows, Mark is *the* molecular biologist. But, to work side by side on a project with him has been one of the best scientific experiences of my life. “10 sec, okay, GO!”

Other people who need to be acknowledged include Drs. Bradley Tebo and Margo Haygood allowed me to be an honorary member of their labs and use most, if not all, or their lab equipment and supplies. Dr. Ron Burton let me to work in his lab during my dinoflagellate days and always provided a sympathetic ear. Other people who provided scientific and technical help along the way include: Aubrey Davis, Luciano Frigeri, Brian Hillier, Gary Moy, Grace Lim, Anna Neill, Sandra Hazelaar, Andy Juhl, and Peter von Dassow. Labmates, Dimitri Deheyn and Elisa Maldonado, have made the lab a great place to spend my days. I want to also thank my former supervisor at Stanford, An Song, because she was the one who introduced me to molecular biology and started me down this path towards a career in research.

Funding, whether for research, stipend, or travel, has been provided by: the SIO Graduate Department, UCSD Biology Department, Art Proceeds Fellowship, David Freeman Memorial Fund, San Diego State Foundation, CEBIC, Air Force MURI, NSF, and various travel awards from meeting organizers.

I also acknowledge the use of published material in this dissertation:

Chapter I, in part, is a reprint of the material as it appears in the Journal of Nanocience and Nanotechnology 5:158-166 and Science First Hand 5:56-60. The dissertation author was the primary investigator and author of these manuscripts. Mark Hildebrand was a co-author.

Chapter II, in full, is a reprint of the material as it appears in the Journal of Phycology 42:822-834. The dissertation author was the primary investigator and

author of this manuscript. Andrew J. Alverson and Mark Hildebrand were co-authors.

Chapter III, in full, has been submitted for publication. The dissertation author was the primary investigator and author of this manuscript. Mark Hildebrand was a co-author.

Chapter IV, in full, is in preparation for submission for publication. The dissertation author was the co-investigator and co-author of this manuscript. Mark Hildebrand was a co-investigator and co-author.

Friends and classmates are critical for surviving grad school. Julie Robidart, the only reason I stayed sane, always knew when to give me a hug or slap me upside the head. Dori Landry, Greg Dick, Ryan Mueller, Monica Lemos, Jessica Harvey, and many others were always supportive.

I wouldn't be here without my parents. Even when they didn't understand what I was doing, they always supported and encouraged me. I think they figured with all the schooling I'd been through, I must be doing something with my life. Thanks also to my brother, Ken, for always picking on me and making me tough.

Kalani makes life possible. Without him, well, I don't even want to think about it. Sage and Jackson are constant reminders that it's the little things in life that matter. Just two walks a day and some outdoor fun on the weekend is all it takes to make them happy. How can you argue with that?

VITA

1997	B.S., Biochemistry & Cell Biology, University of California, San Diego
1997-2000	Research Associate, Department of Immunology Stanford University
2000	M.S., Biological Sciences Stanford University
2000-2006	Graduate Student Researcher, Scripps Institution of Oceanography University of California, San Diego
2002-2003	Teaching Assistant, Division of Biological Sciences University of California, San Diego
2006	Ph.D., Marine Biology Scripps Institution of Oceanography University of California, San Diego

PUBLICATIONS

Thamatrakoln K and M Hildebrand (in preparation). Silicon uptake kinetics in diatoms revisited: a model for saturable and nonsaturable kinetics and the role of silicon transporters.

Thamatrakoln K and M Hildebrand (in review). Analysis of *Thalassiosira pseudonana* silicon transporters indicates distinct regulatory levels and transport activity through the cell cycle. *Eukaryotic Cell.*

Thamatrakoln K and M Hildebrand (2006). Building of silica. *Science First Hand* 5:56-60.

Thamatrakoln K, AJ Alverson, and M Hildebrand (2006). Comparative sequence analysis of diatom silicon transporters: towards a mechanistic model of silicon transport. *Journal of Phycology* 42:822-834.

Thamatrakoln K and M Hildebrand (2005). Approaches for functional characterization of diatom silicic acid transporters. *Journal of Nanoscience and Nanotechnology* 5: 158-166.

Armbrust EV, JA Berges, C Bowler, BR Green, D Martinez, NH Putnam, S Zhou, AE Allen, KE Apt, M Bechner, MA Brzezinski, BK Chaal, A Chiovitti, AK Davis, MS Demarest, JC Detter, T Glavina,D Goodstein, MZ Hadi, U Hellsten, M Hildebrand, BD Jenkins, J Jurka, VV Kapitonov, N Kröger, WWY Lau, TW Lane, FW Larimer, JC Lippmeier, S Lucas, M Medina, A Montsant, M Obornik, MS Parker, B Palenik, GJ Pazour, PM Richardson, TA Rynearson, MA Saito, DC Schwartz, K Thamatrakoln, K Valentin, A Vardi, FP Wilkerson and DS Rokhsar (2004). The genome of the diatom *Thalassiosira pseudonana*: ecology, evolution, and metabolism. *Science* 306: 79-86.

Song A, A Patel, K Thamatrakoln, C Liu, D Feng, C Clayberger, and AM Krensky (2002). Functional domains and DNA-binding sequences of RFLAT-1/KLF13, a Kruppel-like transcription factor of activated T-Lymphocytes. *Journal of Biological Chemistry* 277: 30055-30065.

Song A, YF Chen, K Thamatrakoln, TA Storm, and AM Krensky (1999) RFLAT-1, A new zinc finger transcription factor that activates RANTES gene expression in T-Lymphocytes. *Immunity* 10: 93-103.

FIELDS OF STUDY

Major Field: Marine Biology

Studies in Molecular Biology and Biochemistry
Mark Hildebrand
Julian I. Schroeder
Victor D. Vacquier

Studies in Phytoplankton Physiology
Mark A. Brzezinski
Michael I. Latz
Brian Palenik

ABSTRACT OF THE DISSERTATION

Molecular Insights into the Function and Regulation of Diatom Silicon Transporters

by

Kimberlee Thamatrakoln

Doctor of Philosophy in Marine Biology

University of California, San Diego, 2006

Michael I. Latz, Chair

Diatoms, a major group of primary producers in the ocean, are estimated to be responsible for over 40% of oceanic carbon fixation. As one of the predominant biosilicifying organisms in the world, diatoms are a model system for studying biological interactions with silicon. This research has focused on characterizing a

novel family of transporters, called silicon transporters (SITs), that are specific for the uptake and efflux of silicon in diatoms.

SIT sequences were isolated from evolutionarily diverse diatom species. Multi-gene copies were identified in most species, and phylogenetic analysis showed SITs grouped according to species. Structural analysis suggested SITs evolved through an internal gene duplication. Comparative sequence analysis revealed repeats of a conserved sequence motif, GXQ. A model of silicon transport consistent with known aspects of uptake was developed based on this motif.

Analysis of SIT protein and mRNA expression, as well as measurements of uptake activity, was done on synchronously growing cultures of the diatom, *Thalassiosira pseudonana*. Immunoblot analysis using a newly developed SIT-specific antibody showed peaks in SIT protein levels correlated with active periods of silica incorporation. Quantitative PCR showed each *T. pseudonana SIT* (*TpSIT1-3*) peaked prior to cell wall synthesis. However, a disconnect between protein and mRNA levels suggested SITs were primarily regulated at the translational or post-translational level. In addition, rates of surge uptake suggested SIT activity was internally controlled by the rate of silica incorporation.

Silicon uptake kinetics in diatoms were measured to determine the extent of nonsaturable uptake and the role of SITs. In all diatom species examined, a time-dependent transition from nonsaturable to saturable uptake kinetics was observed. In addition, both forms of uptake were affected by the SIT-specific antibody suggesting SITs were the predominant means of silicon uptake into the cell. Under some conditions, SITs had enormous flexibility in their rate of transport and appeared to act

as selectivity gates rather than controlling agents in uptake. A model of diatom silicon uptake, consistent with this and previously published data, was developed based on the interplay between SITs, intracellular soluble silicon pools, and cell wall silica incorporation.

chapter I

Introduction

Silicon, the second most abundant element in the Earth's crust after oxygen, is an important element in biology (Birchall 1995). In higher plants, silicic acid, the soluble form of silicon, is an important nutrient for growth, while silica, the polymerized form of silicon, is used for rigidity, pathogen resistance, drought tolerance, and defense against grazers (Epstein 1999; Richmond and Sussman 2003). In animals, silicon participates in a variety of metabolic processes (Carlisle 1978) and is required for proper formation of bone, cartilage, and connective tissue formation (Schwarz and Milne 1972; Carlisle 1974, 1981).

The predominant form of silicon in the ocean is silicic acid, produced from the chemical weathering of sediments and rocks and transported to the ocean by rivers and streams (Tréguer et al. 1995). Other minor sources of silicic acid to the ocean include aeolian and hydrothermal input, and seafloor weathering (Tréguer et al. 1995). In the surface layer of the ocean, silicifying organisms take up silicic acid and process it into silica that is used as part of their skeletal structures. Prior to the evolution of silicifying organisms, the world's oceans were nearly saturated with dissolved silicon (1.7-2.5 mM) (Iler 1979; Holland 1984). Today, because of utilization by siliceous organisms, that number has decreased to a global average of 70 μM, but is generally <10 μM and sometimes <1 μM in surface waters (Tréguer et al. 1995; Martin-Jézéquel et al. 2000). The major silicifying organisms are sponges, radiolarians, silicoflagellates, and diatoms; together, they convert 6.7 gigatons of soluble silicon into silica annually (Tréguer et al. 1995; Bäuerlein 2003). Diatoms are by far the largest of these groups; they are unicellular, eukaryotic phytoplankton estimated to contribute up to 40% of marine primary productivity (Nelson et al. 1995).

Diatoms have long been admired for the intricate and diverse microstructure of their cell wall, or frustule, composed primarily of silica. The silicified diatom cell wall is composed of two overlapping halves with the upper half called the epitheca and the lower half the hypotheca. Theca consist of a valve, the species-specific structure capping each end, and girdle bands, a series of overlapping siliceous strips extending on the sides and in the region overlapping the two halves. The reproducibility of a diatom species' silica morphology indicates the process of cell wall synthesis is genetically controlled.

The silica component of the diatom frustule can account for up to 50% of the dry weight of the cell depending on the species (Lewin and Guillard 1963); as such, there is a high demand for silicon to be taken up from the environment. However, intracellular concentrations of silicic acid, ranging from 19 to 340 mM, are nearly 1000 fold higher than extracellular concentrations (Martin-Jézéquel et al. 2000). Thus, diatoms must have an efficient mechanism for transporting limiting amounts of silicic acid into the cell against a steep concentration gradient (Fig. 1.1). Silicon uptake in diatoms has been reported to follow Michaelis-Menten type saturation kinetics with K_s values between 0.2 and 7.7 μM and V_{max} ranging from 1.2 to 950 fmol Si cell^{-1} hr^{-1} (Lewin 1954, 1955; Sullivan 1976, 1977; Bhattacharyya and Volcani 1980; Martin-Jézéquel et al. 2000; Tréguer and Pondaven 2000). The predominant transported form of silicon is orthosilicic acid, but there is evidence in one species, *Phaeodactylum tricornutum,* that the anionic form $SiO(OH)_3^-$ can also be transported (Reidel and Nelson 1985; Del Amo and Brzezinski 1999). Silicic acid is co-transported with sodium in marine diatoms (Fig. 1.1) and it may be sodium and potassium coupled in

freshwater species (Sullivan 1976; Bhattacharyya and Volcani 1980). However, in freshwater species, higher K_s values and increased silicon requirements (Olsen and Paasche 1986) bring into question the extent of ionic coupling (Hildebrand and Wetherbee 2003). Regardless, transport under marine conditions has the characteristics of a sodium/silicic acid symporter and appears to be electrogenic with a 1:1 ratio of $Si(OH)_4$:Na^+ (Bhattacharyya and Volcani 1980). Exposure to sulfhydryl blocking reagents inhibits transport (Lewin 1954; Sullivan 1976).

After silicic acid enters the cell, it must be maintained in an unpolymerized, soluble form. The chemistry of silicic acid is such that, at cytoplasmic pH, it autopolymerizes at concentrations > 2 mM (Iler 1979). Maintenance of supersaturated levels of soluble silicic acid is proposed to occur by association with organic silicon binding components or proteins (Fig. 1.1; Hildebrand 2000; Martin-Jézéquel et al. 2000). Although the mechanism of intracellular transport of silicic acid is relatively unknown, electron spectroscopic imaging shows silicic acid is found throughout the cytoplasm (Rogerson et al. 1987) and not in cytoplasmic vesicles as previously suggested (Schmid and Schulze 1979). Silica polymerization and new cell wall formation occurs in the silica deposition vesicle (SDV), a slighty acidic vesicle (Vrieling et al. 1999) surrounded by a membrane called the silicalemma (Fig. 1.1; Drum and Pankratz 1964; Reimann et al. 1966; Schmid et al. 1981; Crawford and Schmid 1986). Details of how silicic acid enters the SDV are unknown, although it may occur through direct transport, ionophore-mediated diffusion, or electrophoretic transport (Fig. 1.1).

A major step towards understanding the mechanism of cell wall formation was the discovery of two species-specific components directly involved in silica polymerization, silaffins and polyamines (Kröger et al. 1999, 2000, 2002). Siliffins are highly post-translationally modified, lysine and serine rich peptides associated with the cell wall and capable of rapidly polymerizing silica nanospheres in the presence of silicic acid (Kröger et al. 1999, 2001). Long-chained polyamines consisting of repeated oligo-*N*-methyl propylamine units are also associated with diatom biosilica and are capable of rapid polymerization of silica (Kröger et al. 2000). It is proposed the ratio of silaffins and polyamines may direct silica patterning of the diatom cell wall, although a mechanism for the formation of specific micro-scaled structures has not been determined.

Silicon efflux is an often overlooked and under-appreciated aspect of balancing the overall cellular silicon budget (Azam et al. 1974; Sullivan 1976; Milligan et al. 2004). Efflux only occurs in the presence of external silicic acid and increases with increasing external silicic acid (Sullivan 1976). This may occur because as silicic acid concentrations outside the cell rise, surge uptake would increase leading to increased levels of intracellular silicic acid and inducing efflux to a greater extent.

Three modes of silicon uptake have been proposed based on chemostat studies: surge uptake, externally controlled uptake, and internally controlled uptake (Conway et al. 1976; Conway and Harrison 1977). Surge uptake occurs when silicate-starved cells are replenished with silicon. Under these conditions, intracellular silicon pools are depleted resulting in a steep silicon concentration gradient into the cell. Uptake rates during this time are maximal. Externally controlled uptake occurs when

extracellular levels of silicon are low and the rate of uptake is controlled by the external substrate concentration. In internally controlled uptake, the rate of silica incorporation into the cell wall controls the rate of uptake (Conway et al. 1976; Conway and Harrison 1977; Hildebrand and Wetherbee 2003; Hildebrand et al. in press). Thus, there is a temporal coupling between uptake and incorporation that is seen in most diatoms (Chisholm et al. 1978).

Measurements of uptake kinetics in whole cells and extracts have provided critical information about silicon transport, but understanding details of the transport mechanism requires characterizing the molecular components, specifically, the genes and proteins involved in silicon recognition and transport. The first step towards developing a molecular model for silicon transport was the cloning and characterization of silicon transporters (Hildebrand et al. 1997, 1998).

Diatom silicon transporters (SITs) were first identified in the marine pennate diatom *Cylindrotheca fusiformis* (Hildebrand et al. 1997, 1998). Because uptake assays suggested silicon transport was tightly coupled to the cell cycle (Sullivan 1976), synchronously growing cultures of *C. fusiformis* were used to identify cell-cycle regulated genes (Hildebrand et al. 1993). Using subtractive cDNA library techniques, *SITs*, as well as other silicon-responsive genes, were identified and cloned (Hildebrand et al. 1993, 1998). Five distinct *SIT* genes (*CfSIT1-5*) were found in *C. fusiformis*, each with a distinct level or pattern of expression during cell wall synthesis (Hildebrand et al. 1998). *Cf*SIT function is sodium-dependent, specific for silicon and germanium (a commonly used radiotracer for silicon), and sensitive to sulfhydryl blocking reagents (Hildebrand et al. 1997), consistent with diatom whole-cell uptake

experiments. SITs are a novel family of transporters with no known homologs, although a silicon transporter homologous to aquaporins, but with no homology to diatom SITs, was recently described in rice (Ma et al. 2006). Although *SIT*s were among the first silicon-responsive genes to be identified in any organism (Hildebrand et al. 1993), other silicon-interacting proteins have since been identified (Shimizu et al. 1998; Kröger et al. 1999, 2000; Poulsen and Kröger 2004). However, SITs are unique in that they are the only known proteins that recognize silicon, but do not induce its polymerization; thus SITs are a model system for understanding biological interactions with silicon.

*Cf*SITs range between 538-557 amino acids in length and are comprised of two major domains; a region predicted to contain ten transmembrane segments (TMS) and a C-terminus predicted to form a coiled-coil motif, a structure known to play a role in protein-protein interactions (Fig. 1.2). Based on other even-numbered TMS transporters, both the N- and C-terminal ends are proposed to be intracellular (Fig. 1.2, Seckler et al. 1983; Davies et al. 1987). Within the transmembrane domain, *Cf*SITs are highly conserved, having 87-99% amino acid identity. The C-terminus is less conserved with 39-67% amino acid identity. In other transporters, the C-terminus has been shown to play a role in regulating transporter activity, determining intracellular localization, or controlling conformational changes during transport (Verhey et al. 1993; Holman and Cushman 1994; Due et al. 1995; Verhey et al. 1995; Caspari et al. 1996). The sequence disparity within this region among the five SITs may be responsible for functional differences.

Genome sequencing of the centric diatom, *Thalassiosira pseudonana,* led to the identification of three distinct *SIT* genes (*TpSIT1-3*, Armbrust et al. 2004). Similar to *Cf*SITs, *Tp*SITs are predicted to contain ten TMS with an intracellular N- and C-terminus. In contrast, the C-terminus is not predicted to form a coiled-coil motif (Thamatrakoln et al. 2006).

Identification of SITs was an important step in elucidating a key aspect of the molecular mechanisms involved in diatom silicon metabolism. However, since their initial identification, SITs have remained relatively uncharacterized. The goal of this project has been to understand the role of SITs in diatom silicon metabolism through molecular and biochemical characterization of their function and regulation. This dissertation is organized into five subsequent chapters summarized below.

Chapter II describes the identification and comparative sequence analysis of new SIT sequences from evolutionarily distinct diatoms with the goal of identifying conserved residues likely to play a role in the direct recognition and binding of silicic acid. Phylogenetic analysis revealed SITs generally group according to species. Results indicated the presence of a conserved sequence motif proposed to directly coordinate silicic acid. Based on this information, a model for silicon uptake, consistent with known aspects of silicon transport, was developed.

Chapter III describes a multi-level analysis of SIT expression and silicon uptake activity in *Thalassiosira pseudonana* during the course of the cell cycle. Development and characterization of the first SIT-specific antibody, anti-TpEL4, is also described. Analysis of SIT mRNA and protein expression suggests SIT regulation

is predominantly at the translational or post-translational level and uptake data suggest SIT activity is largely controlled through an intracellular mechanism.

Chapter IV investigates silicon uptake kinetics in diatoms and the role of SITs in transport. Previous studies have reported both nonsaturable and saturable Michaelis-Menten type kinetics, although mechanistic explanations for nonsaturable uptake are lacking. Time-course measurements of $Si(OH)_4$ uptake in different diatoms showed a transition from nonsaturable to saturable uptake. Use of anti-TpEL4 suggested $Si(OH)_4$ uptake occurred primarily through SITs and that SITs exhibit enormous flexibility over their transport rate. A model of $Si(OH)_4$ uptake in diatoms, consistent with current as well as previous results, is presented.

Chapter V synthesizes results presented in the previous chapters and discusses implications of this research as well as areas for future study.

Chapter I, in part, is reproduced from the Journal of Nanoscience and Nanotechnology 5:158-166 and Science First Hand 5:56-60. The dissertation author was the primary investigator and author on these manuscripts. Mark Hildebrand was a co-author.

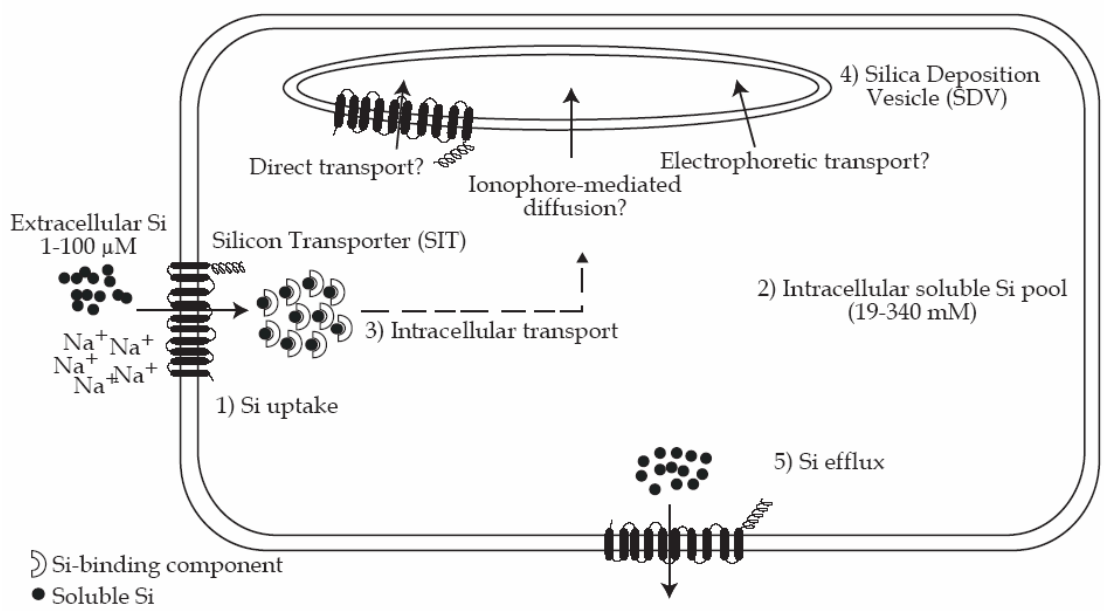

Figure 1.1. Schematic of diatom silicon metabolism. 1) Extracellular silicon, as silicic acid (black circles), is co-transported with sodium (Na^+) across the plasma membrane through silicon transporters (SITs). 2) Supersaturated levels of silicic acid are maintained in soluble form by binding to an intracellular Si-binding component (horseshoe shaped structure). 3) Silicic acid is transported through the cytoplasm to the silica deposition vesicle (SDV), where it is polymerized into silica and molded into the new cell wall. 4) The mechanism by which silicic acid enters the SDV is unknown, but may occur through direct transport by SITs, ionophore-mediated diffusion, or electrophoretic transport. 5) Silicic acid efflux also occurs through SITs, allowing further control over intracellular silicon levels.

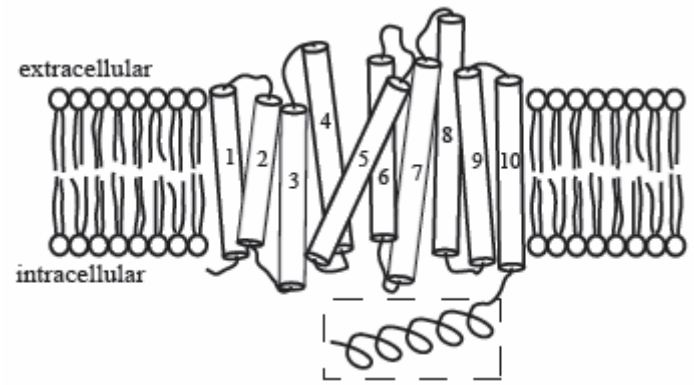

Figure 1.2. Cartoon of computer-based model of silicon transporter topology. SITs are comprised of ten membrane-spanning segments (numbered, white cylinders) connected by hydrophilic loops. The intracellular C-terminus is predicted to form a coiled-coil motif (dashed box) in *C. fusiformis*, but not in *T. pseudonana*.

REFERENCES

Armbrust EV, JA Berges, C Bowler, BR Green, D Martinez, NH Putnam, S Zhou, AE Allen, KE Apt, M Bechner, MA Brzezinski, BK Chaal, A Chiovitti, AK Davis, MS Demarest, JC Detter, T Glavina, D Goodstein, MZ Hadi, U Hellsten, M Hildebrand, BD Jenkins, J Jurka, VV Kapitonov, N Kröger, WWY Lau, TW Lane, FW Larimer, JC Lippmeier, S Lucas, M Medina, A Montsant, M Obornik, MS Parker, B Palenik, GJ Pazour, PM Richardson, TA Rynearson, MA Saito, DC Schwartz, K Thamatrakoln, K Valentin, A Vardi, FP Wilkerson and DS Rokhsar (2004). The genome of the diatom *Thalassiosira pseudonana*: ecology, evolution, and metabolism. *Science* 306: 79-86.

Azam F, BB Hemmsingsen and BE Volcani (1974). Role of silicon in diatom metabolism V. Silicic acid transport and metabolism in the heterotrophic diatom *Nitzschia alba*. *Arch. Microbiol.* 97: 103-114.

Bäuerlein E (2003). Biomineralization of unicellular organisms: An unusual membrane biochemistry for the production of inorganic nano- and microstructures. *Angew. Chem.* 42: 614-641.

Bhattacharyya P and BE Volcani (1980). Sodium dependent silicate transport in the apochlorotic marine diatom *Nitzschia alba*. *Proc. Natl. Acad. Sci. U.S.A.* 77: 6386-6390.

Birchall JD (1995). The essentiality of silicon in biology. *Chem. Soc. rev.* 24: 351-357.

Carlisle EM (1974). Silicon as an essential element. *Fed. Proc.* 33: 1758-1766.

Carlisle EM (1978). Essentiality and function of silicon *in* Biochemistry of Silicon and Related Problems. G Bendz and I Lindqvist. New York, N.Y., Plenum Press**:** 231-253.

Carlisle EM (1981). Silicon in bone formation *in* Silicon and Siliceous Structures in Biological Systems. TL Simpson and BE Volcani. New York, N.Y., Springer-Verlag**:** 69-94.

Caspari T, I Robl, J Stolz and W Tanner (1996). Purification of the *Chlorella* HUP1 hexose-proton symporter to homogeneity and its reconstitution *in vitro*. *Plant J.* 10: 1045-1053.

Chisholm SW, F Azam and RW Eppley (1978). Silicic acid incorporation in marine diatoms on light:dark cycles: use as an assay for phased cell division. *Limnol. Oceanog.* 23: 518-529.

Conway HL and PJ Harrison (1977). Marine diatoms grown in chemostats under silicate or ammonium limitations IV. Transient response of *Chaetoceros debilis*, *Skeletonema costatum*, and *Thalassiosira gravida* to a single addition of the limiting nutrient. *Mar. Biol.* 43: 33-43.

Conway HL, PJ Harrison and CO Davis (1976). Marine diatoms grown in chemostats under silicate or ammonium limitation. II. Transient response of *Skeletonema costatum* to a single addition of the limiting nutrient. *Mar. Biol.* 35: 187-199.

Crawford RM and AMM Schmid (1986). Ultrastructure of silica deposition in diatoms *in* Biomineralization in Lower Plants and Animals. BS Leadbeater and R Riding. London, U.K., The Systematics Society. **30:** 291-314.

Davies A, K Meeran, MT Cairns and ST Baldwin (1987). Peptide-specific antibodies as probes of the orientation of the glucose transporter in the human erythrocyte membrane. *J. Biol. Chem.* 262: 9347-9352.

Del Amo Y and MA Brzezinski (1999). The chemical form of dissolved Si taken up by marine diatoms. *J. Phycol.* 35: 1162-1170.

Drum RW and HS Pankratz (1964). Post mitotic fine structure of *Gomphonema parvulum*. *J. Ultrastruct. Res.* 10: 217-223.

Due AD, Q Zhinchao, JM Thomas, A Buchs, AC Powers and JM May (1995). Role of the C-terminal tail of the GLUT1 glucose transporter in its expression and function in *Xenopus laevis* oocytes. *Biochemistry* 34: 5462-5471.

Epstein E (1999). Silicon. *Annul Rev. Plant Physiol. Plant Mol. Biol.* 50: 641-664.

Hildebrand M (2000). Silicic acid transport and its control during cell wall silicification in diatoms *in* Biomineralization: From Biology to Biotechnology and Medical Applications. E Bäuerlein. Weinheim, Wiley-VCH**:** 171-188.

Hildebrand M, K Dahlin and BE Volcani (1998). Characterization of a silicon transporter gene family in *Cylindrotheca fusiformis*: Sequences, expression analysis, and identification of homologs in other diatoms. *Mol. Gen. Genet.* 260: 480-486.

Hildebrand M, LG Frigeri and AK Davis (in press). Synchronized growth of *Thalassiosira pseudonana* (Bacillariophyceae) provides novel insights into cell wall synthesis processes in relation to the cell cycle. *J. Phycol.*

Hildebrand M, DR Higgins, K Busser and BE Volcani (1993). Silicon-responsive cDNA clones isolated from the marine diatom *Cylindrotheca fusiformis*. *Gene* 132: 213-218.

Hildebrand M, BE Volcani, W Gassmann and JI Schroeder (1997). A gene family of silicon transporters. *Nature* 385: 688-689.

Hildebrand M and R Wetherbee (2003). Components and control of silicification in diatoms *in* Progress in Molecular and Subcellular Biology. WEG Muller. Berlin Heidelberg, Springer-Verlag. **33:** 11-57.

Holland HD (1984). The Chemical Evolution of the Atmosphere and Oceans. Princeton, NJ, Princeton University Press.

Holman GD and SW Cushman (1994). Subcellular localization and trafficking of the GLUT4 glucose transporter isoform in insulin-responsive cells. *BioEssays* 16: 753-759.

Iler RK (1979). The Chemistry of Silica: Solubility, Polymerization, Colloid and Surface Properties, and Biochemistry. New York, John Wiley & Sons.

Kröger N, R Deutzmann, C Bergsdorf and M Sumper (2000). Species-specific polyamines from diatoms control silica morphology. *Proc. Natl. Acad. Sci. U.S.A.* 97: 14133-14138.

Kröger N, R Deutzmann and M Sumper (1999). Polycationic peptides from diatom biosilica that direct silica nanosphere formation. *Science* 286: 1129-1132.

Kröger N, R Deutzmann and M Sumper (2001). Silica-precipitating peptides from diatoms. *J. Biol. Chem.* 276: 26066-26070.

Kröger N, S Lorenz, E Brunner and M Sumper (2002). Self assembly of highly phosphorylated silaffins and their function in biosilica morphogenesis. *Science* 298: 584-586.

Lewin JC (1954). Silicon metabolism in diatoms. I. Evidence for the role of reduced sulfur compounds in silicon utilization. *J. Gen. Physiol.* 37: 589-599.

Lewin JC (1955). Silicon metabolism in diatoms. III. Respiration and silicon uptake in *Navicula pelliculosa*. *Can. J. Microbiol.* 3: 427-433.

Lewin JC and RRL Guillard (1963). Diatoms. *Annu. Rev. Microbiol.* 17: 373-414.

Ma JF, K Tamai, N Yamaji, N Mitani, S Konishi, M Katsuhara, M Ishiguro, Y Murata and M Yano (2006). A silicon transporter in rice. *Nature* 440: 688-691.

Martin-Jézéquel V, M Hildebrand and MA Brzezinski (2000). Silicon metabolism in diatoms: Implications for growth. *J. Phycol.* 36: 821-840.

Milligan A, DE Varela, MA Brzezinski and FMM Morel (2004). Dynamics of silicon metabolism and silicon isotopic discrimination in a marine diatom as a function of *p*CO2. *Limnol. Oceanog.* 49: 322-329.

Nelson DM, P Tréguer, MA Brzezinski and A Leynaert (1995). Production and dissolution of biogenic silica in the ocean: revised global estimates, comparison with regional data and relationship to biogenic sedimentation. *Glob. Biogeochem. Cycles* 9: 359-372.

Olsen S and E Paasche (1986). Variable kinetics of silicon-limited growth in *Thalassiosira pseudonana* (Bacillariophyceae) in response to changed chemical composition of growth medium. *Br. Phycol. J.* 21: 183-190.

Poulsen N and N Kröger (2004). Silica morphogenesis by alternative processing of silaffins in the diatom *Thalassiosira pseudonana*. *J. Biol. Chem.* 279: 42993-42999.

Reidel GF and DM Nelson (1985). Silicon uptake by algae with no known Si requirement. II. Strong pH dependence of uptake kinetic parameters in *Phaeodactylum tricornutum* (Bacillariophyceae). *J. Phycol.* 21: 168-171.

Reimann BEF, JC Lewin and BE Volcani (1966). Studies on the biochemistry and fine structure of silica shell formation in diatoms. II. The structure of the cell wall of *Navicula pelliculosa* (Breb.) Hilse. *J. Phycol.* 2: 74-84.

Richmond KE and M Sussman (2003). Got silicon? The non-essential beneficial plant nutrient. *Curr. Opin. Plant Biol.* 6: 268-272.

Rogerson A, ASW deFreitas and AG McInnes (1987). Cytoplasmic silicon in the centric diatom *Thalassiosira pseudonana*. *Can. J. Microbiol.* 33: 128-131.

Schmid AMM, MA Borowitzka and BE Volcani (1981). Morphogenesis and biochemistry of diatom cell walls *in* Cytomorphogenesis in Plants. O Kiermayer. New York, N.Y., Springer-Verlag. **8:** 63-97.

Schmid AMM and D Schulze (1979). Wall morphogenesis in diatoms: deposition of silica by cytoplasmic vesicles. *Protoplasma* 100: 267-288.

Schwarz K and DB Milne (1972). Growth-promoting effects of silicon in rats. *Nature* 239: 333-334.

Seckler R, J Wright and P Overath (1983). Peptide-specific antibody locates the COOH terminus of the lactose carrier of *Escherichia coli* on the cytoplasmic side of the plasma membrane. *J. Biol. Chem.* 258: 10817-10820.

Shimizu K, J Cha, GD Stucky and DE Morse (1998). Silicatein alpha: Cathepsin L-like protein in sponge biosilica. *Proc. Natl. Acad. Sci. U.S.A.* 95: 6234-6238.

Sullivan CW (1976). Diatom mineralization of silicic-acid. I. $Si(OH)_4$ transport characteristics in *Navicula pelliculosa*. *J. Phycol.* 12: 390-396.

Sullivan CW (1977). Diatom mineralization of silicic acid. II. Regulation of $Si(OH)_4$ transport rates during the cell cycle of *Navicula pelliculosa*. *J. Phycol.* 13: 86-91.

Thamatrakoln K, AJ Alverson and M Hildebrand (2006). Comparative sequence analysis of diatom silicon transporters: towards a mechanistic model for silicon transport. *J. Phycol.* 42.

Tréguer P, DM Nelson, AJ Van Bennekom, DJ DeMaster, A Leynaert and B Queguiner (1995). The silica balance in the world ocean: A reestimate. *Science* 268: 375-379.

Tréguer P and P Pondaven (2000). Silica control of carbon dioxide. *Nature* 406: 358-359.

Verhey KJ, SF Hausdorff and MJ Birnbaum (1993). Identification of the carboxy terminus as important for the isoform-specific subcellular targeting of glucose transporter proteins. *J. Cell Biol.* 123: 137-147.

Verhey KJ, JI Yeh and MJ Birnbaum (1995). Distinct signals in the GLUT4 glucose transporter for internalization and for targeting to an insulin-responsive compartment. *J. Cell Biol.* 132: 1071-1079.

Vrieling EG, WWC Gieskes and TPM Beelen (1999). Silicon deposition in diatoms: control by the pH inside the silicon deposition vesicle. *J. Phycol.* 35: 548-559.

chapter II

Comparative sequence analysis of diatom silicon transporters: towards a mechanistic model of silicon transport

J. Phycol. 42, 822–834 (2006)

DOI: 10.1111/j.1529-8817.2006.00233.x

COMPARATIVE SEQUENCE ANALYSIS OF DIATOM SILICON TRANSPORTERS: TOWARD A MECHANISTIC MODEL OF SILICON TRANSPORT[1]

Kimberlee Thamatrakoln[2]

Marine Biology Research Division, Scripps Institution of Oceanography, University of California, San Diego, 9500 Gilman Drive, La Jolla, California 92037-0202, USA

Andrew J. Alverson

Section of Integrative Biology and Texas Memorial Museum, University of Texas at Austin, 311 Biological Laboratory, Austin, Texas 78712, USA

and

Mark Hildebrand

Marine Biology Research Division, Scripps Institution of Oceanography, University of California, San Diego, 9500 Gilman Drive, La Jolla, California 92037-0202, USA

Silicon is an important element in biology, for organisms ranging from unicellular algae to humans. It acts as a structural material for both plants and animals, but can also function as a metabolite or regulator of gene expression, affecting a wide range of cellular processes. Molecular details of biological interaction with silicon are poorly understood. Diatoms, the largest group of silicifying organisms, are a good model system for studying this interaction. The first proteins shown to directly interact with silicon were diatom silicon transporters (SITs). Because the basis for substrate recognition lies within the primary sequence of a protein, identification of conserved amino acid residues would provide insight into the mechanism of SIT function. Lack of SIT sequences from a diversity of diatoms and high sequence conservation in known SITs has precluded identification of such residues. In this study, PCR was used to amplify partial *SIT* sequences from eight diverse diatom species. Multiple gene copies were prevalent in each species, and phylogenetic analysis showed that SITs generally group according to species. In addition to partial *SIT* sequences, full-length *SIT* genes were identified from the pennate diatom, *Nitzschia alba* (Lewin and Lewin), and the centric diatom *Skeletonema costatum* (Greville) Cleve. Comparing these SITs with previously identified SITs showed structural differences between SITs of centrics and pennates, suggesting differences in transport mechanism or regulation. Comparative amino acid analysis identified conserved regions that may be important for silicon transport, including repeats of the motif GXQ. A model for silicon uptake and efflux is presented that is consistent with known aspects of transport.

Key index words: **diatom; sequence comparison; silicon; silicon transporter**

Abbreviations: **FEL, fixed effects likelihood; IC, IntraCompare; ML, maximum likelihood; PSSM, position-specific score matrix; RACE, rapid amplification of cDNA ends; SIT, silicon transporter; TMS, transmembrane segment**

Silicon is the second most abundant element in the Earth's crust and plays an essential, and often underappreciated, role in biology. However, the molecular basis of biological interactions with silicon is poorly understood. Silicon is an essential element in animals, critical for proper formation of bone and connective tissue (Schwarz and Milne 1972, Carlisle 1978, 1981), and is beneficial, if not essential, for plants, where it contributes to stem rigidity, photosynthetic efficiency, and fungal resistance (Epstein 1994, Fauteux et al. 2005). The most prevalent silicifying organisms are diatoms, unicellular eukaryotic microalgae that use silica as a rigid structural material for their cell walls. Diatom cell walls (or "frustules") are ornately and intricately structured on the nano-scale, generating interest in their use for nanotechnological applications (Gordon et al. 2005). Because diatoms assimilate up to 240 teramoles of silicon each year, they play an important role in silicon biogeochemistry (Nelson et al. 1995, Tréguer et al. 1995). The importance of silicon availability, which limits diatom productivity, in the global carbon cycle has been demonstrated (Tréguer et al. 1995, Smetacek 1999, Tréguer and Pondaven 2000). Diatoms provide an excellent model system to explore biological interactions with silicon because most species have an absolute silicon requirement for growth

[1]Received 23 November 2005. Accepted 9 March 2006.
[2]Author for correspondence: e-mail kthamatr@ucsd.edu.

(Darley and Volcani 1969) and metabolize large amounts of silicon.

Diatoms take up silicon predominantly as silicic acid (Del Amo and Brzezinski 1999), which is polymerized and deposited into the cell wall as silica. The average oceanic concentration of silicic acid is 70 μM, but is generally less than 10 μM in surface waters where diatoms are most common (Tréguer et al. 1995). Intracellular concentrations of silicic acid can be several hundred millimolar, depending on the species (Martin-Jézéquel et al. 2000). Because of the large difference between extra- and intracellular silicon concentration (~1000-fold), diatoms require an efficient uptake system. Whole-cell studies show silicon uptake in diatoms follows Michaelis–Menten kinetics with K_s values between 0.2 and 7.7 μM, and V_{max} ranging from 1.2 to 950 fmol $Si \cdot cell^{-1} \cdot h^{-1}$ (Lewin 1954, 1955, Sullivan 1976, 1977, Bhattacharyya and Volcani 1980, Martin-Jézéquel et al. 2000, Tréguer and Pondaven 2000). Silicic acid is co-transported with sodium in marine diatoms, and it may be sodium and potassium coupled in freshwater species (Sullivan 1976, Bhattacharyya and Volcani 1980). Transport under marine conditions has the characteristics of a sodium-silicic acid symporter and appears to be electrogenic with a 1:1 ratio of $Si(OH)_4$:Na^+ (Bhattacharyya and Volcani 1980). Zinc has also been suggested to play a role in silicic acid uptake (Rueter and Morel 1981).

An important, but often overlooked, aspect of silicon transport is efflux from the cell (Sullivan 1977, Milligan et al. 2004). The importance of efflux in the overall silicon budget of a diatom cell has recently been highlighted (Milligan et al. 2004). Efflux is an essential part of silicon metabolism because it prevents the over-accumulation of intracellular soluble silicon that could auto-polymerize and be detrimental to cell function.

The first step toward understanding the molecular basis of silicon transport was the cloning and functional characterization of the silicon transporter genes, or *SITs* (Hildebrand et al. 1997, 1998). The *SITs* represent a novel family of transporter with no known homologs, and were among the first silicon-responsive genes to be identified in any organism (Hildebrand et al. 1993). Five *SIT* genes were found in the marine pennate diatom, *Cylindrotheca fusiformis* (*CfSIT1-5*), each with a distinct level or temporal pattern of expression during cell wall synthesis (Hildebrand et al. 1998). Each *Cf*SIT is predicted to contain 10 transmembrane segments (TMS) and a coiled-coil motif at the C-terminus (Hildebrand et al. 1998). The *Cf*SITs are 74% identical at the amino acid level, with the highest degree of conservation within the transmembrane domain.

Recently, genome sequencing of the centric diatom, *Thalassiosira pseudonana* (Armbrust et al. 2004) led to the identification of three *SITs* (*TpSIT1-3*), which are 44% identical at the amino acid level. As found for *Cf*SIT1-5, *Tp*SIT1-3 each contain 10 predicted TMS. However, *Tp*SITs appear to have a longer N-terminus and do not contain a C-terminal coiled-coil motif. Genes encoding *Tp*SITs also differ from *Cf*SITs in that they appear to each contain a single intron. Partial SIT sequences have also been reported for the freshwater pennate, *Synedra acus*, and the marine centric diatom, *Chaetoceros muelleri* (Grachev et al. 2002, Sherbakova et al. 2005).

Silicon transporters were the first proteins shown to directly interact with silicon, and although other silicon-interacting proteins have been identified (Shimizu et al. 1998, Kröger et al. 1999, Poulsen and Kröger 2004), SITs are the only ones that do not catalyze silica polymerization. Cloning of a putative silicon transporter in sponge has been reported, but the gene identified is a bicarbonate transporter homolog with no homology to SITs, and only inferential evidence of its role in silicic acid uptake was reported (Schröder et al. 2004). In rice, kinetics of silicon uptake have been measured (Mitani and Ma 2005) and a silicon transport system has been recently described (Ma et al. 2006). However, the rice silicon transporter is an aquaporin homolog and shares no similarity to diatom SITs.

The mechanism by which SITs recognize and bind silicic acid is unknown. Passage of silicic acid must occur through the transmembrane domain, and conserved residues within this region may play an important functional role. Identification of key conserved residues has not been feasible because of the limited number of SIT sequences and high sequence conservation within this region in known SITs. In other transporters, charged residues found within membrane-spanning regions have been shown to be crucial for function (Yamato et al. 1994, Shelden et al. 2003). Hydroxyl groups in aliphatic polyols can directly coordinate silicic acid (Kinrade et al. 1999), suggesting that hydroxylated amino acids could be involved in silicic acid recognition by SITs. Condensation of silicic acid to silica in diatoms occurs via amine-containing molecules (Kröger et al. 1999, 2000), suggesting that amine-containing amino acids could also be involved in silicic acid–SIT interaction. Recently, SITs were hypothesized to contain a conserved zinc-binding domain. Sherbakova et al. (2005) isolated a *SIT* fragment from the centric diatom, *C. muelleri* and compared it against three SITs from GenBank (*C. fusiformis*, *Phaeodactylum tricortum*, and *S. acus*). They proposed that the cysteine found in the conserved sequence, CMLD, binds zinc and coordinates the binding of silicic acid to the SITs.

Our goal is to understand the molecular mechanism by which SITs recognize, bind, and transport silicon. The fundamental basis of ligand recognition lies within the amino acid sequence of a protein, and single residue mutations in other transporters have been shown to significantly alter function (Yamato et al. 1994, Will et al. 1998). Because residues important for function are likely retained during evolution, a comparative sequence analysis of SITs from a diversity of diatoms could help identify such residues. In this study, we report the molecular cloning and sequence comparison of 16 partial and two full-length *SIT* genes from

eight diatom species, including centrics and pennates from both marine and freshwater environments. These data provide new insight into the evolution of these proteins by allowing the identification of conserved amino acid residues possibly involved in SIT function and regulation, as well as provide the basis for a mechanistic model for silicic acid transport.

MATERIALS AND METHODS

Culture conditions. All diatoms (Table 1) were grown in batch culture under continuous illumination with cool white fluorescent lights at approximately 150 µmol quanta · $m^{-2} \cdot s^{-1}$ at 18 to 20° C. *Navicula pelliculosa* FW was grown in fresh water tryptone (FWT) medium (Reimann et al. 1966) and other diatom species in artificial seawater (ASW) medium (Darley and Volcani 1969) or f/2 medium made with 0.2 µm filtered and autoclaved local seawater (Guillard and Ryther 1962, Guillard 1975).

Nitzschia cf. *longissima* was isolated by B. Volcani (date and location unknown) and identified by light microscopy. The 18S rDNA was amplified and sequenced using eukaryotic-specific 18S primers (Medlin et al. 1995). Sequence comparison using BLAST search indicated the closest homolog was *Nitzschia longissima*. *Urosolenia* spp. was isolated by E. Theriot from Yellowstone Lake, Yellowstone National Park, USA (1998). It was identified by light microscopy and provided by E. Theriot. *Bacteriastrum hyalinum* was isolated by M. MacFarland from Narrangansett Bay, USA (2001), identified by light microscopy, and provided by J. Rines. Cultures of *Nitzschia cf longissima*, *Urosolenia* spp., and *Bacteriastrum hyalinum* are no longer viable, however DNA from each species is available.

Isolation of partial SIT sequence. Genomic DNA was isolated as described previously (Jacobs et al. 1992). Degenerate primers were designed based on conserved SIT sequences from *Cylindrotheca fusiformis* (Hildebrand et al. 1998) and *Thalassiosira pseudonana* (Armbrust et al. 2004). Degeneracy is denoted as follows: I = inosine; R = A,G; Y = C,T; M = A,C; W = A,T; The forward primer, SITdegF1, 5′-GGIRAYAAYY-TIGAYMGITA corresponding to amino acids GD/NNLDRY (residues 93–99 in *Cf*SIT1-5) was used in combination with one of the following reverse primers: SITdegR1, 5′-AA-IGCIATIGGRAAIGC (amino acids SAFPIAF, residues 381–387) or SITdegR2, 5′-GTICCIACRTAIWCYTCRTC (amino acids DEV/EYVGT, residues 428–434) to produce an 879 bp or 1 kbp PCR fragment, respectively. The PCR amplification was performed in an Ericomp Thermal Cycler in 50 µL reactions containing 100 ng genomic DNA template, 20 pmol of each primer, 10 mM dNTPs, 1× PCR buffer pH 8.3, and 2.5 U *Taq* DNA polymerase (Roche, Indianapolis, IN, USA). The following "touchdown" PCR protocol was used: 2 min at 96° C, 11 cycles consisting of 30 s at 96° C, 2 min at 60° C (lowering temperature by 2° C every cycle), 2 min at 72° C, followed by 30 cycles of 30 s at 96° C, 2 min at 40° C, 2 min at 72° C, and a final extension of 7 min at 72° C.

Isolation of full-length SIT sequence from genomic DNA. Inverse PCR (Ochman et al. 1988) was used to obtain 5′ and 3′ sequence for *SITs* from *Nitzschia alba* and *Skeletonema costatum*. Two micrograms of genomic DNA was digested with *Eco*RI, *Rsr*I, *Sal*I, *Xho*I, *Xba*I, or *Xmn*I and 100 ng of the restriction fragments were circularized in 100 µL reactions overnight at 12° C using 5 U of T4 ligase (Invitrogen, Carlsbad, CA, USA). The DNA was concentrated by precipitation and used as template in inverse PCR with the following primers: for *N. alba*, forward primer (NaF) 5′-TATGTATTCCTGAACC TTGCT and reverse primer (NaR) 5′-TCAAAATCATGGC AATACCAG; for *S. costatum*, forward primer (ScF) 5′-CCG CATAAGTTAATGATGAAGA and reverse primer (ScR) 5′-AATGAGGATGGCAACATCTTC. Once the 5′ and 3′ sequences were obtained, primers designed within the region flanking the open reading frame were used to amplify

TABLE 1. List of species used in this study.

Name	Abbreviation	Strain	No. and length of SITs
Pennates			
Cylindrotheca fusiformis Reimann et Lewin	*Cf*	CCMP343	SIT1-5 fl
Navicula pelliculosa (freshwater) de Brébisson) Hilse	*Np*FW	SAG1050-3	SIT1-6 ps
Navicula pelliculosa (marine) (Breb. et Kuetzing) Hilse	*Np*M	CCMP543	SIT1 ps
Nitzschia alba Lewin and Lewin	*Na*	CCMP2426	SIT1 fl, SIT2-4 ps
Nitzschia cf. *longissima*[b]	*N*spp		SIT1 ps
Phaeodactylum tricornutum Bohlin	*Pt*	CCMP1327	SIT1 ps
Bacillaria paxillifer (O.F. Muller) Hendey 1951		CCAP 1006/2	NA
Ditylum brightwellii (T. West) Grunow ex van Heurck 1883		CCAP1022/1	NA
Centrics			
Paralia sulcata (Ehrenberg) Cleve 1873	*Ps*	CCAP1059/1	SIT1 ps
Skeletonema costatum (Greville) Cleve	*Sc*	CCMP1281	SIT1 ps, SIT2 fl
Thalassiosira pseudonana (Hustedt) Hasle et Heimdal	*Tp*	CCMP1335	SIT1-3 fl
T. weissflogii (Grun.) Fryxell et Hasle	*Tw*	CCMP1336	SIT1-2 ps
Chaetoceros gracilis Pantocsek		LD2658	NA
Urosolenia[b] species			NA
Bacteriastrum hyalinum[b]			SIT1 ps[a]
Non-diatoms			
Synura echinulata Korschikov (silicoflagellate)		CCMP851	NA
Suberites domuncula (sponge)			NA

Name, abbreviations used in figures, and strain are shown (when available). For *Cf* and *Tp*, number of SITs identified represents total number found in these species as determined by library screening and genome sequencing, respectively (Hildebrand et al. 1998, Armbrust et al. 2004). For other species, number of SITs represent number cloned in this study and length indicates full-length (fl) or partial sequence (ps). NA indicates species that were tested, but in which SITs did not amplify.

[a]Indicates a small fragment (<300 bp) with SIT sequence similarity was found, but because of limited sequence information, was not used in this analysis.

[b]See Materials and Methods for source information.

CCMP, Center for Culture of Marine Phytoplankton; SAG, Culture Collection of Algae at Goettingen University; LD, AlgaeBase; CCAP, Culture Centre of Algae of Protozoa; SIT, silicon transporters.

full-length clones from genomic DNA. The primers used were: for *N. alba* (Na5′UTR) 5′-CTATCAACCGAACCA GAAATT and (Na3′UTR) 5′-ATCCAATCCGTACCATTGT GA; for *S. costatum*, (Sc5′UTR) 5′-CATTGCAGCATTGGAG AGTTC and (Sc3′UTR) 5′-CTAAAAGGGAACAAAATCTGC.

Cloning, sequencing, and analysis of partial and full-length SITs. The PCR products were electrophoresed in a 1% Tris borate agarose gel, excised, and gel purified using a Rapid Gel Extraction System (Marligen Biosciences Inc., Ijamsville, MD, USA). Products were cloned using a TOPO TA for Sequencing Kit (Invitrogen) and sequenced in from both ends with a BigDye® Terminator v3.1 Cycle Sequencing Kit (Applied Biosystems Inc., Foster City, CA, USA). Reactions were precipitated with isoproponal, dried, and sequenced by SeqXcel Inc. (San Diego, CA, USA) using an ABI PRISM® 3100-Avant Genetic Analyzer. Multiple clones from each species were sequenced. Sequence alignments were carried out using ClustalW (Thompson et al. 1994) at the NPS@ Web server (Combet et al. 2000). The 5′ and 3′ gaps were manually removed. A topology model was generated based on hydropathy plots using HMMTOP (Tusnády and Simon 2001). Coiled-coil motifs were predicted using COILS (Lupas et al. 1991).

Rapid amplification of cDNA ends (RACE) cloning of Thalassiosira pseudonana *SIT cDNAs*. RACE (Frohman et al. 1988) was used to verify the 5′ and 3′ *SIT* sequences obtained from genome sequencing of *T. pseudonana*. Cultures of *T. pseudonana* were synchronized (Frigeri et al. 2006) and total RNA was extracted using TriReagent (Sigma, St. Louis, MO, USA) as described (Hildebrand and Dahlin 2000). The 3′ RACE was performed using a 3′ RACE kit (Life Technologies, Bethesda, MD, USA), but using a 3′ Adapter from a First Choice™ RLM-RACE kit (Ambion Corp, Austin, TX, USA) that would allow a nested PCR to be performed. First round PCR amplification was carried out using the 3′ Outer Primer from the First Choice™ RLM-RACE kit and one of the following SIT-specific primers: TpSIT1-3-2′ (5′-TATCTT CACATGCATCCTTGGG), TpSIT2-3-2′ (5′-CATCTTCACG TGCATTCTCGGA), or TpSIT3-3-2′ (5′-CTACCACAAATC ATTGAAGAG). Nested PCR was performed using the outer PCR product as template, the 3′ Inner Primer from the First Choice™ RLM-RACE kit, and one of the following SIT-specific primers: TpSIT1-3′ (5′-ACATCCTTTCTGCCGTCA GT), TpSIT2-3′ (5′-ACATCCTTGCTGCTGTATCC), or TpSIT3-3′ (5′-GACGTCCAAGATGCGAAGAG).

The 5′ RACE was performed using a First Choice™ RLM-RACE kit, with the following modifications: SuperScript II (Life Technologies) was used with the primer Tp5′RT (5′GAAGTAGTTGTTGATRAARTCAATCAT, where R is A or G) for cDNA synthesis. This primer is complementary to all three *TpSITs*. PCR amplification was carried out using the 5′ Inner Primer from the First Choice™ RLM-RACE kit and one of the following SIT-specific primers: TpSIT1-5′-3 (5′-TGGCTATCCTTGTAAAGATCA), TpSIT2-5′-3 (TGGCTGT CTTTGTAGAGGGTG), or TpSIT3-5′-3 (5′-CTCCTTATAA ACCAAGTGATC). The PCR products were electrophoresed, gel purified, and cloned as described above.

IntraCompare (IC) analysis. AveHAS (Zhai and Saier 2001) was used to predict average hydropathy of the 10 full-length SIT sequences. IC (Zhai and Saier 2002) was used to determine homology between the first half and second half of the SITs. Statistical significance is reported as comparison scores in standard deviations (SD).

Phylogenetic analyses. Silicon transporter amino acid sequences were aligned with Clustal X (Chenna et al. 2003) using the Gonnet matrix and default penalties for gap opening and gap extension. Minor adjustments were made to minimize the overall number of indels in similar regions of the alignment, biasing gap extension rather than gap opening. For nucleotide sequences, intron sequences were removed before alignment with Clustal X. Default values for gap opening and gap extension were used, and several manual adjustments were made to ensure that gaps did not interrupt the reading frame and that gaps in the nucleotide alignment corresponded to gaps in the amino acid alignment. Nucleotides were deleted from 5′ and 3′ ends until there were data for at least 50% of the sequences in those regions. All phylogenetic analyses were based on the nucleotide alignment. ModelTest was used to determine that $TrN+I+\gamma$ was an appropriate model of sequence evolution. Subsequent maximum likelihood (ML) analyses were identical to those for the 18S rDNA alignment.

Fixed effects likelihood (FEL) analysis was used to estimate rates of non-synonymous (dN) and synonymous (dS) substitutions to identify codons under positive ($dN/dS>1$), negative ($dN/dS<1$), or neutral ($dN/dS=1$) evolution (Goldman and Yang 1994, Muse and Guat 1994). Kosakovsky Pond and Frost (2005b) recommend FEL for detecting selection on data sets of intermediate size (20–40 sequences) because it has a lower false-positive rate than random effects likelihood methods and greater statistical power than counting methods.

Using the two-rate FEL method, non-neutral evolution was tested on all branches of the ML tree by estimating dN/dS and adjusting dS across sites. For this analysis, a non-standard nucleotide substitution model (012032) was chosen from among 203 possible models with the model selection tool implemented on www.datamonkey.org Kosakovsky Pond and Frost (2005a).

Based on their long-branch lengths, some SIT paralogs appeared to be evolving differently from other paralogs in the genome. HyPhy was used to test whether these branches differed from the rest of the tree in their non-synonymous rate of nucleotide substitution. For these analyses, the entire tree is first fitted with a single dN, then the branch of interest is fitted with its own dN and the rest of the tree with a different dN. A likelihood ratio test is used to determine which model provides a better fit to the data set. A significant result ($P<0.05$) allows one to reject the null hypothesis, in this case that all branches share the same dN. Both synonymous and non-synonymous rates were allowed to vary across sites using four rate classes and the same nucleotide substitution model as the FEL analysis. All analyses to detect selection on codons or branches were performed with the HyPhy software package (Kosakovsky Pond et al. 2005).

Southern Blot. Genomic DNA was digested, electrophoretically separated on 0.7% agarose gels, and transferred to Hybond-N membranes (Amersham, Piscataway, NJ, USA) according to standard procedures (Sambrook and Russell 2001). Blots were probed with a mixture of 1 kbp PCR products of *ScSIT1* and *Np*M*SIT1*, labeled by random priming with ^{32}P-dCTP using a PrimeIt II™ kit (Stratagene Inc. Carlsbad CA, USA). Hybridization was carried out in 6× SSC (1× SSC is 50 mM NaCl, 15 mM NaCitrate, pH 7.0), 0.05× BLOTTO (Johnson et al. 1984), at 62.5° C with 1×10^6 cpm·mL^{-1} of labeled probe for 18 h. Washes were carried out twice for 30 min each in 2× SSC, 0.1% SDS at 62.5° C, then the blot was exposed to X-ray film.

Accession numbers. Sequence data from this study have been deposited in the GenBank data library under the accession numbers DQ256050 (*PtSIT1*), DQ256051–DQ256056 (*Np*FW*SIT1-6*), DQ256057 (*Np*M*SIT1*), DQ256058–DQ 256061 (*NaSIT1-4*), DQ256062 (*Nspp*SIT1), DQ256063 (*PsSIT1*), DQ256064–DQ256065 (*ScSIT1-2*), DQ256066–DQ256068 (*TpSIT1-3*), DQ256069–DQ256070 (*TwSIT1-2*).

RESULTS

Isolation and analysis of partial SIT sequences. To identify members of the *SIT* gene family, degenerate

PCR primers were designed based on conserved regions in the five *Cf*SITs and the three *Tp*SITs. Diatom species used in this study were chosen because they encompassed a diverse array of features, including morphology (centric vs. pennate), salt tolerance (marine vs. fresh water), and silicon metabolism (differences in silicic acid uptake rates and soluble silicon pools. Using genomic DNA from these evolutionarily diverse diatoms, PCR was used to amplify 879 bp or 1 kbp DNA fragments which were then cloned. Multiple clones from each species were sequenced to identify paralogs in the gene family. A total of 16 partial and two complete *SIT* sequences from eight taxa were identified (Table 1) with this approach. Other diatom and non-diatom species were tested, but PCR amplification failed to yield a product (Table 1).

Predicted amino acid sequences were aligned and analyzed using CLUSTAL W (Fig. 1). For simplicity, only one representative SIT is shown for each taxon, with the exception of *T. pseudonana*, which has one highly divergent SIT compared with the others. Analysis of the overlapping region (residues 166–452) showed 19% identity and 40% similarity (identical plus conserved substitutions). Among centric species, there was 35% identity and 65% similarity. The SITs from pennate species showed 34% identity and 69% similarity. Pairwise comparisons of each SIT showed the proportion of identical residues between two SITs ranged from 49% to 99%; similar residues ranged from 73% to 100% (data not shown).

Maximum likelihood analysis of 18S rDNA sequences resulted in a species phylogeny that was congruent with previous phylogenetic analyses of diatoms (data not shown; Medlin and Kaczmarska 2004, Alverson and Theriot 2005). The gene tree, based on phylogenetic analysis of the 26 *SIT* nucleotide sequences (Fig. 2), is unrooted because there are no known SIT homologs outside of diatoms.

Fixed affects likelihood analysis identified 254 codons that were evolving under negative (purifying) selection ($dN/dS<1$; $P<0.1$). The remaining 92 sites had varying dN/dS values, none of which were statistically significant. Although three sites showed some evidence of positive selection ($dN/dS>1$; sites 40, 77, and 129), they were not statistically significant.

Based on branch lengths, *TpSIT3*, *Np*FW*SIT6*, and *Np*M*SIT1* appear to be evolving at elevated rates compared with other *SIT*s. Likelihood ratio tests showed branches leading to *TpSIT3* ($P = 0.063$) and *Np*FW*SIT6* ($P = 0.055$) were evolving under a significantly different dN than the rest of the tree, whereas *Np*M*SIT1* was not ($P = 0.83$).

Isolation and analysis of full-length SIT sequences. Based on genomic sequence, the three SITs from *T. pseudonana* appeared to have a longer N-terminus, and a C-terminus that lacked the predicted coiled-coil motif found in *Cf*SITs. Using RNA from synchronized *T. pseudonana* cultures, 5′ and 3′ RACE was carried out to evaluate these structural features. The 3′ RACE confirmed the lack of a coiled-coil motif in each of the three TpSITs. The 5′ RACE confirmed the predicted start codon for *TpSIT2*, but the start codon for *TpSIT1* was found to be 63 amino acids downstream of that predicted in the genome sequence. The 5′ RACE for *Tp*SIT3 was unsuccessful despite several attempts. Genome sequence data identified two in-frame methionine residues in *Tp*SIT3 located 13 and 34 residues upstream of the start methionine for *Tp*SIT1 and *Tp*SIT2, respectively, but it is unclear which, if either, is the start codon.

Inverse PCR was used to obtain the entire coding sequence for *SIT* genes in the pennate diatom, *N. alba*, and the centric diatom, *S. costatum*. The *NaSIT1* gene contained an open-reading frame of 1647 bp, and *ScSIT2* had a 1524 bp open-reading frame. Because these sequences were obtained from genomic DNA, they may not represent the full-coding region; however, there was strong agreement between the location of both the predicted start and stop codons with *SIT*s from *C. fusiformis* and *T. pseudonana* (Fig. 1). Furthermore, diatom introns are generally small (Armbrust 2000, Hildebrand and Dahlin 2000, Davis et al. 2005), and analysis of upstream and downstream sequences did not reveal any consensus intron splice junctions. As seen with *Cf* and *Tp* SITs, *Na*SIT1 and *Sc*SIT2 each contained 10 predicted TMS. The C-terminus of *Na*SIT1 was predicted to form a coiled-coil motif, whereas the C-terminus of *Sc*SIT2 was not. Amino acid alignment of the 10 available full-length SITs showed 34% amino acid identity and 62% similarity. Pairwise comparisons of each of these SITs showed 43% to 92% amino acid identity and 71% to 96% similarity (data not shown).

Average hydropathy was predicted for the full-length SIT sequences (data not shown) to delineate TMS. Based on this plot, the SITs were cut into two halves of five TMS, and the two halves were compared

FIG. 1. Predicted amino acid alignment of full-length and partial silicon transporter (SIT) sequences. For simplicity, only one representative SIT from each species is shown (but the analysis for conserved residues included all available SIT sequences), with the exception of *Tp*SIT3, which is divergent from *Tp*SIT1 and *Tp*SIT2. Amino acid alignment number is denoted on the right. Bars and circled numbers above sequences denote predicted transmembrane segments. Asterisks (*) below sequence indicate identical amino acids. Colons (:) and dots (.) denote strongly and weakly similar substitutions, respectively. Number symbol (#) denotes residues that are identical in areas where SIT sequence from some species has not been determined. Dashes indicate gaps and regions where sequence data is not available. Shaded residues are conserved hydroxylated amino acids. Boxed residues are conserved amine-containing amino acids. Residues in bold are conserved charged residues. Underlined cysteines are those conserved in most SIT sequences. Underlined italicized residues near the C-terminus indicate regions with a high probability of forming coiled-coils, as predicted by COILS (Lupas et al. 1991) using a window of 28 residues and a probability of >50%.

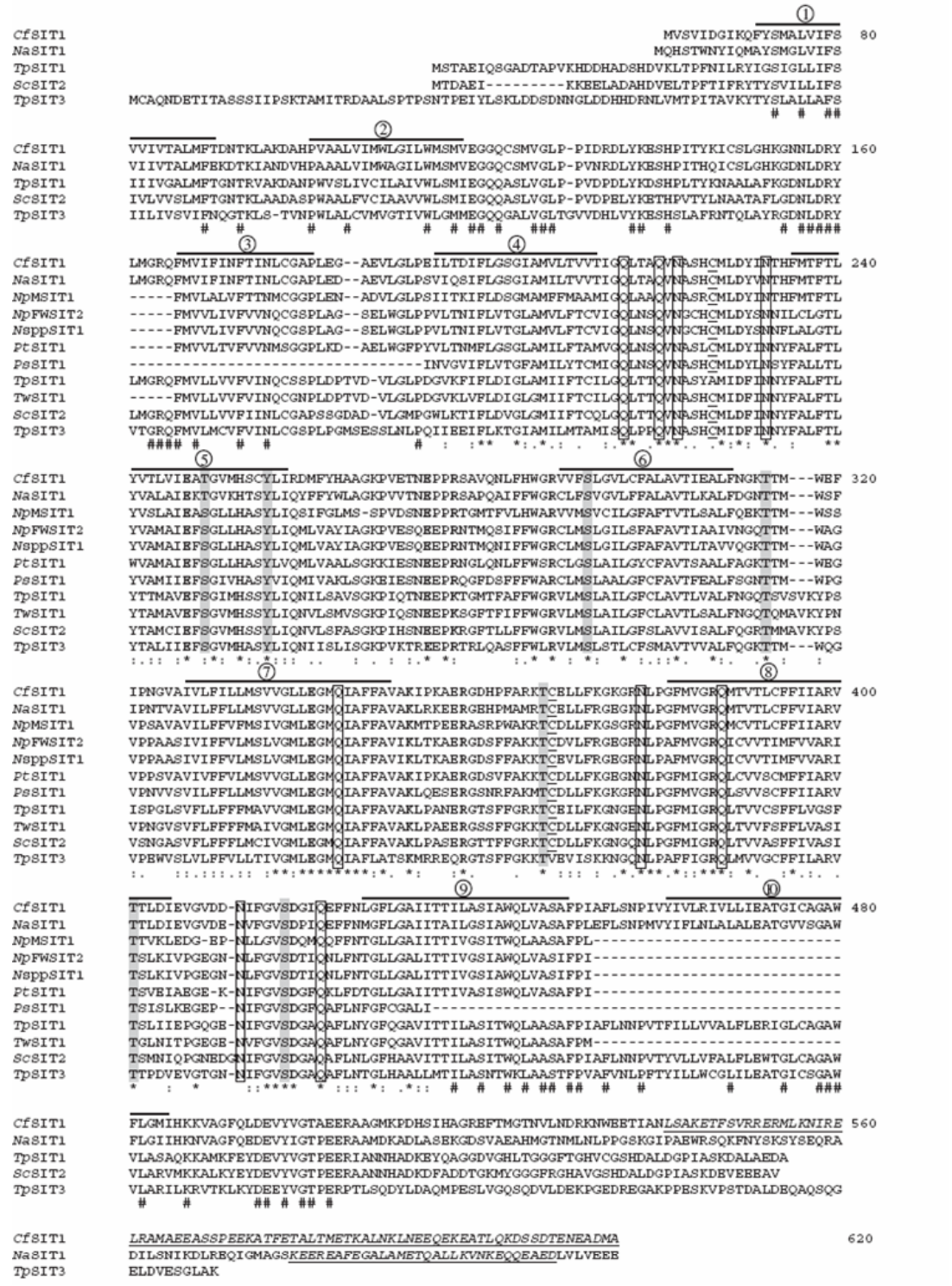
CfSIT1
NaSIT1
TpSIT1
ScSIT2
TpSIT3
NpMSIT1
NpFWSIT2
NsppSIT1
PtSIT1
PsSIT1
TwSIT1

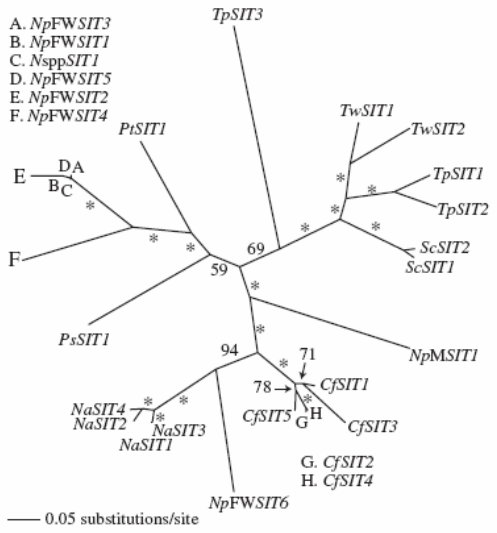

FIG. 2. Unrooted maximum likelihood tree of 26 silicon transporter (SIT) nucleotide sequences. − ln L = 12919.07; estimated base frequencies: A = 0.21, C = 0.29, G = 0.23, T = 0.26; rate matrix: A–C = 1.0, A–G = 2.18, A–T = 1.0, C–G = 1.0, C–T = 2.92, G–T = 1.0; shape parameter [α] for γ distribution = 1.07; proportion of invariant sites = 0.16. Branch labels are bootstrap proportions, with values of at least 95% shown with an asterisk (*).

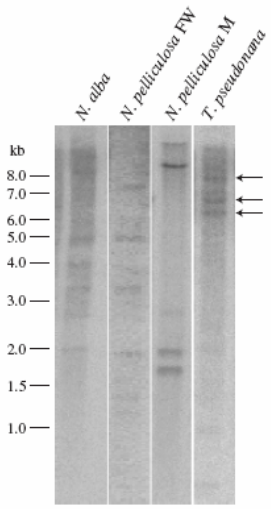

FIG. 3. Southern hybridization analysis of *Nitzschia alba*, *N. pelliculosa* FW, *N. pelliculosa* M, and *Thalassiosira pseudonana* using silicon transporter (SIT)-specific probes. Genomic DNA was digested with *Xba*I (for *N. alba* and *N. pelliculosa* M) or *Sal*I (for *N. pelliculosa* FW and *T. pseudonana*). Molecular size markers (kb) are shown on the left. Arrows on the right denote bands detected in *T. pseudonana*.

with each other. Comparison scores of 10–39 SD were obtained for all combinations tested (data not shown). Because a value of 9 SDs corresponds to a probability of 10^{-19} that the degree of similarity arose by chance (Doolittle 1987), the first halves of the SITs were considered homologous to the second halves.

Overall SIT gene structure. As seen with *CfSITs*, *SITs* from *N. alba*, *P. sulcata*, *P. tricornutum*, *T. weissflogii*, *S. costatum*, *N. pelliculosa* M, and one of the six from *N. pelliculosa* FW (*Np*FW*SIT6*) did not have introns. In contrast, *SITs* from *T. pseudonana*, *N.* spp., and five of the six from *N. pelliculosa FW* (*Np*FW*SIT1-5*) each contained a single predicted or experimentally verified intron ranging in size from 92 to 124 bp. Introns in *TpSIT1-3* were identified by comparison of cDNA and genomic DNA, whereas for other species introns were identified based on amino acid alignment and conserved eukaryotic intron splice junctions at the 5′ and 3′ ends of the intron (Mount 1982, Senapathy et al. 1990). The intron in *NsppSIT1*, *NpFWSIT1-5*, and *TpSIT3* was located in roughly the same position, 473 bases downstream of the start codon predicted by genome sequence data for *TpSIT3*. In contrast, the intron for *TpSIT1* and *TpSIT2* was located 222 bases downstream of their start codon. Intron location corroborated phylogenetic results, which suggested *Tp*SIT1 and *Tp*SIT2 were related through a relatively recent lineage-specific gene duplication (Fig. 2).

In addition to the two *SITs* found in *T. weissflogii*, a putative pseudogene was identified. The pseudogene sequence was identical to *TwSIT1*, but had a 32-base deletion in the first half of TMS five that introduced a downstream stop codon. This deletion was confirmed by PCR using a primer designed against the 5′ and 3′ sequence flanking the gap and an upstream primer.

Southern hybridization analysis. A blot containing digested genomic DNA from *N. alba*, *N. pelliculosa* FW, *N. pelliculosa* M, and *T. pseudonana* was probed with a combination of *ScSIT1* and *Np*M*SIT1* (Fig. 3). Multiple bands of various sizes were revealed in each species, consistent with the presence of multiple *SITs* within a genome. *T. pseudonana* had three distinct bands (Fig. 3), consistent with genome sequence data. Although only one *SIT* in *N. pelliculosa* M was identified by PCR, Southern analysis suggested more were present (Fig. 3). Six *SITs* were identified in *N. pelliculosa* FW by PCR and confirmed by Southern analysis (Fig. 3).

DISCUSSION

Diatom species contain multiple SIT genes. Using degenerate PCR primers, we amplified sizable portions of *SIT* sequences from eight previously unexamined diatom species. Although no attempt was made to isolate all *SITs* from a given species, multiple clones were sequenced to determine if distinct *SIT* paralogs were present in the genome. With the exception of *N. pelliculosa* M, *P. sulcata*, and *P. tricornutum*, multiple

SIT genes were identified by PCR in each species. Southern analysis further supported the presence of multiple *SITs* within species.

Simultaneous PCR amplification of different genes within the same gene family can result in PCR recombination, which produces a product that is a chimera of two distinct genes. The frequency of PCR-mediated recombination can vary depending on a number of factors (Bradley and Hillis 1997, Judo et al. 1998, Qiu et al. 2001, Cronn et al. 2002). Based on these studies, we used PCR conditions to minimize chimera formation, including low template concentration, low-fidelity *Taq* polymerase, and a minimal number of PCR cycles. Although no method can completely eliminate chimera formation, we found no evidence for PCR recombination in the SITs identified.

The degenerate primers designed for this study were not universal because they did not produce a PCR product in all species tested, nor were they able to amplify all *SITs* from a given species (e.g. in *T. pseudonana,* only *SIT1* and *SIT2* were amplified). Attempts to amplify *SIT* homologs from other silicifying organisms, including a silicoflagellate and sponge primmorphs, were unsuccessful. As one of the goals of this study was to identify conserved amino acids necessary for function, SITs less conserved would be of particular interest. Screening genomic libraries may have allowed us to identify more distantly related SITs with the advantage of providing full-length clones, but this approach is far more labor intensive, and our PCR-based survey still provided the data necessary for a thorough comparative sequence analysis of SITs. Our greatly expanded sampling of SIT sequences showed that the overall percent identity is 19%, which is at the low end of what is considered significant for this length in a family of proteins (Doolittle 1987, Pearson 1997). Considering that only particular types of amino acids (as discussed below) are likely to have possible interactions with silicic acid, the number of conserved residues has been reduced to a manageable level for future studies to directly determine their involvement in transport.

SIT evolution. As the success of diatoms is in part due to their ability to utilize silicon, SITs have played an important role in diatom evolution. But, how did SITs themselves evolve? To date, SITs have no described homologs in other organisms, and the additional sequence data obtained in this study, which included *SITs* from one of the earliest branching lineages in the diatom phylogeny (*P. sulcata*), failed to identify any. More powerful than comparing individual sequences is an iterative program called PSI-BLAST, which uses a position-specific score matrix (PSSM) to search a data base for distantly related proteins (Altschul et al. 1997). The PSSM is generated by combining statistically significant alignments identified through BLASTP. A PSSM of 26 partial SIT sequences was generated and used to search the data base for proteins with similar sequence. The top hits were to *Cf*SITs, as expected. Unfortunately, no other significant hits were obtained. Another search of the data base was performed using a PSSM generated from the 10 available full-length SITs, but again, no significant hits were obtained.

The IC analysis of full-length SIT sequences showed homology between the two halves of the SITs, suggesting the protein is comprised of two repeat units, each composed of five membrane spanning segments. This suggests that SITs evolved either by dimerization of two monomers or by internal gene duplication (Fersht 1985, McLachlan 1987, Saier 2003). Intragenic duplication has been documented for a number of membrane transporter proteins (Rubin et al. 1990, Reizer et al. 1993). Proteins comprised of two halves gain complexity over their monomeric component by having an increased range of function, the ability to occupy different subcellular locations, or a wider range of substrate affinity or specificity (Saier 1994). The BLASTP search using each half of the SIT did not yield significant hits to identify the ancestral monomer. Although these results are interesting because they further demonstrate that SITs represent a completely novel family of transporters, they also add to the mystery of how SITs evolved.

A putative pseudogene was identified in *T. weissflogii*. A pseudogene was previously reported in *C. fusiformis* (Hildebrand et al. 1998). Because pseudogenes are unconstrained by evolutionary pressure, they are often considered molecular fossils (Zhang and Gerstein 2004) and analysis of pseudogenes can provide insightful information to the evolutionary history of a gene family (Zhang and Gerstein 2003, D'Errico et al. 2005). However, additional pseudogenes will need to be identified for an accurate picture of SIT evolution to be reconstructed.

In general, *SIT* types from a single species (paralogs) were more closely related to each other than to *SITs* from other species. For example, *SITs* from *C. fusiformis*, *N. alba*, *S. costatum*, and *T. weissflogii* were monophyletic with strong bootstrap support ($\geq$ 95%). In one case, closely related orthologs were detected from somewhat distantly related species (*N*spp*SIT1* nested within a clade of *Np*FW*SITs*). The divergence between *N*spp*SIT1* and *Np*FW*SIT1, SIT3*, and *SIT5* was remarkably small considering the distance between these two species in the 18S-based phylogeny. The *Np*M*SIT1* gene was orthologous to *CfSIT1-5* and was presumably related to *Np*FW*SITs* through an ancient gene duplication. A few highly divergent SIT types were recovered from *T. pseudonana (SIT3), N. pelliculosa* FW (*SIT4* and *SIT6),* and *N. pelliculosa* M (*SIT1),* as evidenced by their relatively long branches and distant relationship to other SIT paralogs from the same genome. These divergent SITs are either ancient SIT types that have had a long time to evolve, or they have evolved more rapidly than other paralogs in the genome, suggesting they may have a distinct function from other SITs.

Presence of multiple SIT types within a genome raises the question of their possible roles in silicon transport, and selective pressures leading to diver-

gence of their sequences. Silicon transporter paralogs may differ in affinity or capacity for transport, and multiple gene copies could allow fine control. Different SITs could be expressed at different times or levels, or there may just be functional redundancy. Some members of transporter families act as sensors and do not actively transport their substrate (Forsberg and Ljungdahl 2001). It is unknown whether the SITs are localized solely to the plasma membrane, or if they are also found in other parts of the cell. Diatoms contain silica deposition vesicles where soluble silicon is polymerized into silica to form the new cell wall (Drum and Pankratz 1964, Pickett-Heaps et al. 1990). Some SITs could be localized in the silicalemma to transport silicon into the silica deposition vesicle, and such SITs would operate in a very different environment than those localized to the plasma membrane.

A number of other factors could be contributing to the evolution of SITs. For example, K_s values for silicic acid uptake is generally lower in centrics than pennates (Martin-Jézéquel et al. 2000). There are also several important differences in silicon physiology of marine versus freshwater diatoms (Martin-Jézéquel et al. 2000, Hildebrand and Wetherbee 2003), including ionic coupling (Olsen and Paasche 1986), the higher availability of silicic acid in freshwater than marine habitats, and the greater extent of silicification in freshwater diatoms (Conley and Kilham 1989). All of these are potentially important factors shaping SIT evolution, although no clear correlation between amino acid substitutions and environmental habitat were found among the species examined.

Analysis of SIT structure. There is no definitive prediction of SIT topology. Analysis indicates the modern SIT structure was derived from a precursor with a single domain of five membrane spanning segments that became duplicated, resulting in 10 membrane spanning segments with the two halves in inverted orientations in the membrane, similar to what has been shown for the *Escherichia coli* YrbG transporter (Sääf et al. 2001). However, the locations of the N- and C-termini are not clear. The positive-inside rule predicts that positively charged amino acids are more abundant on the cytoplasmic side of membrane proteins (von Heijne 1992). Based on this rule, the N-terminus of SITs is predicted to be extracellular. On the other hand, SPLIT 4.0, a program that analyzes clusters of basic residues in addition to the positive-inside rule (Juretić et al. 2002), predicts that SITs have a cytoplasmic N-terminus. Our current hypothesis is that the N- and C-termini of SITs are intracellular. This hypothesis is based, in part, on the C-terminal coiled-coil motif in *Cf*SIT1-5 and *Na*SIT1. The vast majority of coiled-coil motifs are intracellular, and the few proteins with extracellular coiled-coils are generally associated with the extracellular matrix (e.g. laminins, fibrinogens, and lectin; Kammerer 1997). Regardless, direct experimental data are necessary to resolve SIT topology.

Comparison of full-length SITs from the pennate diatoms, *C. fusiformis* and *N. alba*, with SITs from the centric diatoms, *T. pseudonana* and *S. costatum*, revealed the absence of a C-terminal coiled-coil motif in SITs from the centric diatoms. Coiled-coil motifs are involved in protein–protein interactions. The coiled-coil motif in the cobalamin transporter of *E. coli* delivers colicin to a neighboring membrane protein for translocation (Kurisu et al. 2003). The coiled-coil motif at the C-terminus of the *E. coli* transporter, ProP, is an osmosensor that activates transport of osmoprotectants (Culham et al. 2000). Although the exact role of the coiled-coil motif in SITs is unclear, its absence from centric diatoms, which are basal in diatom phylogeny, suggests the ancestral SIT type lacked a coiled-coil motif. Whatever the role of the coiled-coil motif in SITs may be, lack of this structure in the centric diatom SITs suggests that either its function is unnecessary in centrics, or that it is accomplished through another mechanism. Admittedly, our taxonomic sampling is sparse and more full-length SITs from a greater diversity of diatom species are necessary to determine whether this is a general trend between pennates and centrics.

Comparison of amino acid identity in distinct portions of SITs revealed regions of higher and lower overall conservation. Of the hydrophilic loops, the lowest percent conservation was between TMS 6 and 7 (5.5%), and the highest was between TMS 2 and TMS 3, and TMS 4 and 5 (both at 38%). Of the TMS, TMS 7 and 9 had the highest conservation at 46% and 38%, respectively, and TMS 2, 4, and 6 had the lowest, at 22, 21, and 20%, respectively. Other regions ranged from 8% to 30% conservation. The longest stretch of consecutively conserved residues was located at the 3′ end of TMS 7 (residues VGXLEGMQIAF at position 337–347, where X is M or L).

As discussed in the introduction, specific types of amino acids could be likely to interact with silicic acid, including cysteines, amine-containing or hydroxylated amino acids, or charged residues. Analysis of SITs obtained in the study as well as three previously identified SITs (from *S. acus*, accession no. AF492011; *P. tricornutum*, accession no. BI307735; *C. muelleri*, (Sherbakova et al. 2005), revealed conserved residues of these types that may be important for function (Fig. 1). In overlapping regions where there was coverage by at least 75% of SITs, 11 conserved hydroxyl-containing amino acids (Ser, Thr, Tyr) and 12 charged or amine-containing amino acids (Asn, Gln, Arg, His, and Lys) were found. Of these 23 conserved residues, 12 were found in or near (within two residues) a TMS. As passage of silicic acid must occur through the TMS, these 12 residues are of particular interest. Although no conserved cysteines were found, Cys-226, which lies within the fourth hydrophilic loop and Cys-368, which lies within the seventh hydrophilic loop, were found in the majority of SITs. Cys-226 corresponds to the Cys residue that has been proposed to serve as a zinc-binding domain to coordinate SITs and silicic acid

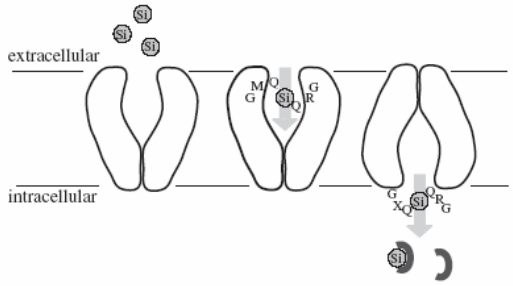

FIG. 4. Proposed model of silicon transport. From left to right is a generalized schematic of sequential silicon transporter (SIT) conformational changes that occur during silicic acid uptake. The outward-facing conformation (left) facilitates interaction with extracellular silicic acid, which is coordinated through hydrogen bonding by two conserved glutamines (center) located in transmembrane segment (TMS) 7 and 8. A conformational change to an inward-facing conformation is induced (right), which allows silicic acid to bind to two additional conserved glutamines located in the hydrophilic loop between TMS 2 and 3. This releases silicic acid into the cell, where it can be bound by as yet uncharacterized intracellular binding components, denoted as horseshoe-shaped structures.

(Sherbakova et al. 2005). The rationale for this hypothesis is in part based on an earlier study describing the effect of zinc on silicon transport in *T. pseudonana* (Rueter and Morel 1981). However, analysis of *Tp*SIT1-3 showed that although this Cys residue was conserved in *Tp*SIT3, it was replaced by Ala in *Tp*SIT1 and *Tp*SIT2. It has been hypothesized that the Ala substitution would abolish SIT uptake activity and that SITs containing this residue would only be involved in efflux of silicic acid (Grachev et al. 2005). However, experimental data on the expression of each *TpSIT* thoughout the cell cycle (unpublished data) are not consistent with *Tp*SIT1 and *Tp*SIT2 being involved only in efflux.

A model for silicon transport. The most common mechanism associated with substrate translocation by secondary membrane transporters is the alternating access model in which the transporter alternates between an inward-facing and outward-facing conformation to enable passage of the substrate across the membrane (Tanford 1983, West 1997, Huang et al. 2003). We propose a similar mechanism of silicic acid transport by SITs (Fig. 4). Based on this mechanism and the data obtained in this study, a general mechanistic model for silicic acid transport can be formulated. While this model is solely based on sequence analysis and not direct experimental data, it will provide a basis for future experimental testing.

Examination of SIT sequences revealed a conserved sequence motif, GXQ, where X is Q, G, R, or M, located in four distinct regions of the protein (Fig. 5). Two of these motifs are located in predicted TMS 7 and 8 and are anchored by highly hydrophobic patches located approximately one-third of the way from the extracellular face (Fig. 5). The other two are in the hydrophilic region between TMS 2 and 3. We propose that the carbonyl group alone or the carbonyl and amine groups on the side chain of the conserved glutamine residues are responsible for coordinating one or two hydroxyls, respectively, of silicic acid via hydrogen bonding, and that full coordination of a single silicic acid molecule (either two or four hydrogen bonds) occurs via the two separated glutamines located in TMS 7 and 8, and similarly with the two glutamines near TMS 2 and 3 (Fig. 4). Sequence analysis shows the glutamines within both coordination sites are closely aligned.

The driving force for silicic acid uptake in marine diatoms is co-transport with sodium (Bhattacharyya and Volcani 1980). Examination of the structure of other sodium-coupled transporters revealed no conserved sequence involved in the interaction with sodium; in some cases several amino acids located in distant regions of the protein are involved in coordination (Hunte et al. 2005, Yamashita et al. 2005). Thus, it was not possible to identify or model similar residues in the SITs.

Regarding the silicic acid uptake mechanism, at least two general mechanisms can be considered. In

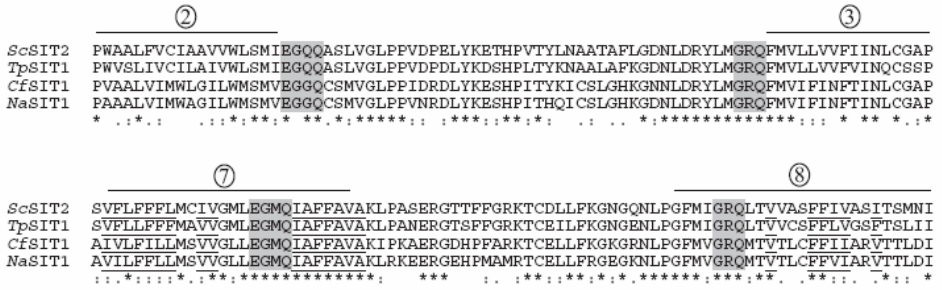

FIG. 5. Alignment of amino acids in the regions proposed to coordinate silicic acid. Predicted transmembrane segments (TMS) are denoted by bars and circled numbers. Asterisks (*), colons (:), and dots (.) denote identical, strongly similar, or weakly similar residues, respectively. Shaded residues denote the conserved regions proposed to directly coordinate silicic acid. Hydrophobic residues in TMS 7 and 8 are underlined.

the first, a conformational change is induced by binding of silicic acid and sodium. Binding of silicic acid (by TMS 7 and 8) and sodium (at an unknown location) to an outward-facing transporter would induce a change to the inward-facing conformation, releasing silicic acid into the cell via the conserved glutamine residues located near TMS 2 and 3 (Fig. 4). Silicic acid then becomes bound by proposed intracellular complexing components that enable maintenance of high levels of soluble silicic acid without auto-polymerization (Fig. 4; Hildebrand 2000). In this scenario, there would be no direct control over transport; whenever extracellular silicic acid was available, the transporter would be active, and excess intracellular silicic acid would be effluxed. An energetic drawback to this would be that sodium would have to be continually pumped out of the cell. The second mechanism is based on observations indicating that silicic acid transport is tightly coupled with silica deposition in the cell wall (Conway and Harrison 1977, Hildebrand and Wetherbee 2003), suggesting that an intracellular component (as yet uncharacterized) may affect the transport properties of SITs. This component would induce a conformational change in SITs only when additional silicic acid was needed by the cell. This would result in tighter control over uptake, with less energy expended pumping out excess sodium. Data suggest that silicic acid efflux occurs after accumulation of excess uncomplexed silicic acid in the cytoplasm (unpublished data). Efflux may occur via a similar mechanism to uptake, but in the reverse. However, the role of sodium in efflux is unclear.

Although the model does not address all details of silicic acid transport, such as the nature of the sodium binding site, and possible involvement of cysteines (Lewin 1954, Sullivan 1976) or zinc (Rueter and Morel 1981), it describes the salient features of silicic acid interaction with the SITs and is consistent with all known aspects of silicic acid uptake, efflux, and regulation. More importantly, this model provides a basis for future studies using site-directed mutagenesis and heterologous SIT expression to experimentally test the role of the proposed GXQ coordination sites.

We would like to thank Luciano Frigeri for technical assistance. Thank you to Nils Kroger for supplying DNA from *Synura echinulata*, Werner E. G. Muller for *Suberites domuncula* primmorph cDNA, Jan Rines for *Bacteriastrum hyalinum* culture, and Edward Theriot for *Urosolenia* sp. culture. *Navicula pelliculosa* CCMP543 was provided as part of a collaborative project with Sandra Hazelaar and Winfried W. C. Gieskes. We appreciate comments on the manuscript by Michael Latz. We would also like to thank Milton Saier, Jr., Ravi Barabote, and Kalani Niheu for assistance with computer analyses. Margo Haygood, Michael Latz, and Brad Tebo generously allowed use of lab space and equipment. This work was supported by the Air Force Office of Scientific Research MURI grant RF00965521 (M. H.), the Center for Environmental BioInorganic Chemistry (M. H.), Art Proceeds Fellowship (K. T.), the David Freeman Memorial Fund (K. T.), and NSF PEET grant DEB 0118883 (A. J. A.). Genomics equipment was purchased through NSF grant DBI 0115801. K. T. was supported in part by the SIO Graduate Department.

Altschul, S. F., Madden, T. L., Schaffer, A. A., Zhang, J., Zhang, Z., Miller, W. & Lipman, D. J. 1997. Gapped BLAST and PSI-BLAST: a new generation of protein database search programs. *Nucleic Acids Res.* 25:3389–402.

Alverson, A. J. & Theriot, E. C. 2005. Comments on recent progress toward reconstructing the diatom phylogeny. *J. Nanosci. Nanotechnol.* 5:57–62.

Armbrust, E. V. 2000. Structural features of nuclear genes in the centric diatom *Thalassiosira weissflogii*. *J. Phycol.* 36:942–6.

Armbrust, E. V., Berges, J. A., Bowler, C., Green, B. R., Martinez, D., Putnam, N. H., Zhou, S., Allen, A. E., Apt, K. E., Bechner, M., Brzezinski, M. A., Chaal, B. K., Chiovitti, A., Davis, A. K., Demarest, M. S., Detter, J. C., Glavina, T., Goodstein, D., Hadi, M. Z., Hellsten, U., Hildebrand, M., Jenkins, B. D., Jurka, J., Kapitonov, V. V., Kröger, N., Lau, W. W. Y., Lane, T. W., Larimer, F. W., Lippmeier, J. C., Lucas, S., Medina, M., Montsant, A., Obornik, M., Parker, M. S., Palenik, B., Pazour, G. J., Richardson, P. M., Rynearson, T. A., Saito, M. A., Schwartz, D. C., Thamatrakoln, K., Valentin, K., Vardi, A., Wilkerson, F. P. & Rokhsar, D. S. 2004. The genome of the diatom *Thalassiosira pseudonana*: ecology, evolution, and metabolism. *Science* 306: 79–86.

Bhattacharyya, P. & Volcani, B. E. 1980. Sodium dependent silicate transport in the apochlorotic marine diatom *Nitzschia alba*. *Proc. Natl. Acad. Sci.* 77:6386–90.

Bradley, R. D. & Hillis, D. M. 1997. Recombinant DNA sequences generated by PCR amplification. *Mol. Biol. Evol.* 14:592–3.

Carlisle, E. M. 1978. Essentiality and function of silicon. *In* Bendz, G. & Lindqvist, I. [Eds.] *Biochemistry of Silicon and Related Problems*. Plenum Press, New York, pp. 231–53.

Carlisle, E. M. 1981. Silicon in bone formation. *In* Simpson, T. L. & Volcani, B. E. [Eds.] *Silicon and Siliceous Structures in Biological Systems*. Springer-Verlag, New York, pp. 69–94.

Chenna, R., Sugawara, H., Koike, T., Lopez, R., Gibson, T. J., Higgins, D. G. & Thompson, J. D. 2003. Multiple sequence alignment with the Clustal series of programs. *Nucleic Acids Res.* 31:3497–500.

Combet, C., Blanchet, C., Geourjon, C. & Deleage, G. 2000. NPS@: network protein sequence analysis. *Trends Biochem. Sci.* 25:147–50.

Conley, D. J. & Kilham, S. S. 1989. Differences in silica content between marine and freshwater diatoms. *Limnol. Oceanogr.* 34:205–13.

Conway, H. L. & Harrison, P. J. 1977. Marine diatoms grown in chemostats under silicate or ammonium limitations IV. Transient response of *Chaetoceros debilis*, *Skeletonema costatum*, and *Thalassiosira gravida* to a single addition of the limiting nutrient. *Mar. Biol.* 43:33–43.

Cronn, R., Credroni, M., Haselkorn, T., Grover, C. & Wendel, J. F. 2002. PCR-mediated recombination in amplication products derived from polyploid cotton. *Theor. Appl. Genet.* 104: 482–9.

Culham, D. E., Tripet, B., Racher, K. I., Voegele, R. T., Hodges, R. S. & Wood, J. M. 2000. The role of the carboxyl terminal alpha-helical coiled-coil domain in osmosensing by transporter ProP of *Escherichia coli*. *J. Mol. Recogn.* 13:309–22.

Darley, W. M. & Volcani, B. E. 1969. Role of silicon in diatom metabolism: A silicon requirement for deoxyribonucleic acid synthesis in the diatom *Cylindrotheca fusiformis* Reimann and Lewin. *Exp. Cell Res.* 58:334–42.

Davis, A. K., Hildebrand, M. & Palenik, B. 2005. Characterization of a cell-surface protein associated with the girdle band region of the diatom *Thalassiosira pseudonana*. *J. Phycol.* 41: 577–89.

D'Errico, I., Dinardo, M. M., Capozzi, O., De Virgilio, C. & Gadaleta, G. 2005. History of the Tfam gene in primates. *Gene* 362:125–32.

Del Amo, Y. & Brzezinski, M. A. 1999. The chemical form of dissolved Si taken up by marine diatoms. *J. Phycol.* 35: 1162–70.

Doolittle, R. F. 1987. *Of URFs and ORFs: A Primer on How to Analyze Derived Amino Acid Sequences*. 1st ed. University Science Books, Mill Valley, 103 pp.

Drum, R. W. & Pankratz, H. S. 1964. Post mitotic fine structure of *Gomphonema parvulum*. *J. Ultrastruct. Res.* 10:217–23.
Epstein, E. 1994. The anomaly of silicon in plant biology. *Proc. Natl. Acad. Sci.* 91:11–7.
Fauteux, F., Remus-Borel, W., Menzies, J. G. & Belanger, R. R. 2005. Silicon and plant disease resistance against pathogenic fungi. *FEMS Microbiol. Lett.* 249:1–6.
Fersht, A. 1985. *Enzyme Structure and Mechanism*. W.H. Freeman & Co., New York, 475 pp.
Forsberg, H. & Ljungdahl, P. O. 2001. Sensors of extracellular nutrients in *Saccharomyces cerevisiae*. *Curr. Genet.* 40:91–109.
Frigeri, L. G., Radabaugh, T. R., Haynes, P. A. & Hildebrand, M. 2006. Identification of proteins from a cell wall fraction of the diatom *Thalassiosira pseudonana*: insights into silica structure formation. *Mol. Cell. Proteomics* 5:182–93.
Frohman, M. A., Dush, M. K. & Martin, G. R. 1988. Rapid production of full-length cDNAs from rare transcripts: amplification using a single gene-specific oligonucleotide primer. *Proc. Natl. Acad. Sci.* 85:8998–9002.
Goldman, N. & Yang, Z. H. 1994. Codon-based model of nucleotide substitution for protein-coding DNA-sequences. *Mol. Biol. Evol.* 11:725–36.
Gordon, R., Sterrenburg, F. & Sandhage, K. [Eds.] 2005. *A Special Issue on Diatom Nanotechnology. Journal of Nanoscience and Nanotechnollogy*. American Scientific Publishers, Stevenson Ranch, 178 pp.
Grachev, M. A., Denikina, N. N., Belikov, S. I., Likhoshvai, E. V., Usol'tseva, M. V., Tikhonova, I. V., Adel'shin, R. V., Kler, S. A. & Sherbakova, T. A. 2002. Elements of the active center of silicon transporters in diatoms. *Mol. Biol. (Moscow)* 36: 534–6.
Grachev, M., Sherbakova, T., Masyukova, Y. & Likhoshway, Y. 2005. A potential zinc-binding motif in silicic acid transport proteins of diatoms. *Diatom Res.* 20:409–11.
Guillard, R. R. L. 1975. Culture of phytoplankton for feed marine invertebrates. *In* Smith, W. L. & Chanley, M. H. [Eds.] *Culture of Marine Invertebrate Animals*. Plenum Press, New York, pp. 29–60.
Guillard, R. R. & Ryther, J. H. 1962. Studies of marine planktonic diatoms. I. *Cyclotella nana* Hustedt and *Detonula confervacea* Cleve. *Can. J. Microbiol.* 8:229–39.
Hildebrand, M. 2000. Silicic acid transport and its control during cell wall silicification in diatoms. *In* Bäuerlein, E. [Ed.] *Biomineralization: From Biology to Biotechnology and Medical Applications*. Wiley-VCH, Weinheim, pp. 171–88.
Hildebrand, M. & Dahlin, K. 2000. Cloning and characterization of nitrate transporter genes from the diatom *Cylindrotheca fusiformis*. *J. Phycol.* 36:30.
Hildebrand, M., Dahlin, K. & Volcani, B. E. 1998. Characterization of a silicon transporter gene family in *Cylindrotheca fusiformis*: sequences, expression analysis, and identification of homologs in other diatoms. *Mol. Gen. Genet.* 260:480–6.
Hildebrand, M., Higgins, D. R., Busser, K. & Volcani, B. E. 1993. Silicon-responsive cDNA clones isolated from the marine diatom *Cylindrotheca fusiformis*. *Gene* 132:213–8.
Hildebrand, M., Volcani, B. E., Gassmann, W. & Schroeder, J. I. 1997. A gene family of silicon transporters. *Nature* 385:688–9.
Hildebrand, M. & Wetherbee, R. 2003. Components and control of silicification in diatoms. *In* Muller, W. E. G. [Ed.] *Progress in Molecular and Subcellular Biology*. Springer-Verlag, Berlin, pp. 11–57.
Huang, Y., Lemiux, J., Song, J., Auer, M. & Wang, D. 2003. Structure and mechanism of the glycerol-3-phosphate transporter from *Escherichia coli*. *Science* 301:616–20.
Hunte, C., Screpanti, E., Venturi, M., Rimon, A., Padan, E. & Michel, H. 2005. Structure of a Na+/H+ antiporter and insights into mechanism of action and regulation by pH. *Nature* 425:1197–202.
Jacobs, J. D., Ludwig, J. R., Hildebrand, M., Kukel, A., Feng, T.-Y., Ord, R. W. & Volcani, B. E. 1992. Characterization of two circular plasmids from the marine diatom *Cylindrotheca fusiformis*: plasmids hybridize to chloroplast and nuclear DNA. *Mol. Gen. Genet.* 233:302–10.
Johnson, D. A., Gautsch, J. W., Sportsman, J. R. & Elder, J. H. 1984. Improved technique utilizing nonfat dry milk for analysis of proteins and nucleic acids transferred to nitrocellulose. *Gene Anal. Tech.* 1:3–8.
Judo, M. S. B., Wedel, A. B. & Wilson, C. 1998. Stimulation and suppression of PCR-mediated recombination. *Nucleic Acids Res.* 26:1819–25.
Juretić, D., Zoranic, L. & Zucic, D. 2002. Basic charge clusters and predictions of membrane protein topology. *J. Chem. Inf. Comput. Sci.* 42:620–32.
Kammerer, R. A. 1997. Alpha-helical coiled-coil oligomerization domains in extracellular proteins. *Matrix Biol.* 15: 555–65.
Kinrade, S. D., Del Nin, J. W., Schach, A. S., Sloan, T. A., Wilson, K. L. & Knight, C. T. G. 1999. Stable five- and six-coordinated silicate anions in aqueous solution. *Science* 285:1542–5.
Kosakovsky Pond, S. L. & Frost, S. D. W. 2005a. Datamonkey: rapid detection of selective pressure on individual sites of codon alignments. *Bioinformatics* 21:2531–3.
Kosakovsky Pond, S. L. & Frost, S. D. W. 2005b. Not so different after all: a comparison of methods for detecting amino-acid sites under selection. *Mol. Biol. Evol.* 22:1208–22.
Kosakovsky Pond, S. L., Frost, S. D. W. & Muse, S. V. 2005. HyPhy: hypothesis testing using phylogenies. *Bioinformatics* 21:676–9.
Kröger, N., Deutzmann, R., Bergsdorf, C. & Sumper, M. 2000. Species-specific polyamines from diatoms control silica morphology. *Proc. Natl. Acad. Sci.* 97:14133–8.
Kröger, N., Deutzmann, R. & Sumper, M. 1999. Polycationic peptides from diatom biosilica that direct silica nanosphere formation. *Science* 286:1129–32.
Kurisu, G., Zakharov, S. D., Zhalnina, M. V., Bano, S., Eroukova, V. Y., Rokitskaya, T. I., Antonenko, Y. N., Wiener, M. C. & Cramer, W. A. 2003. The structure of BtuB with bound colicin E3 R-domain implies a translocon. *Nat. Struct. Mol. Biol.* 10: 948–54.
Lewin, J. C. 1954. Silicon metabolism in diatoms. I. Evidence for the role of reduced sulfur compounds in silicon utilization. *J. Gen. Physiol.* 37:589–99.
Lewin, J. C. 1955. Silicon metabolism in diatoms. III. Respiration and silicon uptake in *Navicula pelliculosa*. *Can. J. Microbiol.* 3:427–33.
Lupas, A., Van Dyke, M. & Stock, J. 1991. Predicting coiled coils from protein sequences. *Science* 252:1162–4.
Ma, J. F., Tamai, K., Yamaji, N., Mitani, N., Konishi, S., Katsuhara, M., Ishiguro, M., Murata, Y. & Yano, M. 2006. A silicon transporter in rice. *Nature* 440:688–91.
Martin-Jézéquel, V., Hildebrand, M. & Brzezinski, M. A. 2000. Silicon metabolism in diatoms: implications for growth. *J. Phycol.* 36:821–40.
McLachlan, A. D. 1987. Gene duplication and the origin of repetitive protein structures. *Cold Spring Harbor Symp. Quant. Biol.* 52:411–20.
Medlin, L. & Kaczmarska, I. 2004. Evolution of the diatoms: V. Morphological and cytological support for the major clades and a taxonomic revision. *Phycologia* 43:245–70.
Medlin, L., Lange, M. & Baumann, M. E. M. 1994. Genetic differentiation among three colony-forming species of Phaeocystis: further evidence for the phylogeny of the Prymnesiophyta. *Phycologia* 33:199–212.
Milligan, A., Varela, D. E., Brzezinski, M. A. & Morel, F. M. M. 2004. Dynamics of silicon metabolism and silicon isotopic discrimination in a marine diatom as a function of pCO_2. *Limnol. Oceanogr.* 49:322–9.
Mitani, N. & Ma, J. F. 2005. Uptake system of silicon in different plant species. *J. Exp. Bot.* 56:1255–61.
Mount, S. M. 1982. A catalogue of splice junction sequences. *Nucleic Acids Res.* 10:459–72.
Muse, S. V. & Guat, B. S. 1994. A likelihood approach for comparing synonymous and nonsynonymous nucleotide substitution rates, with application to the chloroplast genome. *Mol. Biol. Evol.* 11:715–24.
Nelson, D. M., Tréguer, P., Brzezinski, M. A. & Leynaert, A. 1995. Production and dissolution of biogenic silica in the ocean:

revised global estimates, comparison with regional data and relationship to biogenic sedimentation. *Glob. Biogeochem. Cycles* 9:359–72.
Ochman, H., Gerber, A. S. & Hartl, D. L. 1988. Genetic applications of an inverse polymerase chain reaction. *Genetics* 120:621–3.
Olsen, S. & Paasche, E. 1986. Variable kinetics of silicon-limited growth in *Thalassiosira pseudonana* (Bacillariophyceae) in response to changed chemical composition of growth medium. *Br. Phycol. J.* 21:183–90.
Pearson, W. R. 1997. Identifying distantly related protein sequences. *Comput. Appl. Biosci.* 13:325–32.
Pickett-Heaps, J., Schmid, A. M. M. & Edgar, L. A. 1990. The cell biology of diatom valve formation. *In* Round, F. E. & Chapman, D. J. [Eds.] *Progress in Phycological Research*. Biopress Ltd., Bristol, pp. 1–168.
Poulsen, N. & Kröger, N. 2004. Silica morphogenesis by alternative processing of silaffins in the diatom *Thalassiosira pseudonana*. *J. Biol. Chem.* 279:42993–9.
Qiu, X., Wu, L., Huang, H., McDonel, P. E., Palumbo, A. V., Tiedje, J. M. & Zhou, J. 2001. Evaluation of PCR-generated chimeras, mutations, and heteroduplexes with 16S rRNA gene-based cloning. *Appl. Environ. Microbiol.* 67:880–7.
Reimann, B. E. F., Lewin, J. C. & Volcani, B. E. 1966. Studies on the biochemistry and fine structure of silica shell formation in diatoms. II. The structure of the cell wall of *Navicula pelliculosa* (Breb.) Hilse. *J. Phycol.* 2:74–84.
Reizer, J., Reizer, A. & Saier Milton, H. J. 1993. The MIP family of integral membrane channel proteins: sequence comparisons, evolutionary relationships, reconstructed pathway of evolution, and proposed functional differentiation of the two repeated halves of the proteins. *Crit. Rev. Biochem. Mol. Biol.* 28:235–57.
Rubin, R. A., Levy, S. B., Heinrikson, R. L. & Kézdy, F. J. 1990. Gene duplication in the evolution of the two complementing domains of Gram-negative bacterial tetracycline efflux proteins. *Gene* 87:7–13.
Rueter, J. G. Jr. & Morel, F. M. M. 1981. The interaction between zinc deficiency and copper toxicity as it affects the silicic acid uptake mechanisms in *Thalassiosira pseudonana*. *Limnol. Oceanogr.* 26:67–73.
Rueter, J. G. Jr. & Morel, F. M. M. 1981. The interaction between zinc deficiency and copper toxicity as it affects the silicic acid uptake mechanisms in *Thalassiosira pseudoana*. *Limnol. Oceanogr.* 26:67–73.
Sääf, A., Baars, L. & von Heijne, G. 2001. The internal repeats in the Na+/Ca2+ exchanger-related *Escherichia coli* protein YrbG have opposite membrane topologies. *J. Biol. Chem.* 276:18905–7.
Saier, M. H. Jr. 1994. Computer-aided analyses of transport protein sequences: gleaning evidence concerning function, structure, biogenesis, and evolution. *Microbiol. Rev.* 58:71–93.
Saier, M. H. Jr. 2003. Tracing pathways of transport protein evolution. *Mol. Microbiol.* 48:1145–56.
Sambrook, J. & Russell, D. W. 2001. *Molecular Cloning: A Laboratory Manual*. 3rd ed. Cold Spring Harbor Laboratory Press, Cold Spring Harbor.
Schröder, H. C., Perović-Ottstadt, S., Rothenberger, M., Wiens, M., Schwertner, H., Batel, R., Korzhev, M., Müller, I. M. & Müller, W. E. G. 2004. Silica transport in the demosponge *Suberites domuncula*: fluorescence emission analysis using the PDMPO probe and cloning of a potential transporter. *Biochem. J.* 381:665–73.
Schwarz, K. & Milne, D. B. 1972. Growth-promoting effects of silicon in rats. *Nature* 239:333–4.
Senapathy, P., Shapiro, M. B. & Harris, N. L. 1990. Splice junctions, branch point sites, and exons: sequence statistics, identification, and applications to genome project. *Methods Enzymol.* 183:252–78.
Shelden, M. C., Loughlin, P., Tierney, M. L. & Howitt, S. M. 2003. Interactions between charged amino acid residues within transmembrane helices in the sulfate transporter SHST1. *Biochemistry* 42:12941–9.
Sherbakova, T. A., Masyukova, Y., Safonova, T., Petrova, D., Vereshagin, A., Minaeva, T., Adelshin, R., Triboy, T., Stonik, I., Aizdaitcher, N., Kozlov, M., Likhoshway, Y. & Grachev, M. 2005. Conserved motif CMLD in silicic acid transport proteins of diatoms. *Mol. Biol. (Moscow)* 39:269–80.
Shimizu, K., Cha, J., Stucky, G. D. & Morse, D. E. 1998. Silicatein alpha: cathepsin L-like protein in sponge biosilica. *Proc. Natl. Acad. Sci.* 95:6234–8.
Smetacek, V. 1999. Diatoms and the ocean carbon cycle. *Protist* 150:25–32.
Sullivan, C. W. 1976. Diatom mineralization of silicic-acid. I. Si(OH)4 transport characteristics in *Navicula pelliculosa*. *J. Phycol.* 12:390–6.
Sullivan, C. W. 1977. Diatom mineralization of silicic acid. II. Regulation of $Si(OH)_4$ transport rates during the cell cycle of *Navicula pelliculosa*. *J. Phycol.* 13:86–91.
Tanford, C. 1983. Mechanism of free energy coupling in active transport. *Ann. Rev. Biochem.* 52:379–409.
Thompson, J. D., Higgins, D. R. & Gibson, T. J. 1994. CLUSTAL W: improving the sensitivity of progressive multiple sequence alignment through sequence weighting, position-specific gap penalties and weight matrix choice. *Nucleic Acids Res.* 22: 4673–80.
Tréguer, P., Nelson, D. M., Van Bennekom, A. J., DeMaster, D. J., Leynaert, A. & Queguiner, B. 1995. The silica balance in the world ocean: a reestimate. *Science* 268:375–9.
Tréguer, P. & Pondaven, P. 2000. Silica control of carbon dioxide. *Nature* 406:358–9.
Tusnády, G. E. & Simon, I. 2001. The HMMTOP transmembrane topology prediction server. *Bioinformatics* 17:849–50.
von Heijne, G. 1992. Membrane protein structure prediction. Hydrophobicity analysis and the positive-inside rule. *J. Mol. Biol.* 225:487–94.
West, I. C. 1997. Ligand conductance and the gated-pore mechanism of transmembrane transport. *Biochim. Biophys. Acta* 1331:213–34.
Will, A., Grassl, R., Erdmenger, J., Caspari, T. & Tanner, W. 1998. Alteration of substrate affinities and specificities of the *Chlorella* hexose/H+ symporters by mutations and construction in chimeras. *J. Biol. Chem.* 273:11456–62.
Yamashita, A., Singh, S. K., Kawate, T., Jin, Y. & Gouaux, E. 2005. Crystal structure of a bacterial homologue of Na+/Cl-dependent neurotransmitter transporters. *Nature* 437:215–23.
Yamato, I., Kotani, M., Oka, Y. & Anraku, Y. 1994. Site-specific alteration of arginine 376, the unique positively charged amino acid residue in the mid-membrane-spanning regions of the proline carrier of *Escherichia coli*. *J. Biol. Chem.* 269: 5720–4.
Zhai, Y. & Saier, M. H. Jr. 2001. A web-based program for the prediction of average hydropathy, average amphipathicity and average similarity of multiply aligned homologous proteins. *J. Mol. Microbiol. Biotechnol.* 3:285–6.
Zhai, Y. & Saier, M. H. Jr. 2002. A simple sensitive program for detecting internal repeats in sets of multiply aligned homologous proteins. *J. Mol. Microbiol. Biotechnol.* 4:375–7.
Zhang, Z. & Gerstein, M. 2003. The human genome has 49 cytochrome c pseudogenes, including a relic of a primordial gene that still functions in mouse. *Gene* 312:61–72.
Zhang, Z. & Gerstein, M. 2004. Large-scale analysis of pseudogenes in the human genome. *Curr. Opin. Genet. Dev.* 14: 328–35.

Chapter II, in full, is a reprint of the material as it appears in the Journal of Phycology 42:822-834. The dissertation author was the primary investigator and author of this manuscript. Andrew J. Alverson and Mark Hildebrand were co-authors.

chapter III

Analysis of *Thalassiosira pseudonana* silicon transporters indicate distinct levels of regulation and transport activity through the cell cycle

ABSTRACT

A multi-level analysis on expression and activity of silicon transporters (SITs) was done on synchronously growing cultures of *Thalassiosira pseudonana* to provide insight into the role these proteins play in cellular silicon metabolism during the cell cycle. A SIT-specific polyclonal peptide antibody was generated and used in Western blot analysis of whole-cell protein lysates to monitor SIT protein levels during synchronized progression through the cell cycle. Peaks in SIT protein levels correlated with active periods of silica incorporation into cell wall substructures. Quantitative PCR on each of the three distinct *SIT* genes (*TpSIT1-3*) showed mRNA levels of each *SIT* peaked prior to cell wall synthesis, with mRNA levels of *TpSIT1* having an additional peak during girdle band synthesis. Protein and mRNA levels did not correlate, suggesting a significant regulatory step of SITs is at the translational or post-translational level. Surge uptake rates also did not correlate with SIT protein levels suggesting SIT activity was internally controlled by the rate of silica incorporation. This is the first study to characterize SIT mRNA and protein expression and cellular uptake kinetics during the course of the cell cycle and cell wall synthesis and provides novel insight into SIT regulation.

INTRODUCTION

Silicon is an important element in biology, from bacteria to humans (Birchall 1995). The hydrated form of silicon, called silicic acid, is considered an important nutrient for plant growth (Epstein 1994; Richmond and Sussman 2003) and silica, the polymerized form of silicon, is used by certain plants for rigidity, fungal resistance, and defense against grazers. In animals, silicon has a wide range of systemic effects (Bendz and Lindqvist 1978) in additional to being essential for proper bone and collagen formation (Schwarz and Milne 1972; Carlisle 1981). Despite the obvious importance of silicon to life on Earth, the molecular details of biological interactions with silicon and regulatory mechanisms are poorly understood. One of the largest groups of silicifying organisms are diatoms; unicellular, eukaryotic phytoplankton that use silica as a cell wall material. These organisms are found predominantly in aquatic environments, but are capable of living in soils and ice. Diatoms play a dominant role in silicon biogeochemistry (Nelson et al. 1995; Tréguer et al. 1995), and because they are estimated to contribute 40% of global primary production (Nelson et al. 1995), they play an important role in the global carbon cycle. Because most diatom species have an obligate silicon requirement for growth (Darley and Volcani 1969) and naturally process large amounts of silicon, they are an excellent model system for investigations into biological interactions with silicon.

The silicified diatom cell wall, or frustule, is composed of two overlapping halves with the upper half called the epitheca and the lower half the hypotheca. Theca consist of a valve, the species-specific structure capping each end, and girdle bands, a series of overlapping siliceous strips extending on the sides and in the region

overlapping the two theca. Vegetative cell division in certain diatom species begins with the mother cell expanding by synthesizing girdle bands (Pickett-Heaps et al. 1990). Cytokinesis follows and on adjacent faces within the two daughter cell protoplasts (still contained within the mother cell), new valves are formed. Silica polymerization occurs within an organelle called the silica deposition vesicle, bounded by a membrane called the silicalemma (Reimann et al. 1966; Schmid et al. 1981; Crawford and Schmid 1986). Once the valve is completely formed, it is exocytosed and the daughter cells separate. This intimate connection between cell wall synthesis and the cell cycle results in a tight coupling of silicon metabolism and cell division.

In diatoms, silicon is taken up from the environment predominantly as silicic acid (Del Amo and Brzezinski 1999). Although the average oceanic concentration of silicic acid is 70 μM, in surface waters, where diatoms are most common, levels can be less than 10 μM (Tréguer et al. 1995). In contrast, intracellular concentrations of silicic acid can be several hundred millimolar depending on the species (Martin-Jézéquel et al. 2000); therefore, diatoms must posses an efficient uptake system to overcome this 1000 fold difference. Data suggest silicon uptake in diatoms follows Michaelis-Menten saturation kinetics with K_s values between 0.2 and 7.7 μM and V_{max} ranging from 1.2 to 950 fmol Si cell^{-1} hr^{-1} (Lewin 1954; Lewin 1955; Sullivan 1976; Sullivan 1977; Bhattacharyya and Volcani 1980; Martin-Jézéquel et al. 2000; Tréguer and Pondaven 2000). The coupling of the diatom cell cycle and silicon metabolism (Crawford 1981; Brzezinski 1992; Schmid 1994; Claquin et al. 2002) has an effect on transport. Rates of silicon uptake vary during synchronized growth, suggesting silicon uptake may be cell-cycle dependent (Sullivan 1976), which has led to the

understanding that uptake parameters measured in exponentially growing cultures are underestimates because cells are at different stages of the cell cycle and not necessarily utilizing maximum uptake rates (Brzezinski 1992).

Chemostat studies monitoring silicon uptake revealed three modes of uptake: surge uptake, externally controlled uptake, and internally controlled uptake (Conway et al. 1976; Conway and Harrison 1977). Surge uptake occurs upon initial addition of silicon to silicon-starved cells, with maximal uptake rates during this time. Externally controlled uptake occurs when extracellular levels of silicon are low and the rate of uptake is controlled by the external substrate concentration. In internally controlled uptake, the rate of silica deposition into the cell wall is proposed to control the rate of uptake (Conway et al. 1976; Conway and Harrison 1977). On longer time scales (h), uptake is largely internally controlled (Conway et al. 1976; Conway and Harrison 1977; Hildebrand 2000). On shorter time scales (min) silicon transport is a dynamic process, involving both uptake and efflux (Sullivan 1977; Milligan et al. 2004).

Diatom silicon transporters (SITs), first identified in the marine pennate diatom *Cylindrotheca fusiformis* (Hildebrand et al. 1997; Hildebrand et al. 1998), are membrane-associated proteins that directly interact with and transport silicic acid (Hildebrand et al. 1997). SITs are a novel family of transporters with no known homologs, although a silicon transporter homologous to aquaporins, but with no homology to diatom SITs, was recently described in rice (Ma et al. 2006). Five *SIT* genes (*CfSIT1-5*) were identified in *C. fusiformis*, each with a distinct level or pattern of mRNA expression during cell wall synthesis. *Cf*SITs are predicted to contain ten transmembrane segments (TMS), an intracellular N-terminus, and an intracellular C-

terminal coiled-coil motif, a structure known to play a role in protein-protein interactions. Genome sequencing of the centric diatom, *Thalassiosira pseudonana,* led to the identification of three distinct *SIT* genes. Similar to *Cf*SITs, *Tp*SITs are predicted to contain ten TMS with an intracellular N- and C- terminus. However, they are not predicted to contain a coiled-coil motif (Thamatrakoln et al. 2006). Phylogenetic analyses of *TpSITs* suggest *TpSIT1* and *TpSIT2* are related through a relatively recent lineage-specific gene duplication and that *TpSIT3* is evolving at a significantly different rate than *TpSIT1* or *TpSIT2* (Thamatrakoln et al. 2006).

T. pseudonana is an excellent model system for investigations into SIT regulation and function because the exact number of *SIT* genes is known (Armbrust et al. 2004; Thamatrakoln et al. 2006), and a synchronized growth procedure has been recently developed (Frigeri et al. 2006; Hildebrand et al. in press). Synchronized growth enables evaluation of cell cycle effects, providing a unique opportunity to perform a comprehensive investigation into the molecular details of SIT function. In this study, molecular and biochemical analyses of TpSITs, as well as measurements of silicon uptake rates, on synchronously growing cultures of *T. pseudonana* revealed distinct levels SIT regulation.

MATERIALS AND METHODS

Culture conditions

Thalassiosira pseudonana Hasle et Heimdale clone 3H CCMP1335, *Thalassiosira weissflogii* (Grunow) Fryxell et Hasle CCMP1336, *Skeletonema*

costatum (Greville) Cleve CCAP1281, *Cyclotella meneghianana* CCMP338, *Bacillaria paxillifer* (O.F. Müller) N.I. Hendey 1951 CCAP1006/2, *Cylindrotheca fusiformis* Reimann et Lewin CCMP343, *Ditylum brightwellii* (T. West) Grunow ex van Heurck 1883 CCAP1022/1, *Navicula pelliculosa* (Bréb.) Hilse SAG1050-3 (a freshwater strain referred to in the text as *N. pelliculosa* FW), *Navicula pelliculosa* (Breb. et Kuetzing) Hilse CCMP543 (a marine strain referred to in the text as *N. pelliculosa* M), and *Phaeodactylum tricornutum* Bohlin CCMP1327 were grown in batch culture under continuous illumination with cool white fluorescent lights at 150 µmole quanta m^{-2} s^{1}at 18 to 20° C. *N. pelliculosa* FW was grown in fresh water tryptone (FWT) medium (Reimann et al. 1966). *T. pseudonana* was grown in sterile artificial seawater medium (ASW) (Darley and Volcani 1969) supplemented with biotin and vitamin B12, each at 1 ng L^{-1}, with or without Bacto Tryptone added to 1 g L^{-1}. All other diatom species were grown in sterile ASW medium, or f/2 medium made with 0.2 µm filtered and autoclaved local seawater (Guillard and Ryther 1962; Guillard 1975).

Silicon starvation and synchronized cell growth

For gradual silicon starvation, exponential phase cultures of *T. pseudonana* were harvested under sterile conditions by centrifugation at 3,000 x g for 12 min in a Composite KA-14.250 rotor and washed with sterile silicon-free ASW. Cells were resuspended at a concentration of 0.8-1.0 x 10^6 cells ml^{-1} in ASW containing 25 µM sodium silicate, which was enough silicon to allow the cells to complete one division before becoming silicon-starved. Over the next 24 h, 750 ml of cells were harvested

every 4 h by centrifugation at 12,600 x g for 10 min, washed once with 3.5% (w/v) NaCl, and stored at -80°C.

Synchronized growth of *T. pseudonana* was performed as previously described (Frigeri et al. 2006). Briefly, exponential phase cultures of *T. pseudonana* were harvested by centrifugation as above, and washed with silicon-free ASW. Cells were resuspended in silicon-free ASW at 0.8-1.0 x 10^6 cells ml^{-1} and allowed to incubate in the light with aeration for 24 h in a polycarbonate bottle. After 24 h, 200 µM sodium silicate was added to initiate synchronized progression through the cell cycle. Samples (750 ml) were harvested by centrifugation as above every hour, washed in 3.5% (w/v) NaCl and stored at -80°C. Formation of specific cell wall structures was monitored by visualization of Rhodamine 123 (Sigma, St. Louis, MO) staining, as described (Frigeri, et al., 2006), or by 2-(4-pyridyl-5-((4-(2-dimethylaminoethylaminocarbomoyl)methoxy)-phenyl)oxazole (PDMPO, Molecular Probes, Carlsbad, CA) used at 100 nM in the culture.

mRNA extraction, cDNA synthesis, and quantitative PCR

Total RNA was isolated using TriReagent (Sigma, St. Louis, MO) as described (Hildebrand and Dahlin 2000). Aliquots of total RNA were subjected to DNase treatment using an RNeasy kit (Qiagen, Inc. Valencia, CA) according to the manufacturer's protocol. cDNA was prepared from equivalent amounts of DNase-treated RNA using SuperScript II Reverse Transcriptase (Invitrogen, Carlsbad, CA). Quantitative PCR (QPCR) was performed using a LightCycler® System and LightCycler® DNA Master SYBR Green I (Roche Applied Science, Indianapolis, IN).

Because of the high sequence conservation of *TpSITs*, primer sets were designed to amplify different size fragments and PCR was used to verify each primer set only amplified the *SIT* of choice. Primers used were as follows: for *TpSIT1*, *TpSIT1* 5' (5'-AGATGGAAGGGTATTTGACAGAG) and *TpSIT1* 3'-2 (5'-TATCTTCACATGCATCCTTGGG), for *TpSIT2*, *TpSIT2* 5' (5'-GTCCGTTCAACAAGGCAGAA) and *TpSIT2* 3'-2 (5'-CATCTTCACGTGCATTCTCGGA), for *TpSIT3*, *TpSIT3* 5'-2 (5'-CATCCGGAGTAGTTACTCGTG) and *TpSIT3* 3' (5'-GACGTCCAAGATGCGAAGAG). Standards for QPCR were as previously described (Frigeri et al. 2006) using dilutions of *T. pseudonana* genomic DNA. This resulted in genome equivalent ng values for mRNA levels rather than an absolute amount of RNA per cell. Replicates of QCPR data were normalized to the mean of individual experiments. The normalized means were plotted along with standard error. Dilutions of cDNA were done to ensure that amplification was in the linear range. Duplicate technical replicates were performed for each *SIT* during silicon starvation; triplicate technical replicates were done for *TpSIT1* and *TpSIT2* during synchronized cell division.

Anti-TpEL4 production

The sequence of a 15 residue region corresponding to amino acids 318-322 of *Tp*SIT1 (sequence PANERGTSFFGRKTC) was provided to Sigma Genosys (The Woodlands, TX) and used to generate a peptide conjugated to KLH. This peptide was used as antigen to generate polyclonal antibodies in rabbits (Sigma Genosys, The

Woodlands, TX). The antibody was designated anti-TpEL4 because the peptide corresponds to a region of extracellular loop 4 (Thamatrakoln et al. 2006).

SDS-PAGE

During the course of a synchrony, 13 ml samples were harvested by centrifugation at 16,500 x g in an HB-4 rotor at 0 min, 5 min, and every 30 min thereafter for 8 h. Cell pellets were stored at -80°C until ready for use. Either equal cell numbers or equal protein amounts were analyzed. For equal cell numbers, cells were resuspended in 2X SDS-sample buffer (Invitrogen, Carlsbad, CA) and heated to 95°C for 5 min. Thirty microliters of each sample were separated by electrophoresis on 4-20% gradient gels (Bio-Rad, Hercules, CA). For experiments where equal protein concentration was loaded, 50 µl of 2% SDS was added to each sample and protein concentration was measured using a DC Protein Assay kit (Bio-Rad, Hercules, CA) according to manufacturer's instructions. Ten micrograms of total protein were added to 2X SDS-sample buffer, heated at 95°C for 5 min, and electrophoresed as described. Protein lysates from species other than *T. pseudonana* were obtained using the same method as described for equal protein concentration experiments, but samples were electrophoresed on 10% polyacrylamide gels (Bio-Rad, Hercules, CA).

Peptide competition

TpEL4 peptide used as antigen for antibody production was generated and provided by Sigma Genosys (The Woodlands, TX). TpEL4 was reconstituted in 0.2 M boric acid pH 8 to a concentration of 1 mg/ml. Varying concentrations of peptide were

preincubated with 2.5 µl of anti-TpEL4 at 4°C overnight with mixing. This mixture was used as primary antibody for Western analysis as described below.

Western blot

Electrophoretically separated proteins were transferred to PVDF membrane in blotting buffer containing 25 mM Tris, 192 mM glycine, pH 8.3. Transfer efficiency was visualized by using SeeBlue® prestained protein standards (Invitrogen, Carlsbad, CA). Membranes were blocked in 1X TBST pH 7.5 (25 mM Tris HCl, 137 mM NaCl, 27 mM KCl, 0.2% v/v Tween 20) and 3% nonfat dried milk at 4°C overnight with shaking. The membranes were washed 3 x 10 min in 1X TBST, then incubated in blocking buffer containing preimmune or anti-TpEL4 antisera , in initial experiments at 1:5,000 dilution but in subsequent experiments at 1:10,000 dilution, for 1 h at room temperature. After 3 x 10 min washes in 1X TBST, the membranes were incubated in blocking buffer containing horseradish peroxidase-conjugated goat anti-rabbit antibody at 1:10,000 dilution for 1 h at room temperature. Three additional washing steps were done and chemiluminescence detection was performed using a SuperSignal West Pico Chemiluminescent Substrate kit (Pierce, Rockford, IL) and following manufacturer's protocol.

Three Westerns were performed over two independent synchronies. Two of the Westerns had equal cell numbers loaded on the gel, while the third had equal total protein concentration. Densitometry was done for each Western whereby each blot was scanned using an AlphaImager® Imaging System (Alpha Innotech Corp., San Leandro, Ca) and the relative densitometric units (densitometric units minus

background) were determined using AlphaEase®FC (Alpha Innotech Corp., San Leandro, CA). Data were normalized to the mean intensity for all points within a given experiment. The normalized average for all experiments was plotted along with the standard error.

Cloning of *T. pseudonana SITs* and heterologous expression in *Saccharomyces cerevisiae*

TpSIT1, TpSIT2, and *TpSIT3* were amplified by PCR using cDNA as template andthe following primers: EcoRI-*TpSIT1*, 5' CCGGAATTCAAAAATGTCTACCGCTGAAATCCAA and *TpSIT1*-Xba, 5' CTAGTCTAGAGGCATCCTCGGCAAGAGCATC; Bam-*TpSIT2*, 5' CGCGGATCCAAAAATGTCTTCTGCCGAGGTT and *TpSIT2*-Xba, 5' CTAGTCTAGAAGCCTGCGCGTCAACAGCCTC; Bam-*TpSIT3,* 5' CGCGGATCCAAAAATGCGCGCTCAAAACGATGAA and *TpSIT3*-Xba, 5' CTAGTCTAGACTTCGCCAATCCACTTTCAAC. Products were gel purified and ligated into the yeast expression vector, pYES2/CT (Invitrogen, Carlsbad, CA) using the *Eco*RI/*Xba*I site for *TpSIT1* and the *Bam*H1/*Xba*I site for *TpSIT2* and *TpSIT3*. Clones were sequenced by SeqXCel (San Diego, CA) and verified to be in frame.

Saccharomyces cerevisiae INVSc1 (Invitrogen, Carlsbad, CA) were transformed with each construct using the lithium acetate method (Gietz and Woods 2002). *S. cerevisiae* was grown in YPD medium at 30°C to 2 x 10^7 cells ml^{-1}, then harvested by centrifugation at 3,000 x g for 5 min. Cells were washed in sterile water and resuspended at 1 x 10^9 cells ml^{-1}. An aliquot of 100 µl of competent cells was

transferred into a microfuge tube, to which 1 µg of each pYES2-*TpSIT* construct was added, along with 100 µg herring sperm DNA, 36 µl 1 M LiAc, and 240 µl PEG 3500 50% (w/v). After 30 min at 42°C, the cells were centrifuged for 30 sec at maximum speed, resuspended in 1 ml water, and plated at various dilutions onto uracil-deficient synthetic medium plates. Plates were incubated at 30°C until colonies were visible (approximately 3 days). Clones were picked and grown in liquid selection medium.

SIT protein expression was induced in yeast by growing cells in the presence of 2% galactose at 30°C. After 24 h in induction medium, cells were harvested by centrifugation at 1,500 x g for 5 min. Protein lysates were generated by resuspending cells to an OD_{600} = 50 in breaking buffer (50 mM sodium phosphate pH 7.4, 1 mM EDTA, 5% glycerol, and 1 mM PMSF), adding an equal volume of acid-washed glass beads (0.4-0.6 mm size, Sigma-Aldrich, St. Louis, MO), and vortexing 4 x 30 sec intervals at 4°C. After centrifugation at maximum speed for 10 min, the supernatant was removed and stored at -20°C. Proteins were separated by electrophoresis on 10% polyacrylamide gels and Western analysis was performed as described.

Measurements of silicon in the growth medium

Silicon disappearance from the medium was monitored during silicon starvation to monitor extracellular levels or during synchronized growth to measure silicon uptake. Samples were taken at regular intervals by centrifuging cells at 16,500 x g for 5 min. Aliquots of supernatant were removed and stored at -20°C. Silicic acid concentrations were measured using the silicomolybdate assay (Strickland and Parsons 1968) modified for a 96-well plate format. Twenty-five microliters of supernatant

were added to 100 µl Milli-Q water, 50 µl of molybdate reagent was added, mixed, and allowed to incubate for 10 min at room temperature, then 75 µl of reducing agent was added and mixed. Samples were incubated for 3 h at room temperature with occasional mixing, prior to measuring the absorbance at 810 nm on a SpectraMax M2 Microplate Reader (Molecular Devices, Sunnyvale, CA). The standard was sodium hexafluorosilicate (Sigma, St. Louis, MO), used in a range of 0-50 µM.

Measurements of surge uptake kinetics

Silicic acid surge uptake during the course of a synchrony was measured using $^{68}Ge(OH)_4$ as a radiotracer for silicic acid (Azam 1974). We have determined (Thamatrakoln and Hildebrand, in preparation) that short term uptake (2 min) in silicon-replete cultures of *T. pseudonana* is not saturable, even at extremely high silicon concentrations (> 500 µM). The lack of saturability prevents determination of a Michaelis-Menten V_{max} value; therefore uptake was monitored at 100 µM silicate, and V_{100} was determined. Cells were harvested at 3,000 x g for 5 min in an HB-4 rotor, washed and resuspended in silicon-minus ASW to a concentration of 2.5 x 10^5 cells ml^{-1}. One ml of cells was added to 100 µl of 0.1 µCi $^{68}Ge(OH)_4$ and 100 µM silicate (Sullivan 1976; Sullivan 1977), and either immediately vacuum filtered (for 0 min, background measurement) on a Millipore Isopore 1.2 µm RTTP membrane, or incubated for 2 min (surge uptake measurement), then filtered. Filters were washed with 5 ml 3.5% NaCl, placed in a gamma vial, and counted using a LKB Wallac 1282 Compugamma CS Universal gamma counter (Perkin-Elmer, Wellesley, MA). Triplicate samples for each condition were analyzed. Subtraction of 0 min from 2 min

gave net uptake of label, which was converted into fmol $cell^{-1}$ h^{-1}, taking into account counting efficiency, dilution effects, and radioactive decay.

RESULTS

Comparison of SIT sequences

Predicted amino acid sequences of *Tp*SIT1, *Tp*SIT2, and *Tp*SIT3 (Thamatrakoln et al. 2006) were aligned and analyzed using CLUSTAL W (Thompson et al. 1994; Combet et al. 2000) (Fig. 3.1). Analysis showed 44% amino acid identity and 75% similarity (identical plus conserved substitutions) comparing all three SITs. Pairwise comparison between each SIT revealed 88% amino acid identity and 95% similarity between *Tp*SIT1 and *Tp*SIT2. *Tp*SIT1 and *Tp*SIT3 were 46% identical, 74% similar, while *Tp*SIT2 and *Tp*SIT3 were 46% identical, 76% similar. Each *TpSIT* contained a single intron ranging in size from 97 to 124 bp, located at amino acid residue 108 in *Tp*SIT1 and *Tp*SIT2 and residue 158 in *Tp*SIT3 (Fig. 3.1).

Characterization of TpEL4 antibody

Preimmune and anti-TpEL4 antisera were tested for reactivity to whole cell protein lysates of *T. pseudonana*. There was no reactivity with the preimmune serum (Fig. 3.2A), whereas anti-TpEL4 reacted with a single band at approximately 60 kDa (Fig. 3.2A), similar to the predicted molecular weight of *Tp*SITs. A peptide competition assay demonstrated the specificity of the antibody to this band (Fig. 3.2B). To determine whether anti-TpEL4 recognized all three *Tp*SITs, *Saccharomyces*

cerevisiae was transformed to express individual SITs. Western analysis of whole cell lysates showed anti-TpEL4 recognized each *Tp*SIT (Fig. 3.2C). To determine whether anti-TpEL4 recognized SITs from other diatom species or phytoplankton, whole cell protein lysates were analyzed by Western blot (Fig. 3.2D). Anti-TpEL4 recognized a protein of approximately 60 kDa in the centric diatoms, *T. pseudonana*, *Skeletonema costatum, Chaetoceros gracilis, Cyclotella meneghianana, Ditylum brightwellii,* and the pennate diatoms, *Cylindrotheca fusiformis, Navicula pelliculosa* M, and *Phaeodactylum tricornutum*, but did not recognize proteins in lysates from the centric diatom *T. weissflogii*, or the pennate diatoms, *N. pelliculosa* FW, or *Bacillaria paxillifer*. In addition, there was no reactivity with protein lysate from the coccolithophore, *Emiliania huxleyi*. For those species where SIT sequences were available (Thamatrakoln et al. 2006), the region corresponding to the peptide used as antigen was compared to *Tp*SIT1 (Fig. 3.2E). No distinct pattern of sequence conservation among SITs that did or did not cross-react with anti-TpEL4 was apparent. For example, SIT2 of *T. weissflogii* (*Tw*SIT2, Fig. 3.2E) had only one amino acid substitution when compared to *Tp*SIT1, but did not cross-react with anti-TpEL4.

Analysis of SIT protein expression in synchronized cultures of *T. pseudonana*

SIT protein was monitored through a synchrony using anti-TpEL4 and Western blot (Fig. 3.3, upper panel). For the same synchrony, net silicic acid uptake was determined by measurement of silicon disappearance from the medium (Fig. 3.3, middle panel). Densitometry analysis for three Westerns was performed and normalized relative densitometric units (see Materials and Methods) were compared

between experiments (Fig. 3.3, lower panel). This analysis showed SIT protein was expressed throughout the synchrony, but at variable levels. SIT protein levels increased approximately 1.5 h after silicon replenishment and then decreased to a minimum at t = 3.5 h (Fig. 3.3). At t = 4.5 h, protein levels again increased and remained high until the end of the experiment. The timing of cellular processes during the synchrony, shown in Fig. 3.3 (bottom) were determined in repeated synchronies by observation of Rhodamine 123 incorporation coupled with flow cytometric analysis to determine cell cycle stage (Hildebrand et al. in press)

Analysis of *SIT* mRNA levels during silicon starvation and synchronized growth

mRNA levels of each *SIT* were monitored during gradual silicon starvation and synchronized cell division using quantitative PCR (QPCR) (Fig. 3.4). During silicon starvation, mRNA levels of each *TpSIT* peaked at t = 4 h, coincident with decreased silicon in the medium (Fig. 3.4A). *TpSIT1* and *TpSIT2* had an additional peak at t = 12-16 h, with mRNA levels 12 fold higher than initial levels for *TpSIT1* and 5 fold higher for *TpSIT2* (Fig. 3.4A). At the end of the starvation phase, when silicon was minimal in the medium, *TpSIT1* and *TpSIT2* levels decreased, but remained 6 and 3 fold higher than initial levels, respectively (Fig. 3.4A). Levels of *TpSIT3* mRNA were, on average, 30 fold lower than those of *TpSIT1* or *TpSIT2* (Fig. 3.4A).

During synchronized cell growth, mRNA levels of each *SIT* peaked at t = 3 h, increasing relative to t = 0 h by 8 fold for *TpSIT1*, 12 fold for *TpSIT2*, and 1.5 fold for *TpSIT3* (Fig. 3.4B). A transient 2.5 fold increase in *TpSIT1* mRNA was also measured at t = 1 h (Fig. 3.4B). By t = 4 h, mRNA levels of each *SIT* returned to levels similar to

t = 0 h. *TpSIT1* and *TpSIT2* mRNA levels were relatively constant for the remainder of the experiment, whereas *TpSIT3* mRNA had a slight increase at t = 8 h (Fig. 3.4B). *TpSIT3* mRNA levels were, on average, 200-300 fold lower than those of *TpSIT1* and *TpSIT2* (Fig. 3.4B).

Surge uptake rate through the cell cycle

Surge uptake rates were measured using radiolabeled germanic acid as a tracer for silicic acid (Fig. 3.5). The rate was low at t = 0 h, but increased and was relatively constant between t = 2-4 h of the synchrony at approximately 30 fmol $cell^{-1}$ h^{-1}. At t = 5 h, the rate increased and eventually peaked at t = 8 h at 147 fmol $cell^{-1}$ h^{-1}. At t = 9 h, the rate decreased to 113 fmol $cell^{-1}$ h^{-1}.

DISCUSSION

Biochemical, molecular, and physiological tools were used to determine the relationship of SIT protein and mRNA expression to silicon uptake during progression through the cell cycle in *T. pseudonana*. Because of the tight coupling between silicon uptake and the cell cycle, it is only with the ability to synchronize growth of *T. pseudonana* that these analyses were possible. Interpretation of the data requires discussion about events occurring during synchronized growth of *T. pseudonana*, details of which are the subject of a manuscript in press (Hildebrand et al.), but are summarized here. *T. pseudonana* starved for silicon for 24 h arrest predominantly in the G1 stage of the cell cycle. Upon silicate replenishment, cells progress through G1 for 3 h while girdle band synthesis occurs. As the cells enter S-phase (t = 3-4 h), girdle

band production ceases. Cytokinesis follows and valve synthesis is observed between t = 4-6 h, although the exact timing of this can vary between synchronized cultures. The timing of valve synthesis in a given synchrony can be monitored either by direct visualization by fluorescence microscopy of Rhodamine 123 or PDMPO stained cells, or by a characteristic 5 fold increase in net silicic acid uptake over that occurring during girdle band synthesis (Hildebrand et al. in press). Upon completion of valve synthesis, cells separate and additional girdle bands are synthesized. The net rate of silicic acid uptake during this process, measured by silicate disappearance from the medium, is 4 fmol $cell^{-1}$ h^{-1} for the first phase of girdle band synthesis, 20 fmol $cell^{-1}$ h^{-1} for valve synthesis, and 4 fmol $cell^{-1}$ h^{-1} for the second phase of girdle band synthesis. Similar to other diatom species (Brzezinski et al. 1990), synchronized growth in *T. pseudonana* does not result in all of the cells entrained at the same stage of the cell cycle; typically, 80% are arrested under silicate starvation in G1 and the remaining 20% in G2+M (Hildebrand et al. in press).

In general, the pattern and levels of SIT protein determined by Western analysis (Fig. 3.3) correlated with active periods of silica incorporation into cell wall substructures. Upon silicate replenishment, SIT protein levels increased coincident with girdle band synthesis, until t = 3 h (Fig. 3.3). During S-phase (t = 3-4 h) cells are not making silica structures (Hildebrand et al. in press), and SIT levels are minimal (Fig. 3.3). Considering that 20% of the cells may not be in S-phase at that time, it is possible that SIT protein levels are even lower or undetectable in S-phase cells. During valve synthesis when silicon demands are high, SIT protein levels increased to maximal levels measured (Fig. 3.3).

SIT protein levels and silicon uptake were not strictly correlated. Comparing t = 0.5-2.5 h with t = 5-8 h, SIT protein levels were not substantially different, yet net silicic acid uptake, as measured by its disappearance from the medium (Fig. 3.3, middle panel), and surge uptake, as measured by short-term uptake of radiolabeled $^{68}Ge(OH)_4$ (Fig. 3.5) increased 5 fold. Furthermore, comparison of surge uptake rates with net uptake suggests the cells are capable of taking up 7.5 fold more silicon than they actually do on longer time scales. These observations are consistent with net uptake being largely dictated by the rate of silica incorporation, as in internally controlled uptake (Conway and Harrison 1977), in which case, the cell may rely more on regulating the activity of SITs rather than the actual amount of SIT protein. Alternatively, because Western analysis only measures total SIT protein, some of the SITs measured may not be present at the plasma membrane. If, as has been demonstrated for glucose transporters (Bryant et al. 2002; Dugani and Klip 2005), SITs cycle between the plasma membrane and intracellular vesicles as part of a regulatory mechanism, changes in uptake rates without a concomitant change in total protein could result.

Care must be taken when interpreting mRNA expression patterns during silicon starvation (Fig. 3.4A) because the cells are initially unsynchronized and at different stages of the cell cycle. However, it is nonetheless important because data obtained from unsynchronized cultures are more likely representative of natural environmental conditions where cells may experience periods of gradual starvation. One conclusion that can be made is that *SIT* mRNA levels were not strictly controlled by extracellular silicon concentrations. Between t = 0-4 h, silicon concentrations were

relatively similar, but there was almost a 7 fold increase in *TpSIT1* and *TpSIT2* mRNA levels and a 2 fold increase in *TpSIT3* mRNA. *TpSIT1* and *TpSIT2* were induced when extracellular silicon dropped to lowest levels (t = 12 h) and remained elevated until t = 16 h, suggesting cells upregulated *TpSIT1* and *TpSIT2* mRNA in response to the immediate absence of silicon. At the end of the silicon starvation phase, mRNA levels of *TpSIT1* and *TpSIT2* decreased, possibly as a response to longer term starvation or because the cells were becoming arrested at the same stage of the cell cycle. *TpSIT3* showed a different response, increasing slightly in response to immediate silicon starvation and possibly increasing at the end of the starvation phase (Fig. 3.4A), suggesting *TpSIT3* may be induced in response to prolonged exposure to silicon starvation. However, standard error between replicates at the later timepoint makes interpretation of the data tenuous. One interesting feature unique to *Tp*SIT3 is the presence of additional N-terminal sequence when compared to *Tp*SIT1 or *Tp*SIT2, however, BLAST search (Altschul et al. 1990) using this sequence did not reveal significant similarity to known proteins, nor were any conserved functional domains identified. In addition, SignalP (Nielsen et al. 1997) did not predict the presence of a signal peptide cleavage site.

One goal of this study was to gain insight into the regulation of SITs during the cell cycle using synchronously grown cells. This requires analysis and comparison of protein and mRNA expression data. Due to the number of manipulations required, it is not technically feasible to analyze both protein and mRNA on the same synchrony; however, synchronies are quite reproducible with the only variation being the timing of valve structure formation (Hildebrand et al. in press). Thus, data obtained from

separate synchronies can be related by comparing the timing of valve formation as indicated either by fluorescence microscopy examination of Rhodamine 123-stained cells, or by a characteristic 5-fold increase in net silicic acid uptake (Hildebrand et al. in press). Valve formation in the synchrony used for mRNA analysis began at t = 4 h; for protein analysis, it began one hour later at t = 5 h. Considering this, the 2 fold increase in *TpSIT1* mRNA at t = 1 h (Fig. 3.4B) occurs prior to the 2 fold increase in SIT protein levels between t = 0.5-2.5 h (Fig. 3.3). In addition, the large increase in mRNA level seen for each *SIT* at t = 3 h (Fig. 3.4B) may occur prior to the increase in SIT protein between t = 5-8 h (Fig. 3.3), however, in this case, the fold increase in mRNA (5-8 fold) did not result in a similar fold increase in SIT protein (2 fold) and levels of SIT protein remained high well after *SIT* mRNA decreased. These data suggest a disconnect between mRNA and protein levels and are consistent with the hypothesis that a significant regulatory step over SIT expression is at the translational or post-translational (protein degradation) level. Differentiating between the two possibilities would require pulse-labeling techniques which are not well-developed for diatoms.

One interesting result from the QPCR analysis was the low levels of *TpSIT3* mRNA compared with the other *TpSITs* (Fig. 3.4). This and other data, lead us to hypothesize that *Tp*SIT3 may serve as a silicon sensor in *T. pseudonana*. In addition to being able to transport silicon, diatoms could also have a mechanism for sensing silicon; for example, to evaluate whether enough extracellular silicon is present to complete a round of valve and girdle band synthesis. Specific members of other transporter families have been shown to function as substrate sensors that regulate the

expression of other members in the family through a signal transduction cascade (Özcan et al. 1996; Iraqui et al. 1999). While some sensors do not themselves exhibit transport capability, they are critical in the cells' ability to adapt to changing environments. Some known substrate sensors have distinct characteristics that differentiate them from the functional transporters (Forsberg and Ljungdahl 2001; Van Belle and André 2001). One of these features is the lack of sequence conservation of sensors to other members of the transporter family. In the ammonium transporter family in yeast, Mep1 and Mep3 share 80% amino acid identity, but are only 41% and 39% identical, respectively, to the ammonium sensor, Mep2 (Dubois and Grenson 1979; Marini et al. 1994; Marini et al. 1997; Lorenz and Heitman 1998). Similarly, the yeast glucose sensors Snf3p and Rgt2p are only 26-30% identical to other members of the family, HXT1-4 (Ko et al. 1993), while the other members share 64-87% identity (Ko et al. 1993; Kasahara and Kasahara 2003). In addition to low sequence similarity, genes encoding Snf3p and Rgt2p are weakly expressed compared to HXT1-4, approximately 100-300 fold lower (Neigeborn et al. 1986; Özcan et al. 1996). Structural differences have also been identified in known substrate sensors. For example, Snf3p and Rgt2p have an extended C-terminus compared to the other glucose transporters (Özcan et al. 1996), and the amino acid permease sensor, Ssy1p, has a 140 amino acid longer N-terminus and an extra 25-35 amino acid region in a hydrophilic loop (Iraqui et al. 1999).

Sequence analysis of *Tp*SITs revealed *Tp*SIT1 and *Tp*SIT2 shared 88% amino acid identity, but only 46% to *Tp*SIT3 (Fig. 3.1). QPCR data also showed *TpSIT3* mRNA was expressed 200-300 fold lower than *TpSIT1* and *TpSIT2* (Fig. 3.4). In

addition, the predicted amino acid sequence based on genome data for *Tp*SIT3 indicates a 34 amino acid extension at the N-terminus when compared to *Tp*SIT1 and *Tp*SIT2 (Fig. 3.1). These points are consistent with the possibility of *Tp*SIT3 being a silicon sensor, although one alternative hypothesis could be that *Tp*SIT3 plays a specialized role in uptake (e.g. specific intracellular targeting). High expression levels for *Tp*SIT1 and *Tp*SIT2 suggest they are active transporters, but amino acid differences between them could result in differing affinities or capacities for silicic acid. For example, one could be a high-affinity/low capacity transporter and the other a low-affinity/high capacity transporter allowing the cell to take advantage of a wider range of silicic acid concentrations. Definitively determining whether *Tp*SIT3 is a silicon sensor and whether *Tp*SIT1 or *Tp*SIT2 have different affinities or capacities for silicic acid will require additional investigations.

In conclusion, data obtained in this study indicate a major regulatory step for SIT expression is at the translational or post-translational level and SIT activity is controlled largely by intracellular requirements and not by protein levels. Circumstantial data suggests *Tp*SIT3 may be a silicon sensor and future work focusing on determining the transport capacity and silicon affinity of SITs should provide further insight into the roles each SIT plays in meeting the overall transport needs of the cell. In addition, the first SIT-specific antibody is now available, which will be integral in future investigations into SIT function and regulation.

ACKNOWLEDGEMENTS

We thank Luciano Frigeri and Sandra Hazelaar for technical assistance, Brian Palenik for the use of an epifluorescence microscope, and Dori Landry for kindly providing a frozen *Emiliania huxleyi* cell pellet. We would also like to thank Michael Latz for use of lab space and equipment. *Navicula pelliculosa* (Breb. et Kuetzing) Hilse CCMP543 was provided as part of a collaborative project with Sandra Hazelaar and Winfried W.C. Gieskes.

This work was supported by Air Force Office of Scientific Research Multidiscplinary University Research Initiative Grant RF00965521.

Chapter III, in full, has been submitted for publication. The dissertation author was the primary investigator and author of this manuscript. Mark Hildebrand was a co-author.

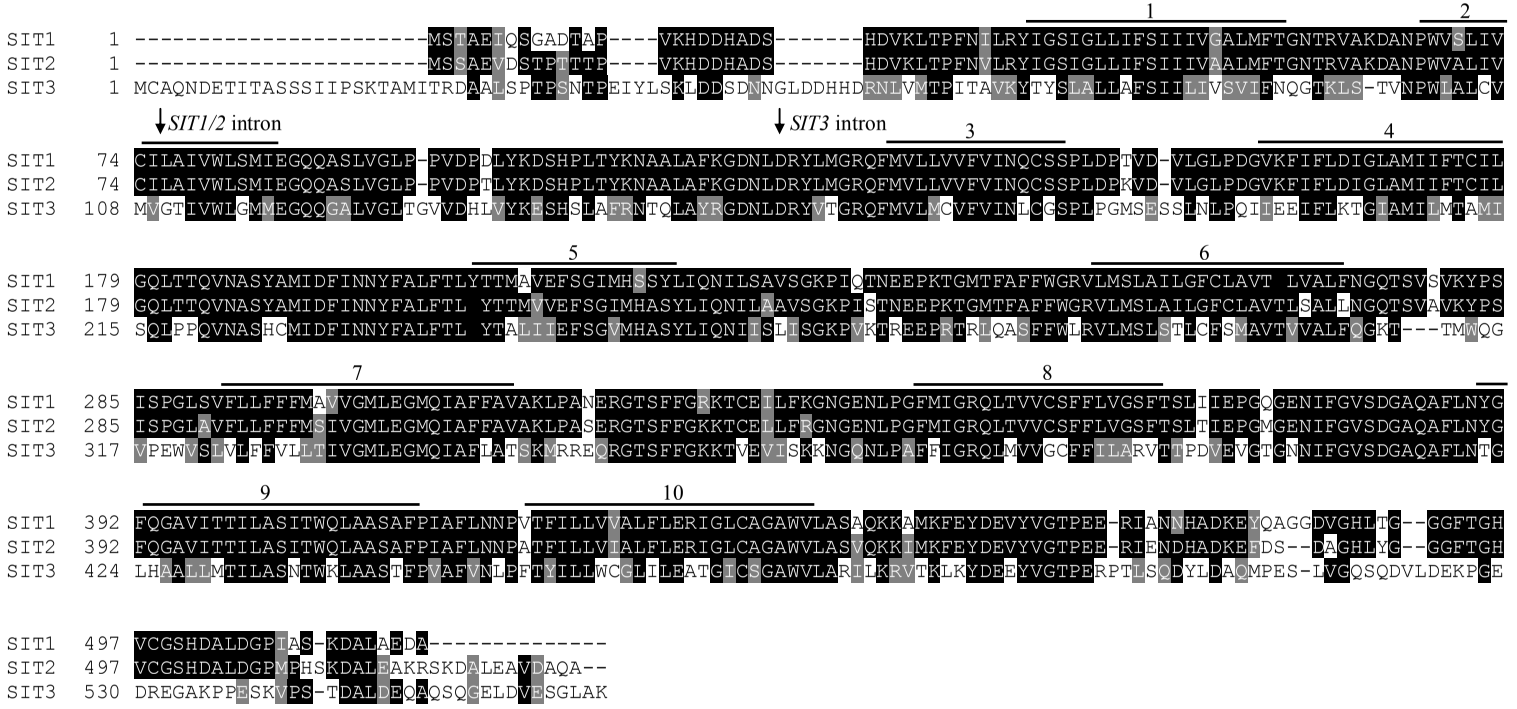

Figure 3.1. Predicted amino acid alignment of TpSITs. Residue number is shown on the left. Black shading indicates identical residues and gray shading represents conserved substitutions. Black lines and numbers over alignment denote transmembrane segments as predicted by HMMTOP (Tusnády and Simon 2001) on a multiple sequence alignment of 10 SIT sequences (Thamatrakoln et al. 2006). Arrows indicate location of introns in each SIT.

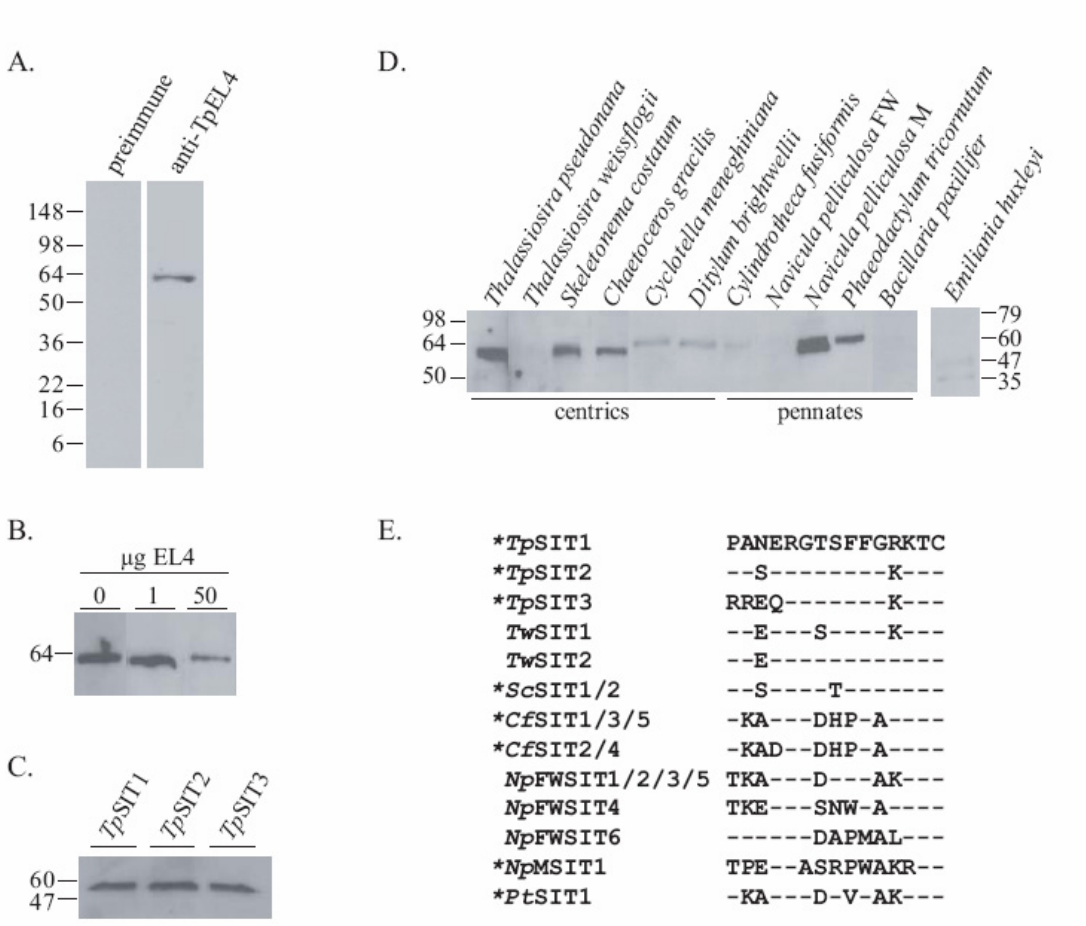

Figure 3.2. Characterization of anti-TpEL4. Molecular weight markers (kDa) are shown for each Western blot. A. Western blot of *T. pseudonana* whole cell protein lysates using preimmune serum and anti-TpEL4. B. Western blot on protein lysates using anti-TpEL4 preincubated with 0, 1, or 50 µg of EL4 peptide. C. Western blot of *S. cerevisiae* transformed to express TpSIT1, TpSIT2, or TpSIT3. D. Western blot on protein lysates from various diatom species and the coccolithophore, *Emiliania huxleyi*. E. Amino acid alignment of SITs from different diatoms in the region used to generate anti-TpEL4. TpSIT1 is shown on the first line. SIT sequences are identified by the initials for genus and species as follows: *Tp, Thalassiosira pseudonana; Tw, T. weisflogii; Sc, Skeletonema costatum; Cf, Cylindrotheca fusiformis; NpFW, Navicula pelliculosa FW; Np*M*, N. pelliculosa* M*; Pt, Phaeodactylum tricornutum*. Dashes indicate residues identical to TpSIT1. Stars indicate those species that cross-reacted with anti-TpEL4.

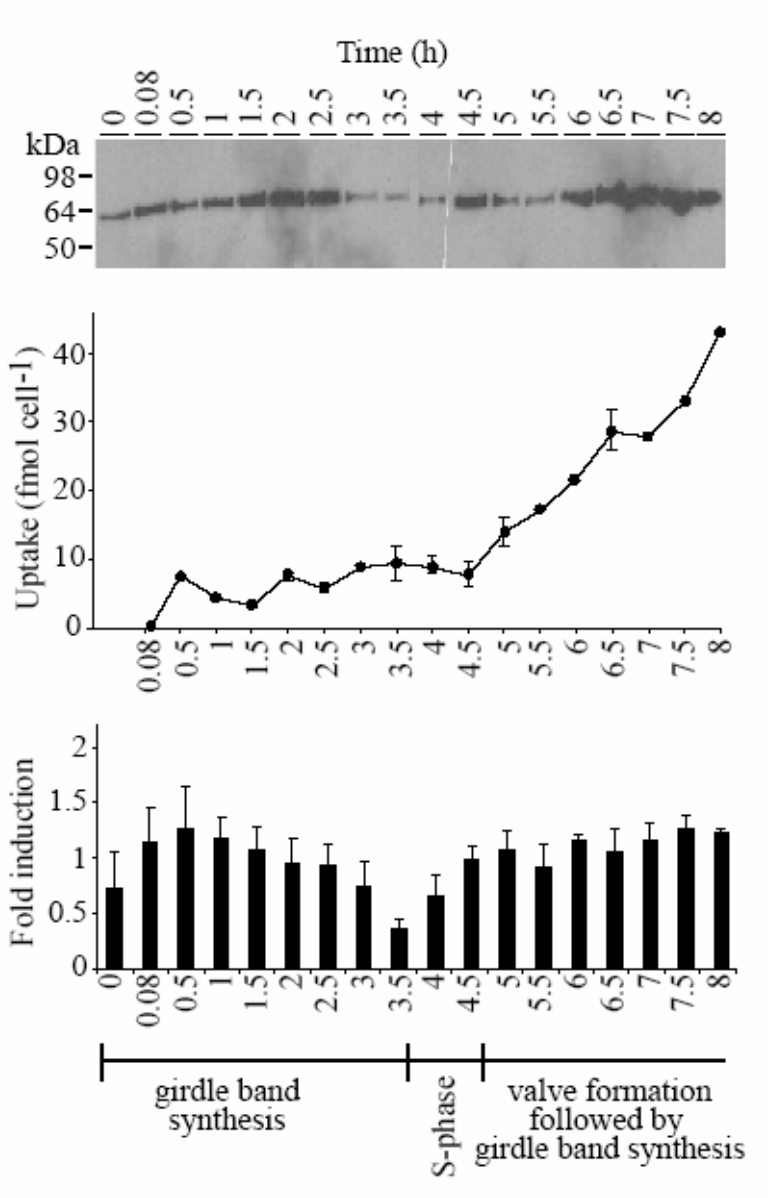

Figure 3.3. Analysis of SIT protein levels during synchronized cell growth. Time (h) during synchronized cell growth is shown. Top panel is Western analysis of whole cell protein lysates of equal cell number using anti-TpEL4. Middle panel is net silicic acid uptake during the synchrony. Bottom panel shows the mean fold induction based on relative densitometric units of three separate experiments (see Materials and Methods). Error bars are standard error. Cellular events during the synchrony are denoted at bottom.

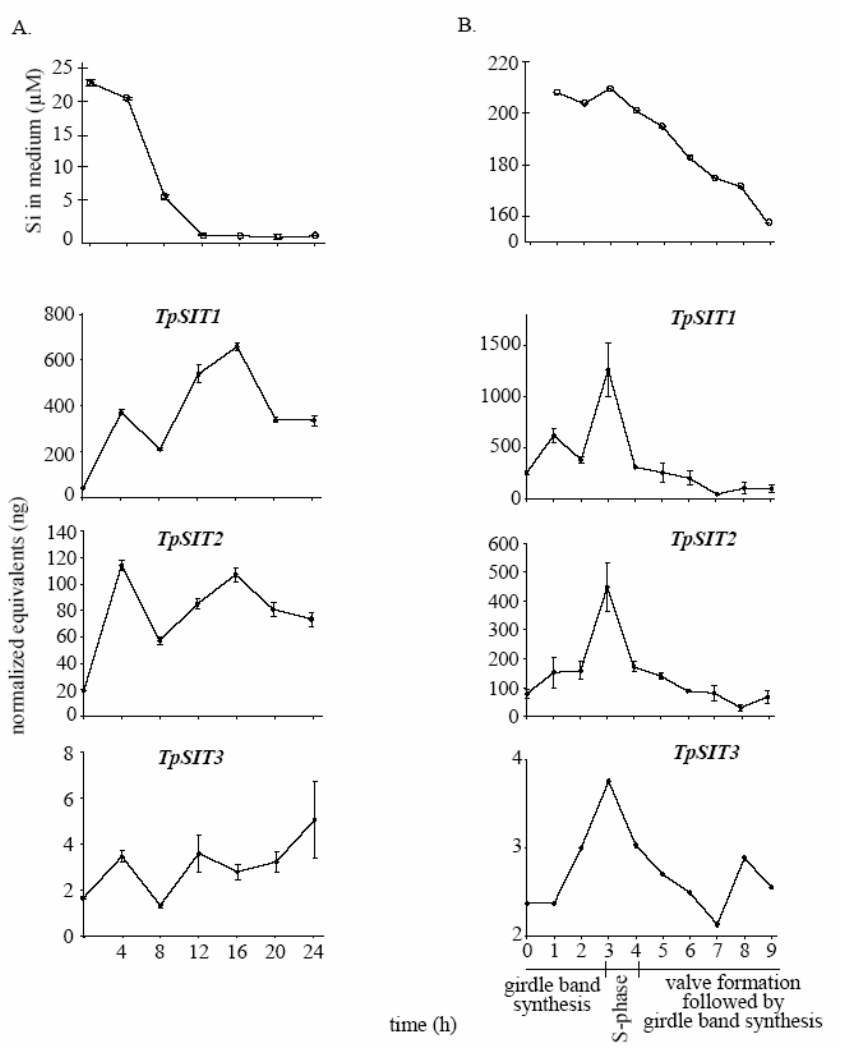

Figure 3.4. mRNA levels of *TpSIT1*, *TpSIT2*, and *TpSIT3* determined by QPCR during a gradual silicon starvation experiment (A), or a synchronized growth experiment (B). Top graphs in A and B are the mean value of triplicate measurements of silicon concentration in the medium with error bars showing standard deviation. A. Bottom three graphs are QPCR data for cells harvested during gradual silicon starvation. Time zero represents cells harvested just after inoculation. Mean values of duplicate technical replicates are shown with standard error. B. Bottom three graphs are data obtained during synchronized cell division. Time zero represents cells harvested prior to the addition of silicon. Mean values of triplicate technical replicates are shown for *TpSIT1* and *TpSIT2*, with the exception of t = 1 h for *TpSIT1* which is mean value of duplicate experiments. Errors bars represent standard error. Data from a single experiment for *TpSIT3* is shown. Note the difference in scale of the y-axis for *TpSIT3* in both panels. mRNA levels are plotted as normalized ng equivalents of standards of genomic DNA (see Materials and Methods). Cellular events during the synchrony are shown at bottom. (Frigeri et al. 2006).

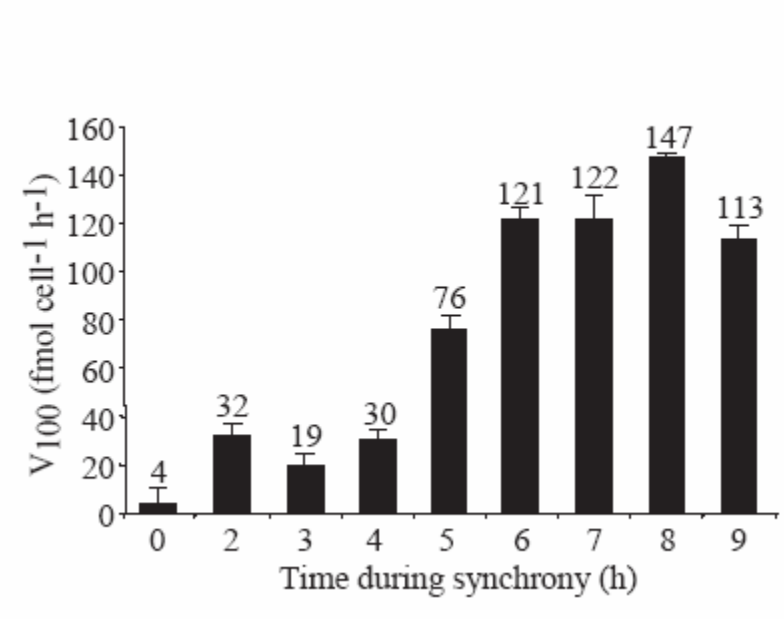

Figure 3.5. Maximum rates of surge uptake at 100 μM silicate (V100) during synchronized cell growth. Average values from triplicates are shown, with error bars as standard deviations. Numbers above bars are V100 values.

REFERENCES

Altschul SF, W Gish, W Miller, EW Myers and DJ Lipman (1990). Basic local alignment search tool. *J. Mol. Biol.* 215: 403-410.

Armbrust EV, JA Berges, C Bowler, BR Green, D Martinez, NH Putnam, S Zhou, AE Allen, KE Apt, M Bechner, MA Brzezinski, BK Chaal, A Chiovitti, AK Davis, MS Demarest, JC Detter, T Glavina, D Goodstein, MZ Hadi, U Hellsten, M Hildebrand, BD Jenkins, J Jurka, VV Kapitonov, N Kröger, WWY Lau, TW Lane, FW Larimer, JC Lippmeier, S Lucas, M Medina, A Montsant, M Obornik, MS Parker, B Palenik, GJ Pazour, PM Richardson, TA Rynearson, MA Saito, DC Schwartz, K Thamatrakoln, K Valentin, A Vardi, FP Wilkerson and DS Rokhsar (2004). The genome of the diatom *Thalassiosira pseudonana*: ecology, evolution, and metabolism. *Science* 306: 79-86.

Azam F (1974). Silicic acid uptake in diatoms studied with [^{68}Ge] germanic acid as a tracer. *Planta* 121: 205-212.

Bendz G and I Lindqvist, Eds. (1978). The Biochemistry of Silicon and Related Problems. New York, N.Y., Plenum Press.

Bhattacharyya P and BE Volcani (1980). Sodium dependent silicate transport in the apochlorotic marine diatom *Nitzschia alba*. *Proc. Natl. Acad. Sci. U.S.A.* 77: 6386-6390.

Birchall JD (1995). The essentiality of silicon in biology. *Chem. Soc. rev.* 24: 351-357.

Bryant N, R Govers and D James (2002). Regulated transport of the glucose transporter GLUT4. *Nat Rev Mol Cell Biol* 3: 267-277.

Brzezinski MA (1992). Cell-cycle effects on the kinetics of silicic acid uptake and resource competition among diatoms. *J. Plankton Res.* 14: 1511-1539.

Brzezinski MA, RJ Olson and SW Chisholm (1990). Silicon availability and cell cycle progression in marine diatoms. *Mar. Ecol. Prog. Ser.* 67: 83-96.

Carlisle EM (1981). Silicon in bone formation *in* Silicon and Siliceous Structures in Biological Systems. TL Simpson and BE Volcani. New York, N.Y., Springer-Verlag: 69-94.

Claquin P, V Martin-Jézéquel, JC Kromkamp, MJ Veldhuis and GW Kraay (2002). Uncoupling of silicon compared with carbon and nitrogen metabolisms and the role of the cell cycle in continuous cultures of *Thalassiosira pseudonana* (Bacillariophyceae) under light, nitrogen, and phosphorous control. *J. Phycol.* 38: 922-930.

Combet C, C Blanchet, C Geourjon and G Deleage (2000). NPS@: Network Protein Sequence Analysis. *Trends Biochem. Sci.* 25: 147-150.

Conway HL and PJ Harrison (1977). Marine diatoms grown in chemostats under silicate or ammonium limitations. IV. Transient response of *Chaetoceros debilis*, *Skeletonema costatum*, and *Thalassiosira gravida* to a single addition of the limiting nutrient. *Mar. Biol.* 43: 33-43.

Conway HL, PJ Harrison and CO Davis (1976). Marine diatoms grown in chemostats under silicate or ammonium limitation. II. Transient response of *Skeletonema costatum* to a single addition of the limiting nutrient. *Mar. Biol.* 35: 187-199.

Crawford RM (1981). The siliceous components of the diatom cell wall and their morphological variation *in* Silicon and Siliceous Structures in Biological Systems. TL Simpson and BE Volcani. New York, N.Y., Springer-Verlag: 129-156.

Crawford RM and AMM Schmid (1986). Ultrastructure of silica deposition in diatoms *in* Biomineralization in Lower Plants and Animals. BS Leadbeater and R Riding. London, U.K., The Systematics Society. 30: 291-314.

Darley WM and BE Volcani (1969). Role of silicon in diatom metabolism: A silicon requirement for deoxyribonucleic acid synthesis in the diatom *Cylindrotheca fusiformis* Reimann and Lewin. *Exp. Cell Res.* 58: 334-342.

Del Amo Y and MA Brzezinski (1999). The chemical form of dissolved Si taken up by marine diatoms. *J. Phycol.* 35: 1162-1170.

Dubois E and M Grenson (1979). Methylamine/ammonia uptake systems in *Saccharomyces cerevisiae*: multiplicity and regulation. *Mol Gen Genet* 175: 67-76.

Dugani CB and A Klip (2005). Glucose transporter 4: cycling, compartments and controversies. *EMBO reports* 12: 1137-1142.

Epstein E (1994). The Anomaly of Silicon in Plant Biology. *Proc. Natl. Acad. Sci. U.S.A.* 91: 11-17.

Forsberg H and PO Ljungdahl (2001). Sensors of extracellular nutrients in *Saccharomyces cerevisiae*. *Curr. Genet.* 40: 91-109.

Frigeri LG, TR Radabaugh, PA Haynes and M Hildebrand (2006). Identification of proteins from a cell wall fraction of the diatom *Thalassiosira pseudonana*: Insights into silica structure formation. *Mol. Cell. Proteomics* 5: 182-193.

Gietz RD and RA Woods (2002). Transformation of yeast by the LiAc/SS carrier DNA/PEG method. *Methods Enzymol.* 350: 87-96.

Guillard RR and JH Ryther (1962). Studies of marine planktonic diatoms. I. *Cyclotella nana* Hustedt and *Detonula confervacea* Cleve. *Can. J. Microbiol.* 8: 229-239.

Guillard RRL (1975). Culture of phytoplankton for feed marine invertebrates *in* Culture of Marine Invertebrate Animals. WL Smith and MH Chanley. New York, N.Y., Plenum Press: 29-60.

Hildebrand M, LG Frigeri and AK Davis (in press). Synchronized growth of *Thalassiosira pseudonana* (Bacillariophyceae) provides novel insights into cell wall synthesis processes in relation to the cell cycle. *J. Phycol.*

Hildebrand M (2000). Silicic acid transport and its control during cell wall silicification in diatoms *in* Biomineralization: From Biology to Biotechnology and Medical Applications. E Bäuerlein. Weinheim, Wiley-VCH: 171-188.

Hildebrand M and K Dahlin (2000). Cloning and characterization of nitrate transporter genes from the diatom *Cylindrotheca fusiformis*. *J. Phycol.* 36: 30-.

Hildebrand M, K Dahlin and BE Volcani (1998). Characterization of a silicon transporter gene family in *Cylindrotheca fusiformis*: Sequences, expression analysis, and identification of homologs in other diatoms. *Mol. Gen. Genet.* 260: 480-486.

Hildebrand M, BE Volcani, W Gassmann and JI Schroeder (1997). A gene family of silicon transporters. *Nature* 385: 688-689.

Iraqui I, S Vissers, F Bernard, J-O de Craene, E Boles, A Urrestarazu and B Andre (1999). Amino acid signaling in *Saccharomyces cerevisiae*: a permease-like sensor of external amino acids and F-box protein Grr1p are required for transcriptional induction of the AGP1 gene, which encodes a broad-specificity amino acid permease. *Mol. Cell. Biol.* 19: 989-1001.

Kasahara T and M Kasahara (2003). Transmembrane segments 1, 5, 7, and 8 are required for high-affinity glucose transport by *Saccharomyces cerevisiae* Hxt2 transporter. *Biochem. J.* 372: 247-252.

Ko CH, H Liang and RF Gaber (1993). Roles of multiple glucose transporters in *Saccharomyces cerevisiae*. *Mol. Cell. Biol.* 13: 638-648.

Lewin JC (1954). Silicon metabolism in diatoms. I. Evidence for the role of reduced sulfur compounds in silicon utilization. *J. Gen. Physiol.* 37: 589-599.

Lewin JC (1955). Silicon metabolism in diatoms. III. Respiration and silicon uptake in *Navicula pelliculosa*. *Can. J. Microbiol.* 3: 427-433.

Lorenz MC and J Heitman (1998). The MEP2 ammonium permease regulates pseduohyphal differentiation in *Saccharomyces cerevisiae*. *EMBO J* 17: 1236-1247.

Ma JF, K Tamai, N Yamaji, N Mitani, S Konishi, M Katsuhara, M Ishiguro, Y Murata and M Yano (2006). A silicon transporter in rice. *Nature* 440: 688-691.

Marini A-M, S Soussi-Boudekou, S Vissers and B André (1997). A family of ammonium transporters in *Saccharomyces cerevisiae*. *Mol. Cell. Biol.* 17: 4282-4293.

Marini A-M, S Vissers, A Urrestarazu and B André (1994). Cloning and expression of the *MEP1* gene encoding an ammonium transporter in *Saccharomyces cerevisiae*. *EMBO J* 13: 3456-3463.

Martin-Jézéquel V, M Hildebrand and MA Brzezinski (2000). Silicon metabolism in diatoms: Implications for growth. *J. Phycol.* 36: 821-840.

Milligan A, DE Varela, MA Brzezinski and FMM Morel (2004). Dynamics of silicon metabolism and silicon isotopic discrimination in a marine diatom as a function of *p*CO2. *Limnol. Oceanog.* 49: 322-329.

Neigeborn L, P Schwartzberg, R Reid and M Carlson (1986). Null mutations in the *SNF3* gene of *Saccharomyces cerevisiae* cause a different phenotype than do previously isolated missense mutations. *Mol. Cell. Biol.* 6: 3569-3574.

Nelson DM, P Tréguer, MA Brzezinski and A Leynaert (1995). Production and dissolution of biogenic silica in the ocean: revised global estimates, comparison with regional data and relationship to biogenic sedimentation. *Global Biogeochemical Cycles* 9: 359-372.

Nielsen H, J Engelbrecht, S Brunak and G von Heijne (1997). Identification of prokaryotic and eukaryotic signal peptides and prediction of their cleavage sites. *Protein Eng.* 10: 1-6.

Özcan S, J Dover, AG Rosenwald and SJ Wölfl, M. (1996). Two glucose transporters in *Saccharomyces cerevisiae* are glucose sensors that generate a signal for induction of gene expression. *Proc. Natl. Acad. Sci. U.S.A.* 93: 12428-12432.

Pickett-Heaps J, AMM Schmid and LA Edgar (1990). The cell biology of diatom valve formation *in* Progress in Phycological Research. FE Round and DJ Chapman. Bristol, Biopress Ltd. 7: 1-168.

Reimann BEF, JC Lewin and BE Volcani (1966). Studies on the biochemistry and fine structure of silica shell formation in diatoms. II. The structure of the cell wall of *Navicula pelliculosa* (Breb.) Hilse. *J. Phycol.* 2: 74-84.

Richmond KE and M Sussman (2003). Got silicon? The non-essential beneficial plant nutrient. *Curr. Opin. Plant Biol.* 6: 268-272.

Schmid AMM (1994). Aspects of morphogenesis and function of diatom cell walls with implication for taxonomy. *Protoplasma* 181: 43-60.

Schmid AMM, MA Borowitzka and BE Volcani (1981). Morphogenesis and biochemistry of diatom cell walls *in* Cytomorphogenesis in Plants. O Kiermayer. New York, N.Y., Springer-Verlag. 8: 63-97.

Schwarz K and DB Milne (1972). Growth-promoting effects of silicon in rats. *Nature* 239: 333-334.

Strickland JDH and TR Parsons (1968). A practical handbook of sea water analysis. *Bull. Fish. Res. Board. Canada* 167: 1-311.

Sullivan CW (1976). Diatom mineralization of silicic-acid. I. $Si(OH)_4$ transport characteristics in *Navicula pelliculosa*. *J. Phycol.* 12: 390-396.

Sullivan CW (1977). Diatom mineralization of silicic acid. II. Regulation of $Si(OH)_4$ transport rates during the cell cycle of *Navicula pelliculosa*. *J. Phycol.* 13: 86-91.

Thamatrakoln K, AJ Alverson and M Hildebrand (2006). Comparative sequence analysis of diatom silicon transporters: towards a mechanistic model for silicon transport. *J. Phycol.* 42: 822-834.

Thompson JD, DR Higgins and TJ Gibson (1994). CLUSTAL W: improving the sensitivity of progressive multiple sequence alignment through sequence weighting, position-specific gap penalties and weight matrix choice. *Nucleic Acids Res.* 22: 4673-4680.

Tréguer P, DM Nelson, AJ Van Bennekom, DJ DeMaster, A Leynaert and B Queguiner (1995). The silica balance in the world ocean: A reestimate. *Science* 268: 375-379.

Tréguer P and P Pondaven (2000). Silica control of carbon dioxide. *Nature* 406: 358-359.

Tusnády GE and I Simon (2001). The HMMTOP transmembrane topology prediction server. *Bioinformatics* 17: 849-850.

Van Belle D and B André (2001). A genomic view of yeast membrane transporters. *Curr. Opin. Cell Biol.* 13: 389-398.

chapter IV

Silicon uptake kinetics in diatoms revisited: a model for saturable and nonsaturable kinetics and the role of silicon transporters

ABSTRACT

Previous work measuring $Si(OH)_4$ uptake in diatoms demonstrate both nonsaturable and Michaelis-Menten type saturable kinetics. Reasons for this are unclear and mechanistic explanations for nonsaturable kinetics are lacking. Using ^{68}Ge as a radiotracer for $Si(OH)_4$ uptake, we showed a time-dependent transition occurred from nonsaturable to saturable uptake kinetics in multiple diatoms species, including *Thalassiosira pseudonana.* Use of a specific antibody against *T. pseudonana* silicon transporters (SITs) affected both nonsaturable and saturable kinetics, suggesting SITs are the predominant means of $Si(OH)_4$ transport in diatoms. Cells grown under Si-replete conditions showed nonsaturable short-term uptake kinetics, while those prestarved for silicon were saturable. Data suggest nonsaturability was due to surge uptake when intracellular silicon pool capacity exceeded the requirement of silica for cell wall incorportion, and saturability occurred when these two factors became equilibrated. In addition, at low $Si(OH)_4$ concentrations, when pool capacities were high, saturable kinetic features indicative of SITs were visible. SITs appeared to have enormous flexibility in transport rate and, if left unregulated, allowed $Si(OH)_4$ uptake into the cell very quickly at high substrate concentrations. We also demonstrated that zinc is not directly involved in $Si(OH)_4$ uptake, as was previously suggested. A model for $Si(OH)_4$ uptake in diatoms based on the interplay between SITs, intracellular pools, and cell wall silica incorporation was developed and consistently explains results in this and previous investigations. Data suggest previous studies most likely measured kinetics of cell wall silica incorporation, but that these values could still reasonably correspond with the uptake kinetics at low $Si(OH)_4$ concentrations.

INTRODUCTION

For decades, models of Michaelis-Menten type saturable kinetics of nutrient uptake and assimilation in phytoplankton have guided our understanding of how the cell translates nutrient availability into growth (Eppley et al. 1969; Sullivan 1976; 1977; McCarthy 1981; Del Amo and Brzezinski 1999). However, several studies suggest uptake, under certain conditions, is nonsaturable and in some cases, biphasic (Wheeler et al. 1982; Collos et al. 1992; Watt et al. 1992; Collos et al. 1997; Lomas and Glibert 1999). Conclusions regarding uptake kinetics of nutrients have been variable, due in part to differences in the methods applied, making comparison of data difficult. Factors contributing to these variations include species-specific or cell size differences, the physiological state of cultures, the incubation period, and nutrient concentration range over which uptake is measured (Sullivan 1976; Wheeler et al. 1982; Harrison et al. 1989; Collos et al. 1992; Lomas and Glibert 1999; Leynaert et al. 2004). The attractive simplicity of a Michaelis-Menten kinetic model for uptake (control by the transporter itself, similar to an enzymatic process) in some cases may have precluded efforts to explain factors involved in nonsaturating kinetics. However, transporters generally do not convert a molecule from one form to another (i.e. they are not enzymes), but are engaged in generating what is oftentimes a non-equilibrium gradient of a molecule across a lipid bilayer. Thus, other factors involved in generating and maintaining the state of equilibrium will influence the kinetic properties of transport.

Most diatoms have an obligate requirement for silicon for cell wall formation, with the predominant transported form of silicon being silicic acid, or $Si(OH)_4$ (Del

Amo and Brzezinski 1999). Factors influencing the equilibrium state of $Si(OH)_4$ uptake in diatoms include, low extracellular $Si(OH)_4$ concentrations (less than 100 μM; Tréguer et al. 1995; Martin-Jézéquel et al. 2000), high intracellular concentrations (up to hundreds of mM), and different forms of silicon - extracellular being silicic acid or silicate, intracellular consisting of soluble pools of free silicic acid and silicic acid complexed to organic compounds, and the solid form of silica in the cell wall (Martin-Jézéquel et al. 2000). Unlike other nutrients, silicic acid has a unique chemistry in that it autopolymerizes into silica at concentrations above 2 mM (Iler 1979). Intracellular binding to organic compounds are proposed to maintain supersaturated levels in a soluble form (Hildebrand 2000) and the balance between these organic binding-components and free $Si(OH)_4$ will also influence the equilibrium state of $Si(OH)_4$ uptake. Silicon efflux is an often overlooked and under-appreciated aspect of balancing the overall cellular silicon budget (Azam et al. 1974; Sullivan 1976; Milligan et al. 2004), and net uptake involves both uptake and efflux (Milligan et al. 2004).

Numerous studies have reported Michaelis-Menten type saturation kinetics of $Si(OH)_4$ uptake in diatoms, but occasionally nonsaturable or biphasic kinetics have been observed (Table 4.1). In each study documenting Michaelis-Menten type saturation kinetics, either, 1) cultures were preincubated in Si-minus medium prior to measuring uptake, 2) uptake was measured over long (h) incubation times, or 3) low $Si(OH)_4$ concentrations were used (Table 4.1). When these conditions were not followed, nonsaturable uptake kinetics were observed (Table 4.1). Possible

explanations for nonsaturating kinetics have been lacking, perhaps because this has not been consistently (or controllably) seen.

Silicic acid transport occurs through specific membrane-associated proteins called silicon transporters (SITs), originally identified in the marine pennate diatom, *Cylindrotheca fusiformis* (Hildebrand et al. 1997; Hildebrand et al. 1998). Consistent with data from whole cell uptake studies, SITs are specific for silicic acid and uptake is sodium-dependent (Hildebrand et al. 1997). SITs have since been identified in numerous other diatom species as well as the Chrysophytes, *Synura petersenii* and *Ochromonas ovalis* (Grachev et al. 2002; Sherbakova et al. 2005; Likhoshway et al. 2006; Thamatrakoln et al. 2006). Mechanistic models for transport have recently been proposed (Sherbakova et al. 2005; Thamatrakoln et al. 2006), including one (Sherbakova et al. 2005) with an explanation for a proposed involvement of zinc in $Si(OH)_4$ uptake (Rueter and Morel 1981).

Three modes of silicon uptake in diatoms, surge uptake, externally controlled uptake, and internally controlled uptake, have been defined from chemostat experiments, (Conway et al. 1976; Conway and Harrison 1977). Surge uptake occurs upon initial addition of silicon to silicon-starved cells with maximal uptake rates occurring at this time. Externally controlled uptake occurs when extracellular silicon is low, and the rate of uptake is dictated by external silicon concentrations. In internally controlled uptake, rates are regulated by the intracellular utilization of silicon, proposed to be the rate of silica incorporation into the cell wall (Conway et al. 1976; Conway and Harrison 1977). In most diatom species tested, silica incorporation and silicic acid uptake are temporally coupled (Chisholm et al. 1978), and experiments

monitoring uptake and incorporation under different conditions confirm a direct correlation between these two processes (Hildebrand and Wetherbee 2003; Hildebrand et al. in press). Although surge uptake occurs, during which short-term uptake rates are higher than the cells' need for silicon, over longer time scales, the rate of silica incorporation is the major controlling factor over the rate of silicon transport into cell (Conway et al. 1976; Conway and Harrison 1977; Hildebrand and Wetherbee 2003; Hildebrand et al. in press).

Based on previous studies, a model for silicic acid transport into the diatom cell has been developed, which involves control by the rate of silica incorporation through the intermediary of intracellular soluble silicon pools (Conway et al. 1976; Conway and Harrison 1977; Hildebrand 2000; Hildebrand and Wetherbee 2003). Intracellular pools are at extremely high concentrations in diatoms, with measurements ranging from 19 – 340 mM (Martin-Jézéquel et al. 2000). Such concentrations are far above saturability for silica polymerization (c.a. 2 mM at neutral pH – Iler 1979), suggesting there must be a mechanism for stabilizing silicic acid in an unpolymerized form, possibly through interaction with intracellular silicon-binding components (Hildebrand 2000; Hildebrand and Wetherbee 2003). Electron spectroscopic imaging of *Thalassiosira pseudonana* showed silicon is dispersed throughout the cytoplasm (Rogerson et al. 1987) and not sequestered in vesicles, as was previously suggested (Schmid and Schulze 1979). A hypothesis most consistent with the data is that intracellular silicon is bound by as yet uncharacterized organic molecules (Azam et al. 1974; Sullivan 1979; Hildebrand 2000; Hildebrand and Wetherbee 2003). In this case, the chemical form of bound intracellular silicon would be different from extracellular

silicic acid, and this would contribute to maintenance of a high (>1,000 fold) concentration gradient across the plasma membrane. It was suggested that under conditions of internally controlled uptake the level of saturation of intracellular pools provided a feedback mechanism that connected silica incorporation with uptake (Conway and Harrison 1977). When incorporation rates were high, intracellular pools would be depleted and uptake stimulated, and when incorporation rates were low, pools would be saturated and uptake inhibited. Subsequent work (Hildebrand and Wetherbee 2003) showed general agreement with this, however in an experiment in which incorporation was inhibited, resulting in a similar inhibition of uptake, intracellular pools did not reach their maximum level, indicating the pools do not have to be saturated (at maximum levels) to control uptake. It was proposed (Hildebrand 2000; Hildebrand and Wetherbee 2003) that the ratio of bound to unbound intracellular silicic regulated uptake. In the presence of excess binding component, uptake would be induced, and in the presence of excess unbound silicic acid, efflux would be induced by the favorable concentration gradient for export of the same chemical moiety that was transported into the cell (i.e. $Si(OH)_4$). This is consistent with data showing that efflux does not occur in the absence of extracellular silicon and increases with increasing extracellular concentrations due to excess surge uptake (Sullivan 1976). The capacity of the cell to maintain soluble silicic acid in the cytoplasm could vary, as has been shown experimentally (Martin-Jézéquel et al. 2000; Hildebrand and Wetherbee 2003; Claquin and Martin-Jézéquel 2005), depending on the amount of binding component present. Thus, measurements of intracellular soluble silicon may be underestimates of the total *capacity* of the pools.

The described model for silicic acid transport deals mainly with equilibrium processes, and is not integrated with kinetic parameters. In order to do so, previous kinetic results (Table 4.1) must be clarified and specific conditions in which saturating or nonsaturating kinetics are observed must be determined. Because surge uptake and efflux over short time scales (min) are major aspects of transport (Conway et al. 1976; Conway and Harrison 1977; Milligan et al. 2004), measuring short term uptake kinetic parameters is essential. Of the available methods, the radiotracer analog of silicic acid, $^{68}Ge(OH)_4$, is ideal because it is available in high specific activity and carrier-free form, has a relatively long half-life of 282 days, and has well-established protocols for measuring silicic acid transport in diatoms (Azam 1974; Azam et al. 1974; Sullivan 1976; 1977). The alternative ^{32}Si is cost-prohibitive and available only in low specific activity, preventing its use in short-term incubations where high activity is needed. ^{31}Si has the drawback of a half life of only 156 min, making it technically challenging to use, particularly in long term (h) incubations. Using ^{30}Si is laborious because it requires samples be analyzed by mass spectrometry (Nelson and Goering 1977). In this report, we determine the conditions that produce nonsaturable and saturable $Si(OH)_4$ uptake kinetics, leading to a consistent picture of factors controlling the kinetics of $Si(OH)_4$ uptake in diatoms and the role of silicon transporters.

MATERIALS AND METHODS

Culture conditions

Thalassiosira pseudonana Hasle et Heimdale clone 3H CCMP1335 (Provasoli-Guillard National Center for Culture of Marine Phytoplankton, Bigelow Laboratory

for Ocean Sciences), *Thalassiosira weissflogii* (Grunow) Fryxell et Hasle CCMP1336, *Cylindrotheca fusiformis* Reimann et Lewin CCMP343, *Navicula pelliculosa* (Bréb.) Hilse UTEX 688 (The Culture Collection of Algae at the University of Texas at Austin; a freshwater strain, referred to as *N. pelliculosa* FW in text), *Navicula pelliculosa* (Breb. et Kuetzing) Hilse CCMP543 (a marine strain, referred to as *N. pelliculosa* M in text), *Phaeodactylum tricornutum* Bohlin CCMP1327, *Chaetoceros gracilis* Schütt UTEX LB2658, and *Nitzschia alba* Lewin and Lewin CCMP2426 were grown in batch culture under continuous illumination with cool white fluorescent lights at approximately 150 µmole quanta m^{-2} s^{1} at 18 to 20° C. *N. pelliculosa* FW was grown in fresh water tryptone (FWT) medium (Reimann et al. 1966). All other diatom species were grown in artificial seawater (ASW) medium (Darley and Volcani 1969) with biotin and vitamin B12 added to 1 ng L^{-1}or f/2 medium made with 0.2 µm filtered and autoclaved local seawater (Guillard and Ryther 1962; Guillard 1975).

$Si(OH)_4$ uptake kinetic measurements

To avoid possible cell cycle and cell phasing effects, exponentially growing, non-phased cultures were used in all measurements. Cells were harvested by centrifugation at 3000 x g for 5 min, then washed and resuspended in Si-minus medium, and cell counts determined to cell cocentration. Preliminary measurements were done to determine the optimal cell concentration for each species that would result in counts significantly above background. This was $2.5x10^5$ cells ml^{-1} for most species with the exception of *Phaeodactylum tricornutum* and *Navicula pelliculosa* FW, which required $2.0x10^6$ cells ml^{-1}. Silicic acid uptake was measured using

$^{68}Ge(OH)_4$ as a radiotracer for silicic acid (Azam 1974; Sullivan 1976). Stock solutions containing 1.0 µCi ml^{-1} of $^{68}Ge(OH)_4$ and ten-fold concentrations of freshly made sodium silicate in 3.5% NaCl (MilliQ-treated water for *N. pelliculosa* FW) were prepared, and for a given concentration of silicate, 100 µl of ^{68}Ge:silicate stock per 1 ml of cells were assayed. The volume needed to cover all time points in a given experiment was calculated (e.g. 7 ml for 6 time points) and the amount of stock and cells used scaled appropriately, with the ^{68}Ge:silicate stock being placed in the tube first, then cells added and mixed. For most experiments, 1, 2, 4, 8, 10 15, 30 and 100 µmol L^{-1} final silicate concentrations were used, with duplicates being done for 8-30 µmol L^{-1} because initial experiments indicated interesting features in this range. For experiments using different concentrations, these are described in the figure legend for the experiment. Cells were incubated in the light at approximately 150 µmole quanta m^{-2} s^{1} at 18 to 20° C, and aliquots removed at different times, vacuum filtered on a Millipore Isopore 1.2 µm RTTP membrane, and washed once with 5 ml 3.5% NaCl (MilliQ-treated water for *N. pelliculosa* FW). Background was minimal with this wash treatment. For measurement of background, 1 ml of cells was added to separate tubes containing 100 µl of ^{68}Ge:silicate, and immediately pipetted onto a Millipore membrane and washed. This manipulation took 8-10 sec, so cellular binding and some uptake may have occurred during this time, but because this would be minimal, and a consistent procedure was used in all experiments, subtraction of 0 min from the longer time points was used to calculate net uptake for those time points. After washing, filters were placed in a gamma counter vial, and counted using a LKB Wallac 1282 Compugamma CS Universal gamma counter (Perkin-Elmer, Wellesley, MA). Counts

per minute were converted to fmol $cell^{-1}$ h^{-1}, taking into account counting efficiency, dilution effects, and radioactive decay. Data obtained using this method will be referred to as $Si(OH)_4$ uptake (Sullivan 1976).

Measurements of cell wall silica and intracellular soluble silicon pools

Aliquots of cells (approximately 1.3 x 10^7 each) during exponential growth were harvested in 14 ml Falcon 1029 polypropylene tubes and pelleted at 16,500 x g in an HB-4 rotor (Sorvall™, Thermo Electron Corporation, Asheville, NC, USA) for 4 min. The supernatant was aspirated, cells were resuspended in 1 ml Si-minus medium, transferred to a microfuge tube, and repelleted. Supernatant was aspirated, and cell pellets stored at –20° C. Intracellular soluble silicon pool levels were measured using the boiling water method of Sullivan (1979). Frozen cells were resuspended in 1 ml MilliQ treated water, placed in a boiling water bath for 10 min, cooled, and then centrifuged for 5 min at 16,500 x g in an HB-4 rotor. Triplicate samples of supernatant were assayed for intracellular silicon. Cell wall silica was determined by resuspending the boiled cell pellet in 4 ml 0.5N NaOH (made from solid NaOH dissolved in MilliQ water) and placing the tube in a boiling water bath for 15 min. After cooling, 2 ml 1N HCl was added to neutralize the sample, which was then centrifuged for 5 min at 16,500 x g in an HB-4 rotor. Triplicate samples of supernatant were assayed to measure cell wall silica. Silicic acid concentrations were measured using the silicomolybdate assay (Strickland and Parsons 1968) modified for a 96-well plate format. Twenty-five microliters of supernatant was added to 100 µl MilliQ water, 50 µl of molybdate reagent was added, mixed, and allowed to incubate for 10 min at

room temperature, and then 75 µl of reducing agent was added and mixed. Samples were incubated for 3 h at room temperature with occasional mixing, prior to measuring the absorbance at 810 nm on a SpectraMax M2 Microplate Reader (Molecular Devices, Sunnyvale, CA). The standard was sodium hexafluorosilicate (Sigma, St. Louis, MO), used in a range of 0-50 µmol L^{-1}.

Statistical analysis

Nonlinear regressions were obtained using the software program GraphPad Prism 4 (San Diego, CA). Best-fit curves were obtained using Michaelis-Menten hyperbolas, or an allosteric-enzyme model using built-in equations in the Prism software.

Preincubation with antibody specific for *T. pseudonana* silicon transporters

Anti-TpEL4 is a polyclonal antibody generated against a peptide sequence of *T. pseudonana* SIT1 that cross reacts with each of the three *T. pseudonana SIT* genes (Thamatrakoln and Hildebrand, submitted for publication). Exponentially growing cells of *T. pseudonana* were incubated with a 1:10 dilution of anti-TpEL4 for 1 h. Cells were then harvested by centrifugation, washed and resuspended in Si-minus ASW. Short-term uptake (2 min) was measured as described.

Effect of zinc chelators on silicon uptake

A control experiment was done to test the effect of the membrane impermeable zinc chelator CaEDTA and membrane permeable zinc chelator N,N,N',N-tetrakis(2-

pyridylmethyl) ethylenediamine (TPEN) on growth of *T. pseudonana*. A stock solution of 25 mM CaEDTA was made in water at high pH (c.a. 12), and of TPEN in 100% DMSO. Five milliter cultures of *T. pseudonana* were established with 1 x 10^5 cells ml^{-1} in the presence of CaEDTA and TPEN concentrations ranging from 0 – 1 mM. Culture cell density was monitored after 8 d. For both chelators, no growth occurred above a concentration of 25 μmol L^{-1}, and equivalent volumes of DMSO alone as in the TPEN additions did not affect growth. To monitor the effect of the chelators on $Si(OH)_4$ uptake, exponentially growing cultures of *T. pseudonana* were harvested by centrifugation and washed in Si-minus ASW. Cells were resuspended in Si-minus ASW at a cell density of 2.5 x 10^5 ml^{-1}. Chelators were added to separate tubes at a final concentration of 50 μmol L^{-1}. Control tubes had no addition or addition of an equivalent amount of DMSO as in the TPEN addition. These were allowed to incubate for 5 min after which 15 μmol L^{-1} ^{68}Ge:$Si(OH)_4$ was added. Uptake was measured after 30 min as described with the 0 min timepoint used to calculate background.

RESULTS

Uptake rates in *T. pseudonana* over different incubation periods

To determine the effect of incubation time on $Si(OH)_4$ uptake kinetics, uptake rates were measured in *T. pseudonana* harvested from exponentially growing silicon replete cultures by incubating samples with various silicate concentrations and measuring uptake after removing aliquots at 2 min, 10 min, 30 min, 1 h, 2 h, or 3 h incubation. In Fig. 4.1A, curves were fitted by nonlinear regression using Michaelis-

Menten hyperbolas. For 2 min uptake, Michaelis-Menten curves resulted in a poor fit of the data (r^2=0.9033). At 10 min, $Si(OH)_4$ uptake was nonsaturable. Comparing Michaelis-Menten plots from 30 min - 3 h, the curves gradually sloped over and saturation was observed between 1-2 h (Fig. 4.1A). Based on measurements of silicon requirements for the cell wall of *T. pseudonana* (Hildebrand et al. in press), $Si(OH)_4$ would not be depleted in the long term incubations. Data for 2 and 10 min were examined more closely in Fig. 4.1B. By excluding data from the higher $Si(OH)_4$ concentrations, kinetic parameters for 2 and 10 min could be calculated. For 2 min (Fig. 4.1B), two Michaelis-Menten hyperbolas could be fit, one for lower $Si(OH)_4$ concentrations (1-10 μmol L^{-1}) and one for higher $Si(OH)_4$ concentrations (10-30 μmol L^{-1}). For 10 min, a Michaelis-Menten curve did not fit, but an allosteric enzyme model could be fit to data for 1-15 μmol L^{-1} $Si(OH)_4$ concentrations (Fig. 4.1B). Kinetic parameters (K_s and V_{max}) calculated for curves shown in Fig. 4.1A for 30 min - 3 h, and Fig. 4.1B for 2 and 10 min are shown in Fig. 4.1C. For comparison, Michaelis-Menten curves plotted for 2 min (Fig. 4.1A) gave a K_s of 78 μmol L^{-1} and V_{max} of 60 fmole $cell^{-1}$ h^{-1}, and for 10 min (Fig. 4.1A) a K_s of 868 μmol L^{-1} and V_{max} of 152 fmole $cell^{-1}$ h^{-1}. These data (Fig. 4.1) reflect nonsaturable $Si(OH)_4$ uptake kinetics for incubations of 1 h or less.

Nonsaturability of short-term uptake in *T. pseudonana*

To determine the extent of nonsaturability of short-term uptake (defined as 2 min) observed in Fig. 4.1, we measured uptake in cells harvested from exponentially growing cultures of *T. pseudonana* using concentrations of $Si(OH)_4$ that ranged up to

500 μmol L^{-1} (Fig. 4.2). Saturation did not occur, and an allosteric enzyme curve fit to the data suggested $Si(OH)_4$ uptake rates increased with increasing $Si(OH)_4$ concentrations (Fig. 4.2).

Determining whether nonsaturability was a property of silicon transporters

To determine whether short-term nonsaturable uptake (Figs. 4.1 and 4.2) involved silicon transporters (SITs) or another uptake mechanism, exponential cultures of *T. pseudonana* were preincubated with the SIT-specific antibody, anti-TpEL4 (Thamatrakoln and Hildebrand, submitted for publication), prior to measuring short-term $Si(OH)_4$ uptake. The hypothesis was that if SITs played a role in nonsaturable uptake, anti-TpEL4 would bind SITs and possibly cause a change in uptake rates. Comparison of antibody-treated with untreated cultures (Fig. 4.3) showed a similar shaped curve, however antibody-treated cultures had consistently higher uptake rates at higher $Si(OH)_4$ concentrations. The difference between the curves at higher $Si(OH)_4$ concentrations was statistically significant as determined by t-test (p = 0.05), suggesting nonsaturable uptake occurred through SITs. In addition, the saturable component of uptake seen between 10-30 μmol L^{-1} (as also seen in Fig. 4.1B), is also affected by anti-TpEl4 suggesting this features is also a property of SITs.

Uptake kinetics in *Navicula pelliculosa* FW and the effect of silicon starvation

To test if nonsaturability of $Si(OH)_4$ uptake (Figs. 4.1 and 4.2) observed in *T. pseudonana* was due to the experimental design, or was specific to this species, $Si(OH)_4$ uptake was monitored in the previously studied *Navicula pelliculosa* FW

(Sullivan 1976; 1977) where short-term uptake (2 min) was shown to be saturable. To compare the effect of experimental design, $Si(OH)_4$ uptake was measured using both the current method (exponentially growing cells with no preincubation in Si-minus medium), as well as Sullivan's method (preincubation of cells in Si-minus medium). *N. pelliculosa* FW was harvested from a Si-replete exponential culture and $Si(OH)_4$ uptake was assayed after 2 and 30 min incubations in Si-minus medium. For 2 min incubation, Michaelis-Menten hyperbola resulted in a poor fit of the data (r^2 = 0.8557), indicating nonsaturable kinetics (Fig. 4.4A, right graph). However, at $Si(OH)_4$ concentrations less than 30 μmol L^{-1}, a Michaelis-Menten saturating hyperbola could be fit, with K_s = 17.4 μmol L^{-1} and V_{max} = 3.2 fmol $cell^{-1}$ h^{-1} (data not shown). Uptake after 30 min incubation saturated (Michaelis-Menten hyperbola, r^2 = 0.9968) with K_s = 48.5 μmol L^{-1} and V_{max} = 5.0 fmol $cell^{-1}$ h^{-1} (Fig. 4.4A, left graph). When cultures of *N. pelliculosa* FW were incubated in Si-minus medium 24 h prior to measuring short-term uptake (2 min), uptake saturated as previously observed (Sullivan 1976; 1977)). For short-term uptake in both experiments, K_s and V_{max} were lower than uptake measured after 30 min (Fig. 4.4).

Comparison of uptake capacity in different diatom species

A survey of different diatom species was done to determine how common nonsaturable $Si(OH)_4$ uptake on short time scales was and whether uptake saturated on longer time scales. $Si(OH)_4$ uptake was measured in different diatom species using the same method for *T. pseudonana* (Fig. 4.1). For each species tested, full kinetic curves were obtained for each incubation period, but for simplicity, V_{max} at the higher

$Si(OH)_4$ concentrations for each incubation period is shown (Fig. 4.5). For *T. pseudonana*, *C. fusiformis*, *C. gracilis*, *P. tricornutum*, and *N. pelliculosa* FW, V_{max} at 100 μmol L^{-1} $Si(OH)_4$ is shown. For *T. weissflogii*, *N. pelliculosa* M, and *N. alba*, V_{max} at 30 μmol L^{-1} $Si(OH)_4$ is shown. In each species, $Si(OH)_4$ uptake was maximal in 2 min incubations, and decreased with increased incubation time (Fig. 4.5). *T. weissflogii* had the highest V_{max}, while *N. pelliculosa* FW had the lowest. Saturation was achieved in all species, but the timing varied. By plotting the percentage of uptake relative to the maximum at 2 min over time (Fig. 4.5B), the response of different species could be compared, and exponential decay curves were used to calculate when saturation (based on the appearance of the curves, defined as 15% of the 2 min value) was achieved. *N. pelliculosa* FW (4.8 min saturation time), *Chaetoceros gracilis* (10.8 min), and *N. pelliculosa* M (13.8 min) saturated earlier than the others, and *T. pseudonana* (43.3 min) took the longest.

Comparison of cell wall silica to intracellular pool size in different diatom species

Intracellular soluble silicon pool concentrations and the amount of cell wall silica were measured in each species during exponential growth to determine whether these parameters might influence uptake characteristics, in particular the rate at which saturation was achieved. The ratio of cell wall silica to soluble intracellular pools is shown in Fig. 4.6. There were no consistent relationships between this ratio and the rate of saturation; however selected examples will be discussed below.

DISCUSSION

The goal of this study was to re-evaluate $Si(OH)_4$ uptake kinetics in diatoms to whether specifically controlled conditions could generate saturable or nonsaturable uptake kinetics. For all diatom species tested, exponentially growing cells isolated from Si-replete medium exhibited nonsaturable short-term (min) $Si(OH)_4$ uptake kinetics at environmentally relevant concentrations, but saturable long-term (h) uptake that followed Michaelis-Menten type kinetics (Fig. 4.5A). Short-term saturable uptake was achieved only if cells were incubated in Si-minus medium prior to measuring uptake. $Si(OH)_4$ uptake appeared to be predominantly controlled by silicon transporters (Fig. 4.3), which were saturable at low extracellular $Si(OH)_4$ concentrations, but at higher concentrations could no longer control the rate of uptake (Figs. 4.1-4.3). Based on changes in kinetic parameters over time (Figs. 4.1 and 4.5) or upon silicon starvation (Fig. 4.4) we propose the capacity of intracellular pools to complex free $Si(OH)_4$ is the major determinant over whether transport is saturable. Transport over the longer term is controlled by the rate of silica incorporation into the cell wall (Fig. 4.1 and Hildebrand et al. in press). These data suggest that under some conditions SITs are selectivity gates more than controlling agents in $Si(OH)_4$ transport. Here, we discuss these observations individually, then bring the data together to detail $Si(OH)_4$ uptake in diatoms as a process involving multi-level control between SITs, intracellular pools, and cell wall silica incorporation.

Cell cycle effects on $Si(OH)_4$ uptake

In all experiments, cells were grown under continuous illumination to avoid possible cell cycle and cell phasing effects. Because $Si(OH)_4$ uptake occurs at specific times in the cell cycle (Sullivan 1977), uptake parameters K_s and V_{max} will be underestimates in exponentially growing cultures (Brzezinski 1992). However, because cell-cycle associated silicon requirements vary in different diatom species (Brzezinski et al. 1990; Martin-Jézéquel et al. 2000), non-phased cultures were examined. Differences in kinetic parameters determined for nonsaturable and saturable conditions (Fig. 4.1) are far greater than those measured as a result of cell cycle effects (Chisholm et al. 1978; Brzezinski 1992).

Short-term $Si(OH)_4$ uptake in *T. pseudonana* is nonsaturable; long-term uptake is saturable and follows Michaelis-Menten type kinetics.

We determined short-term uptake kinetics (defined as 2 min) in exponentially growing *T. pseudonana* cells isolated from silicon-replete medium was nonsaturable, even at $Si(OH)_4$ concentrations as high as 500 μmol L^{-1} (Fig. 4.2), but that saturation occurred upon longer incubations (Fig. 4.1). V_{max} values at 2 and 3 h are consistent with previous measurements of silica incorporation rates (Hildebrand et al. in press), but the values at 2, 10, and 30 min (calculated by Michaelis-Menten curves) are far higher, consistent with surge uptake transitioning to internally controlled uptake (Conway et al. 1976; Conway and Harrison 1977) between 30 min and 2 h. We propose the transition is due to a gradual equilibration of intracellular pool capacity (which is high in the beginning, enabling surge uptake) with silicon requirements for

cell wall silica incorporation. Because of nonsaturability, K_s values calculated over the full range of $Si(OH)_4$ concentrations from Michaelis-Menten curves at 2, 10, 30 min and 1 h are not accurate indications of transporter affinity, but V_{max} values do indicate the uptake capacity of the transporters, which is in extreme excess of cellular silicon requirements. High K_s values could relate to the affinity of binding of $Si(OH)_4$ by intracellular pool components.

Nonsaturable uptake and kinetics features of short-term uptake at low $Si(OH)_4$ concentrations in *T. pseudonana* are a property of SITs

If nonsaturable uptake kinetics were due to non-specific transport though another cellular transporter protein, then saturation could possibly still occur if turnover rate for the non-specific transporter became limiting. This is not seen in Fig. 4.2. If nonsaturability was due to diffusion, the curve in Fig. 4.2 should be linear (Reed 1990; Lobban and Harrison 1997), or even hyperbolic due to saturation of intracellular pools, which it is not. In addition, treatment with a SIT-specific antibody affected nonsaturable transport rates in parallel with untreated cells (Fig. 4.3), indicating nonsaturation was a property of SITs. Anti-TpEL4 was designed against a predicted extracellular loop in the SIT protein, and if transport occurs via an alternating access model as proposed (Thamatrakoln et al. 2006), then perhaps antibody bound to the transporter favors an open extracellular conformation (due to steric hindrance or mass effects) resulting in increased uptake or decreased efflux.

Even though short-term uptake was nonsaturable at high $Si(OH)_4$ concentrations, examination of curves at less than 30 μmol L^{-1} $Si(OH)_4$ for 2 min and

less than 15 μmol L^{-1} for 10 min revealed distinct kinetic features. For 2 min uptake, two Michaelis-Menten saturation curves could be fit (Fig. 4.1B). One possible explanation for this could be related to the presence of multiple silicon transporters (SITs) that may have different transport properties. Of the three SITs in *T. pseudonana*; two are expressed at mRNA levels 200-300 fold higher than the third (Thamatrakoln and Hildebrand, submitted for publication). The data in Fig. 4.1B may relate to the two highly expressed SITs, which would indicate they have different transport characteristics, with a slight difference in affinity (K_s), but a 3.5 fold difference in capacity (V_{max}). In the antibody incubation experiment (Fig. 4.3), a curve for the proposed higher capacity transporter shifted to higher V_{max} in the presence of the antibody, consistent with these kinetic features being a property of SITs. Data were ambiguous for the lower capacity transporter.

For 10 min uptake, data for low $Si(OH)_4$ concentrations did not fit to a Michaelis-Menten curve, but did fit to an allosteric enzyme curve (Fig. 4.1B). Allostery is a regulatory process (Monod et al. 1965) in which activation of one subunit of a multi-subunit protein complex affects other subunits. One interpretation of the data is that after initial silicic acid uptake, SITs may begin to interact with each other or with other cellular proteins between 2 and 10 min, and an allosteric inhibition regulatory process could come into play. V_{max} for 10 min is lower than V_{max} for 2 min (Fig. 4.1C), indicating uptake was reduced. If excess surge $Si(OH)_4$ uptake (2 min) is detrimental to the cell, one mechanism for controlling it would be to reduce transport capacity (10 min).

Our data (Figs. 4.1 and 4.3) are consistent with previous studies showing Michaelis-Menten type kinetics at low extracellular $Si(OH)_4$, with nonsaturation occurring at higher concentrations (Del Amo and Brzezinski 1999), suggesting SITs can exert an energetic influence over transport at low $Si(OH)_4$ concentrations. However, at higher concentrations, a threshold is reached (30 μmol L^{-1} in Fig. 4.3) where the $Si(OH)_4$ concentration gradient into the cell (uptake gradient) overcomes the energetic limitations. The antibody data (Fig. 4.3) are also consistent with SITs being the predominant means of $Si(OH)_4$ transport into the cell.

Silicon starvation affects short-term $Si(OH)_4$ uptake kinetics in *N. pelliculosa* FW

Most previous measurements of silicon uptake in diatoms demonstrated saturable Michaelis-Menten kinetics; however in most studies, uptake was either measured during long (≥1 h) incubations, or after cells were starved for silicon for appreciable time periods prior to measuring uptake (Table 4.1). Figs. 4.1 and 4.5A show short-term uptake was nonsaturable, but under long-term incubations, saturability was achieved. These features were not species-specific, nor artifacts of experimental design as confirmed by results obtained with the previously studied *N. pelliculosa* FW. When cultures of *N. pelliculosa* FW were preincubated in Si-minus medium (as had been previously done by Sullivan (1976) or when uptake was measured in Si-replete cells over longer time periods (this study), uptake followed Michaelis-Menten type saturation kinetics (Fig. 4.4). Short-term uptake in Si-replete cells was nonsaturable as had been seen in all other species tested (Figs. 4.4 and 4.5).

These data support the hypothesis that reduction in intracellular pool capacity leads to saturable uptake.

Short-term nonsaturable uptake kinetics and long-term saturable kinetics occurs in all diatoms tested

The change in kinetic properties from short-term (min) nonsaturable to long-term (h) saturable was shown in other diatom species (Fig. 4.5A), and we propose this occurs for the same reasons as mentioned for *T. pseudonana* – that the capacity of intracellular pools becomes equilibrated with the needs for cell wall silica incorporation. The rate at which saturability was achieved varied depending on the species (Fig. 4.5B). At least three variables could come into play regarding how fast saturability is achieved, the rate of uptake (how fast the pools would be replenished), the rate of silica incorporation (how fast the pools would be depleted), and the capacity of the pools to bind free $Si(OH)_4$. The first two parameters can be measured, but with current approaches, the third cannot. A crude way of determining the effect of pools on saturability would be to compare the ratio of cell wall silica to pools (Fig. 4.6), with the assumption that a higher ratio would mean that pools would be depleted more rapidly and saturation would occur faster. Analyzing data for uptake and rate of saturation (Fig. 4.5) and cell wall silica:pools (Fig. 4.6) did not reveal any clear trends in this regard; however, two interesting observations could be made. First, in comparing the two *N. pelliculosa* species, which are from the same genus and have similar cell sizes and shapes, *N. pelliculosa* FW had a 4.3 fold higher cell wall:pools and a 2.9 fold faster rate of saturation, consistent with the pools/incorporation

equilibration hypothesis. Second, there is a general correlation between cell size (data not shown) and rate to achieve saturation (Fig. 4.5B), which suggests cell volume or geometry may have an effect (because there should be a distance component to the rate at which silicic acid is transported to the cell wall). Direct measurements of $Si(OH)_4$ uptake in *C. fusiformis* have shown kinetic parameters do vary with cell size (Leynaert et al. 2004) and depending on geometry, some cells may have a higher surface to volume ratio. Interestingly, *C. gracilis*, which has 80% of its cell wall silica in the form of long and narrow spines (Rogerson et al. 1986), had one of the fastest saturation times (Fig. 4.5B), even though its cell wall:pools ratio was near the average of the species examined.

A model for $Si(OH)_4$ uptake kinetics in diatoms

Based on the data obtained, we propose the following model to explain the kinetic properties of $Si(OH)_4$ uptake in diatoms (Fig. 4.7). In cells growing under Si-replete conditions, intracellular pool capacity is relatively high, and when incubated with high $Si(OH)_4$, maximum surge uptake occurs (Fig. 4.7A). Uptake is nonsaturable because of the high pool capacity. When cells are starved for silicon prior to measuring uptake (Fig. 4.4), or during long-term measurements of uptake (Figs. 4.1 and 4.5), intracellular pool capacity is reduced or minimized, surge uptake is reduced or eliminated, and overall uptake is coupled to cell wall silica incorporation and is saturable (Fig. 4.7B). However, short-term uptake in cells growing in Si-replete conditions is controlled by SITs at low extracellular $Si(OH)_4$ concentrations because

uptake is not yet connected to incorporation kinetics and pool capacity is not minimized (Fig. 4.7C).

An important question is why is excess surge uptake of $Si(OH)_4$ allowed to occur at all, even at the environmentally relevant concentrations we tested? Although $Si(OH)_4$ efflux is predicted to be energetically favorable, uptake is not because of the energy required to pump out sodium co-transported with $Si(OH)_4$ (Bhattacharyya and Volcani 1980). In addition, excess uncomplexed silicic acid in the cell could be prone to autopolymerization, which would be detrimental to the cell. One possible explanation is that surge uptake provides a means for diatoms to take advantage of nutrient patchiness by being able to take up silicic acid rapidly and in excess of immediate needs, but this would be of little use if the amount taken up induces efflux.

Comparison of results with previously published data

Data obtained in this study suggest most previous measurements of $Si(OH)_4$ uptake kinetics (Table 4.1) were actually measurements of kinetics of silica incorporation into the cell wall. Kinetic parameters for uptake controlled by SITs or internally controlled by silica incorporation are similar in *T. pseudonana* (Figs. 4.1B and C), suggesting that if the same is true for other diatom species, previously determined kinetic parameters (Table 4.1), could be reasonable estimates for uptake controlled by SITs. In some studies, nonsaturation was observed (Table 4.1), but explanations not provided. Del Amo and Brzezinski (1999) reported long-term nonsaturable uptake in the diatom *Phaeodactylum tricornutum*, however, *P. tricornutum* is a lightly silicified diatom and one of the few known to be capable of

transporting both silicate and silicic acid. Long-term nonsaturable uptake reported for *T. pseudonana* clone 3H (Nelson et al. 1976) contradict current results, but uptake in that study was only measured for $Si(OH)_4$ concentrations up to 15 μmol L^{-1} so it is difficult to say what kinetic features would have been present at higher concentrations. Our results showed long-term uptake in *T. pseudonana* saturated at 30 μmol L^{-1} $Si(OH)_4$ (Fig. 4.1A).

Zinc does not appear to be involved in $Si(OH)_4$ uptake

Previous work (Reuter and Morel 1981) suggested zinc may be involved in silicic acid transport because transport rates varied with concentration of available zinc. These experiments utilized long term incubations to measure uptake, and based on our data, this raises the possibility that the kinetics of silica incorporation were being measured, and not uptake. We tested whether zinc was directly involved in uptake by monitoring uptake in the presence of two zinc chelators, TPEN (N,N,N',N'-tetrakis (2-pyridylmethyl) ethylenediamine), which is membrane permeable, and CaEDTA which is membrane impermeable (Fig. 4.8). These were used at concentrations approximately10 fold higher than added zinc, which were shown in control experiments to completely inhibit cell growth (data not shown). A control using the same volume of DMSO as in the TPEN stock was included in the analysis. Results monitoring uptake at 30 min showed no significant difference between untreated cells and those treated with DMSO, TPEN, or CaEDTA (Fig. 4.8), suggesting $Si(OH)_4$ uptake by SITs does not involve zinc. One concern in interpreting these results is whether uptake could have occurred through SITs bound to zinc prior

to treatment with the zinc chelators. However, the zinc dissociation constant for TPEN is several orders of magnitude lower than that for zinc binding enzymes, including ZntR, the protein with the highest zinc dissociation constant known to date (Hitomi et al. 2001). Thus, it is reasonable to assume that any zinc previously bound to SITs would have dissociated upon treatment with TPEN.

Implications for SIT function

Our results indicate SITs can exert control over short-term $Si(OH)_4$ uptake at low extracellular $Si(OH)_4$ (<30 μM) concentrations (Fig. 4.1B). These concentrations are environmentally relevant (Tréguer et al. 1995), and control by SITs at these levels would provide an energy savings to the cell because sodium co-transported during excess uptake would require energy supplied by ATP hydrolysis to be pumped out (Bhattacharyya and Volcani 1980). During long-term incubation (Fig. 4.1), the kinetic features seen at less than 30 μM are not visible; suggesting any control SITs had on uptake is masked by the rate of silica incorporation into the cell wall. In addition, because K_s and V_{max} values for long-term uptake (incorporation rate) are in close agreement with those for short-term uptake at low $Si(OH)_4$ concentration (uptake rate), this suggests that there is not a significant difference for the cell when uptake is controlled by either of these processes.

The data indicate that SITs have enormous flexibility in their rate of transport and, if left unregulated, transport $Si(OH)_4$ into the cell very quickly under high substrate concentration. This, coupled with their tight coupling to incorporation rates has implications on the regulation of their expression. Having a transporter with highly

flexible transport capacity would require less control over the actual amount of transporter present, which is consistent with recent results monitoring SIT protein levels in *T. pseudonana* (Thamatrakoln and Hildebrand, submitted for publication).

In summary, although SITs can exert control over short-term uptake at low $Si(OH)_4$ concentrations, long-term uptake is controlled by the rate of cell wall silica incorporation, and SITs are not capable of control during surge uptake at high extracellular $Si(OH)_4$ concentrations. Thus, under some conditions, SITs function more as selectivity gates rather than controlling agents in diatom silicon transport.

Environmental relevance

Concentrations of $Si(OH)_4$ in most of the ocean's photic zone average 10 μmol L^{-1} (Tréguer et al. 1995). Based on our data, $Si(OH)_4$ uptake by field assemblages would be either 1) directly controlled by SITs, which would minimize the associated costs of excess surge uptake and efflux, or 2) controlled by the rate of cell wall silica incorporation because under low extracellular $Si(OH)_4$ concentrations, intracellular pools should be minimized and in equilibrium with the needs for cell wall silica. In coastal environments or upwelling zones, conditions favoring surge uptake can occur; for example, cells exposed to high levels of $Si(OH)_4$ would have a higher intracellular pool capacity allowing surge uptake to occur more frequently. The amount of cell wall silica in a given diatom species can vary up to four-fold (Lewin 1957; Paasche 1980; Taylor 1985; Brzezinski et al. 1990), and under conditions of chronically high $Si(OH)_4$ concentrations, cell wall silica content increases (Martin-Jézéquel et al. 2000). Such silica would become available to future generations of diatoms upon death and silica

dissolution. Freshwater diatoms on average have an order of magnitude more cell wall silica per unit area than marine diatoms (Conley and Kilham 1989), therefore, their rate of response from surge uptake to saturability may be quicker, as was the case with the only freshwater diatom in this study (Fig. 4.6B).

ACKNOWLEDGMENTS

We thank Michael Latz and Bradley Tebo for use of lab space and equipment. Dimitri Deheyn helped with statistical analysis. We appreciate both encouraging words and helpful comments from Mark Brzezinski. *Navicula pelliculosa* (Breb. et Kuetzing) Hilse CCMP543 was provided as part of a collaborative project with Sandra Hazelaar and Winfried W.C. Gieskes. This work was supported by Air Force Office of Scientific Research Multidisciplinary University Research Initiative Grant RF00965521.

Chapter IV, in full, is in preparation for submission. The dissertation author was the co-investigator and co-author of this manuscript. Mark Hildebrand was a co-investigator and co-author.

Table 4.1. List of previously published studies on $Si(OH)_4$ uptake in diatoms. Listed are species used in the study, whether cultures were prestarved for silicon prior to measuring uptake, the incubation period and $Si(OH)_4$ concentrations over which uptake was measured, the method, the results, and the reference.

Species	Pre-starved?	Incubation period	$[Si(OH)_4]$ ($\mu mol\ L^{-1}$)	Method	Results	Reference
Thalassiosira pseudonana clone 3H	No	> 1 h	0-14	Silico-molybdate	Michealis-Menten hyperbola	Paasche 1973a
Skeletonema costatum *Thalassiosira pseudonana* *T. decipiens* *Ditylum brightwellii* *Licmophora sp.*	Yes	1 h	0-15	Silico-molybdate	Michealis-Menten hyperbola	Paasche 1973b
Nitzschia alba	Yes	< 10 min	0-20	^{31}Si	Michaelis-Menten hyperbola	Azam et al. 1974
Nitzschia alba	Yes	15 sec–3 min	0-80	^{68}Ge	Michaelis-Menten hyperbola	Azam 1974
Nitzschia alba	Yes	< 2 min	0-32	^{68}Ge	Biphasic	Azam and Volcani, 1974
Thalassiosira pseudonana clone 3H clone 13-1	Both Si-replete and prestarved	4 h	0-15	^{30}Si	Clone 3H Replete: nonsaturable Prestarved: Michaelis-Menten hyperbola Clone 13-1 Replete and prestarved: Michaelis-Menten hyperbola	Nelson et al. 1976
Navicula pelliculosa FW	Yes	2 min	0-100	^{68}Ge	Michaelis-Menten hyperbola	Sullivan 1976
Phaeodactylum tricornutum	Yes	2 h	up to 160	^{30}Si	Michaelis-Menten hyperbola	Reidel and Nelson, 1985
Thalassiosira pseudonana *T. weissflogii* *Cylindrotheca fusiformis* *Phaeodactylum tricornutum*	Yes	3-4 h	0-35 or 0-300	^{32}Si	*T. pseudonana, T. weissflogii, C. fusiformis*: Michaelis-Menten hyperbola *P. tricornutum*: Michaelis-Menten hyperbola at 0-25 $\mu M\ Si(OH)_4$, nonsaturable at 25-300 $\mu M\ Si(OH)_4$	Del Amo and Brzenzinski 1999
Cylindrotheca fusiformis	No	4 h	0-15	^{32}Si	Michaelis-Menten hyperbola	Leynaert et al. 2004
Thalassiosira weissflogii	No	1 h	0-30	^{32}Si	Michaelis-Menten hyperbola	Milligan et al. 2004

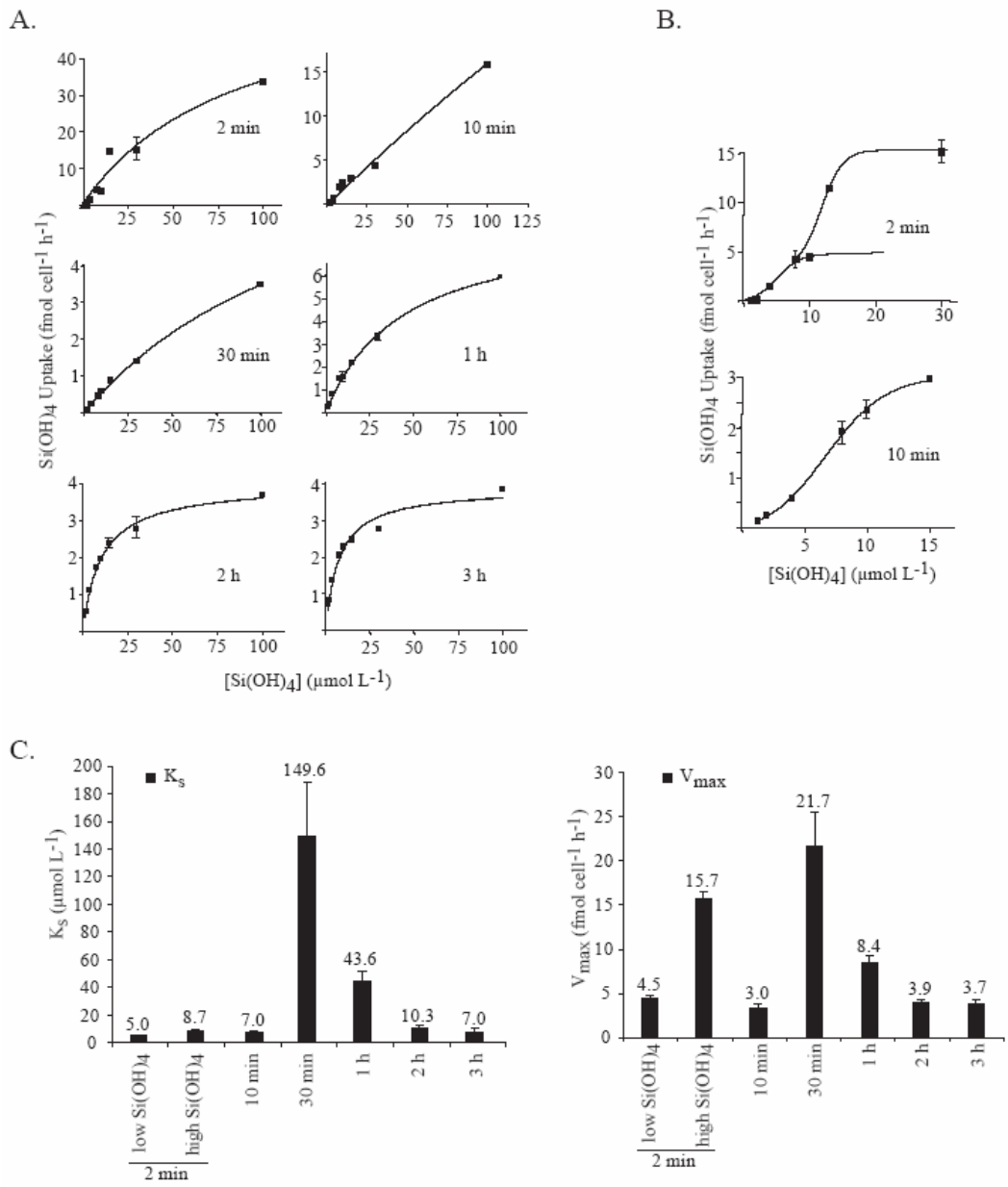

Figure 4.1. $Si(OH)_4$ uptake kinetics of *T. pseudonana*. A. Effect of incubation time on uptake kinetics. Uptake rates were measured in cells incubated for 2 min, 10 min, 30 min, 1 hr, 2 hr, or 3 h. Curves represent fitted Michaelis-Menten hyperbolas obtained by nonlinear regression. For 8-30 µmol L^{-1} $Si(OH)_4$ concentrations, the average of duplicates is plotted. Error bars are standard error. B. Fitted curves for 2 min and 10 min incubations for 1-30 µmol L^{-1} $Si(OH)_4$ (2 min) and 1-15 µmol L^{-1} $Si(OH)_4$ (10 min). For 2 min uptake, two Michaelis-Menten hyperbolas were fit to low and high $Si(OH)_4$ concentrations. For 10 min uptake, best-fit curve was based on an allosteric enzyme model. C. K_S and V_{max} calculated for each incubation period. Values are based on curves shown in B for 2 min and 10 min and for curves shown in A for other times. Errors bars are 95% confidence interval.

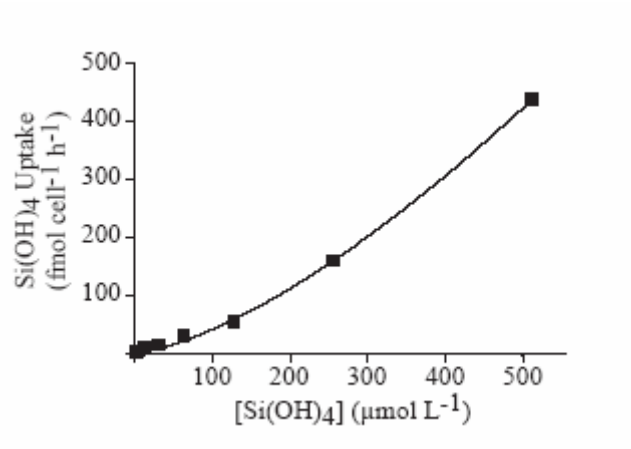

Figure 4.2. Short-term (2 min) $Si(OH)_4$ uptake kinetics of *T. pseudonana* over $Si(OH)_4$ concentrations ranging from 1 to 500 µmol L^{-1}. Best-fit curve is based on allosteric enzyme model obtained by nonlinear regression.

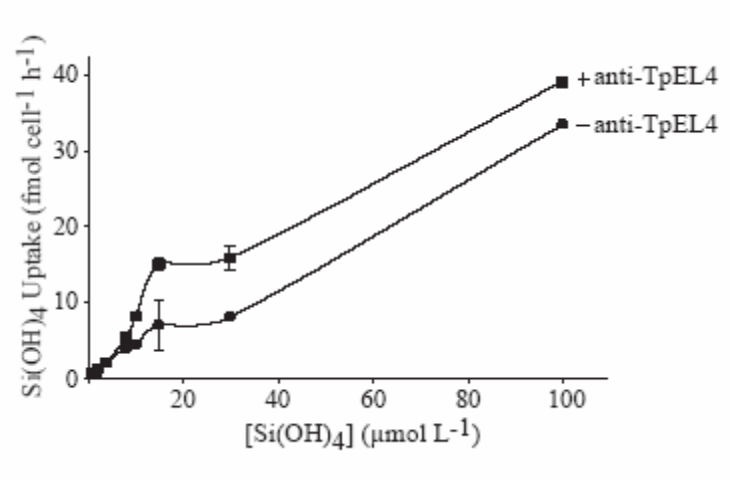

Figure 4.3. Effect of SIT-specific antibody on short-term $Si(OH)_4$ uptake kinetics. *T. pseudonana* cells were preincubated in the presence (■) or absence (●) of the SIT-specific antibody anti-TpEL4 (Thamatrakoln and Hildebrand, submitted for publication) for 60 min prior to measurement of uptake kinetics. Error bars for 8-30 µmol L^{-1} are standard error of duplicate samples. Curves were significantly different between 10-100 µmol L^{-1} as determined by t-test ($p = 0.05$).

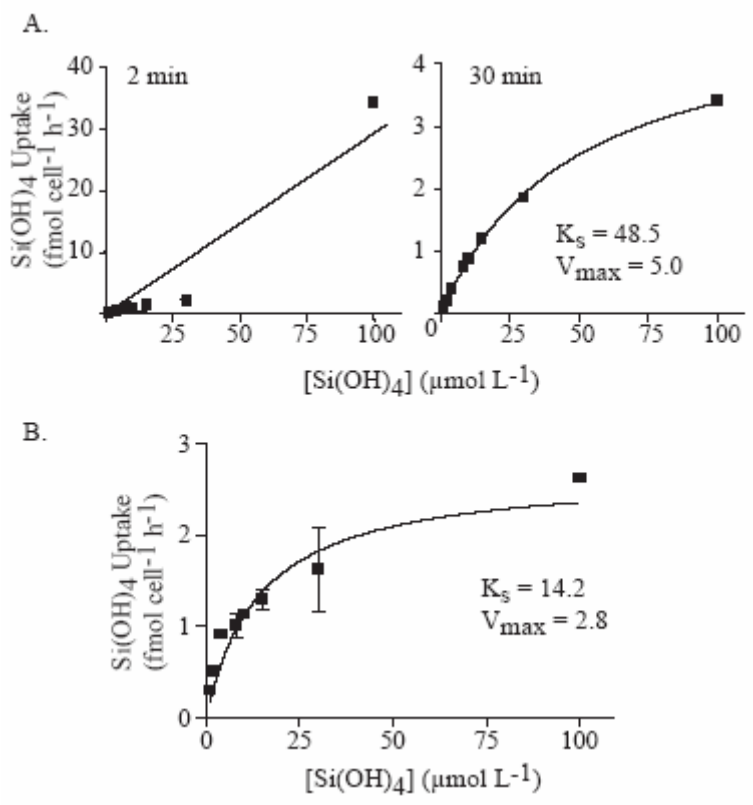

Figure 4.4. $Si(OH)_4$ uptake kinetics of *N. pelliculosa* FW. All data were fit by non-linear regression using Michaelis-Menten hyperbolas. A. Left graph is uptake kinetics for cells harvested from Si-replete medium after 2 min incubation. Right graph is uptake kinetics for the same cells measured after 30 min incubation. B. Cells were preincubated in Si-minus medium for 24 h prior to measuring short-term uptake kinetics (2 min incubations). Error bars for 8-30 µmol L^{-1} $Si(OH)_4$ concentrations are standard error of duplicates. Values for K_s (in µmol L^{-1}) and V_{max} (in fmol $cell^{-1}$ h^{-1}) were calculated using GraphPad Prism 4.

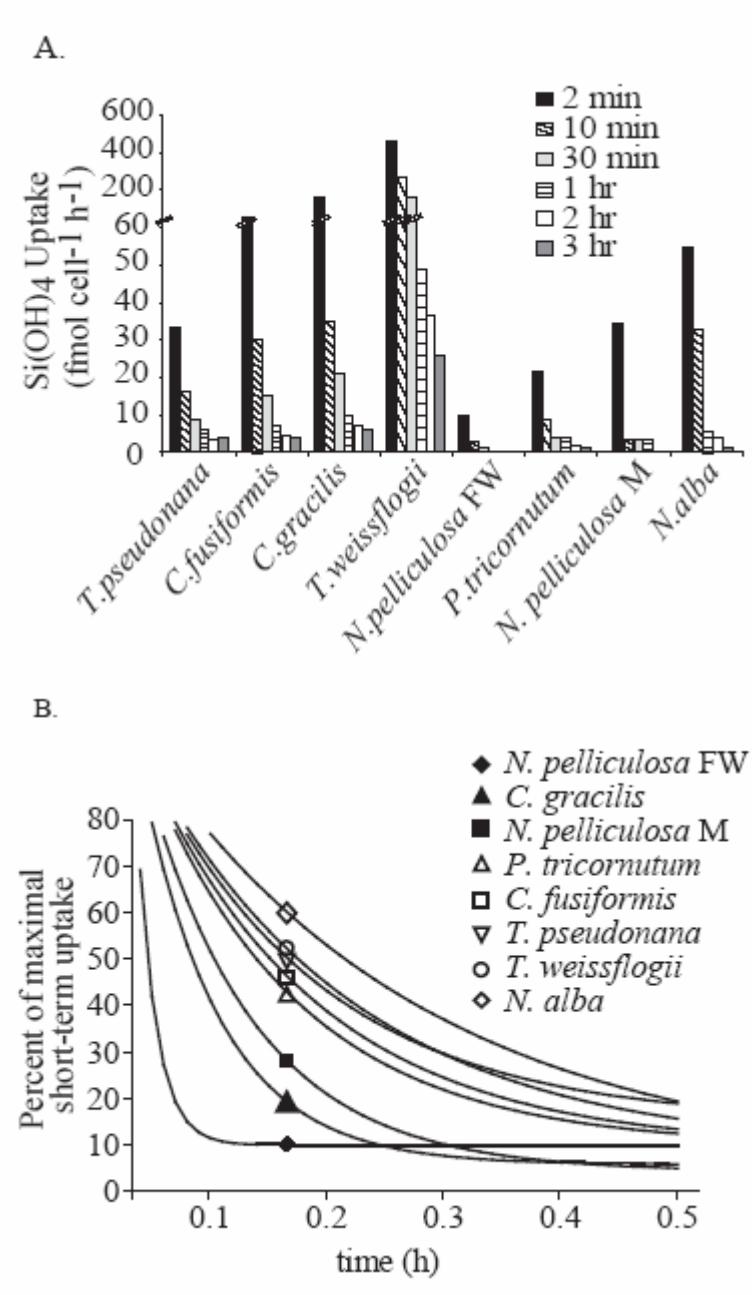

Figure 4.5. Maximum $Si(OH)_4$ uptake rates and time to saturation for different diatom species. A. Maximum rate of $Si(OH)_4$ uptake for different diatom species incubated for 2 min, 10 min, 30 min, 1 hr, 2 h, or 3 h. *T. pseudonana, C. fusiformis, C. gracilis, P. tricornutum*, and *N. pelliculosa* FW were incubated with 100 µmol L^{-1} $Si(OH)_4$. *T. weissflogii, N. pelliculosa* M, and *N. alba* were incubated with 30 µmol L^{-1} $Si(OH)_4$. Break in y-axis is shown. B. Rate of decrease in uptake for different species based on percent of maximal uptake at 2 min over time. Exponential decay curves were fit; symbols denote the different species.

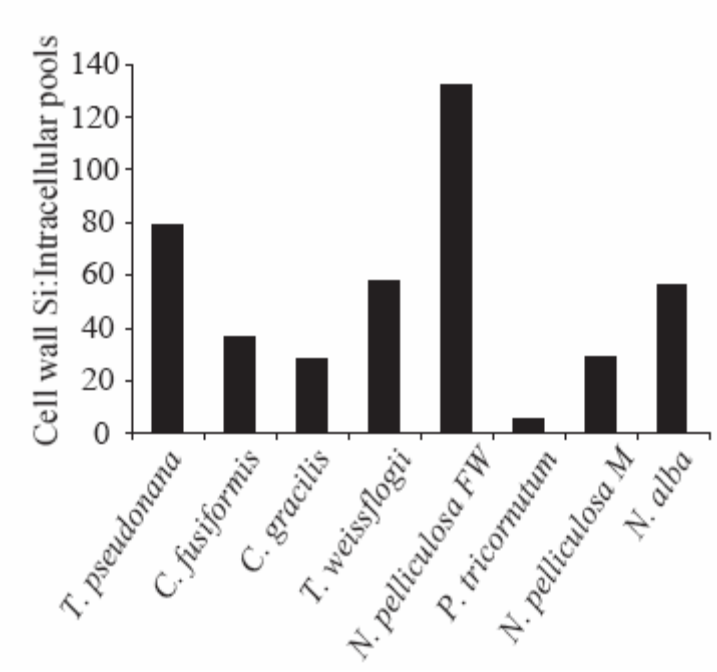

Figure 4.6. Ratio of cell wall silica to intracellular soluble silicon pools for exponentially growing diatom species used in this study. See Materials and Methods for experimental details.

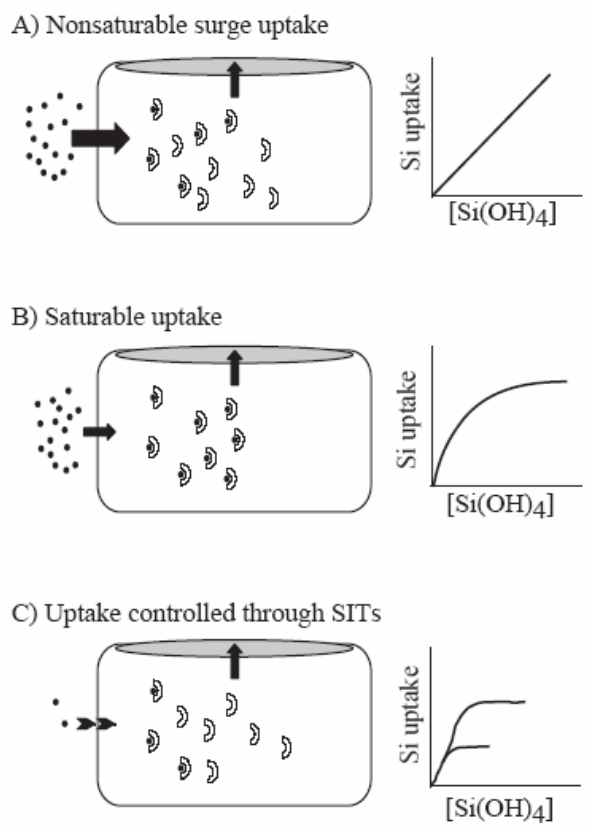

Figure 4.7. A model of silicon uptake kinetics. On the left a diatom cell is represented as a rectangular box and cell wall silica is represented as a gray oval. Black dots represent $Si(OH)_4$. Horseshoe-shaped structures represent silicon-binding components. Arrows denote direction of transport with magnitude indicated by their thickness. On the right are stylized graphs of uptake kinetics during each mode of uptake. A. In nonsaturable surge uptake, cells are isolated from silicon replete conditions and silicon-binding components are abundant. Upon addition of high concentrations of silicon, uptake is in excess of silica incorporation and is nonsaturable because of excess binding components. B. Saturable uptake under high silicon concentrations can occur by two means. Cells prestarved in Si-minus medium will decrease levels of the binding components. Upon addition of $Si(OH)_4$, short-term uptake saturates because binding components are minimized and equilibration between uptake and cell wall silica incorporation occurs quickly. Alternatively, saturation is achieved in Si-replete cells by monitoring uptake over longer incubation times. In this case, the longer incubation time enables equilibration between the level of binding component and cell wall silica incorporation leading to saturation. C. Short-term uptake controlled through SITs occurs at low $Si(OH)_4$ concentrations. In *T. pseudonana*, uptake follows a biphasic curve because of the presence of two predominant SITs (denoted by the broken arrow) which are able to exert control over uptake at low silicon concentrations under conditions when uptake is not tightly coupled to cell wall silica incorporation. Each SIT is proposed to contribute to the separate portions of the curve.

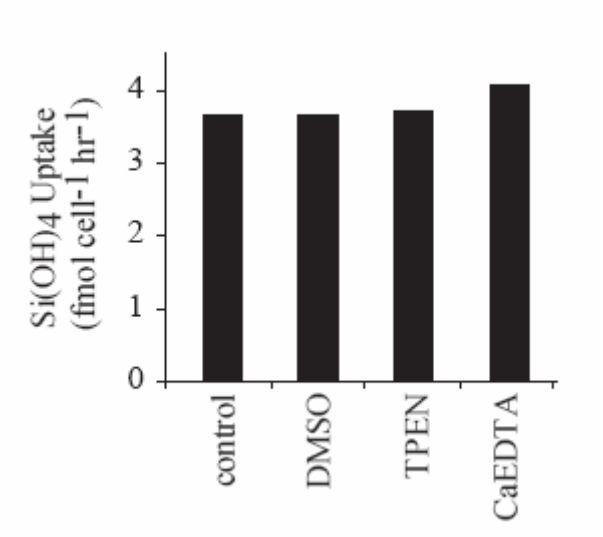

Figure 4.8. Effect of zinc chelators on $Si(OH)_4$ uptake. Membrane permeable chelator TPEN and membrane impermeable chelator CaEDTA were added to cells at 50 µmol L^{-1} and uptake monitored after 30 min. Control cells had no addition, and another control had an equal volume of DMSO as used for the TPEN solution.

REFERENCES

Azam F (1974). Silicic acid uptake in diatoms studied with [^{68}Ge] germanic acid as a tracer. *Planta* 121: 205-212.

Azam F, BB Hemmsingsen and BE Volcani (1974). Role of silicon in diatom metabolism V. Silicic acid transport and metabolism in the heterotrophic diatom *Nitzschia alba*. *Arch. Microbiol.* 97: 103-114.

Azam F and BE Volcani (1974). Role of diatom silicon metabolism. VI. Active transport of germanic acid in the hetertrophic diatom *Nitzschia alba*. *Arch. Microbiol.* 101: 1-8.

Bhattacharyya P and BE Volcani (1980). Sodium dependent silicate transport in the apochlorotic marine diatom *Nitzschia alba*. *Proc. Natl. Acad. Sci. U.S.A.* 77: 6386-6390.

Brzezinski MA (1992). Cell-cycle effects on the kinetics of silicic acid uptake and resource competition among diatoms. *J. Plankton Res.* 14: 1511-1539.

Brzezinski MA, RJ Olson and SW Chisholm (1990). Silicon availability and cell cycle progression in marine diatoms. *Mar. Ecol. Prog. Ser.* 67: 83-96.

Chisholm SW, F Azam and RW Eppley (1978). Silicic acid incorporation in marine diatoms on light:dark cycles: use as an assay for phased cell division. *Limnol. Oceanog.* 23: 518-529.

Claquin P and V Martin-Jézéquel (2005). Regulation of the Si and C uptake and of the soluble free-silicon pool in a synchronized culture of *Cylindrotheca fusiformis* (Bacillariophyceae): effect on the Si/C ratio. *Marine Biology* 146: 877-886.

Collos Y, MY Siddiai, MY Wang, ADM Glass and PJ Harrison (1992). Nitrate uptake kinetics by two marine diatoms using the radiotracer ^{13}N. *J. Exp. Mar. Biol. Ecol.* 163: 251-260.

Collos Y, A Vaquer, B Bibent, G Slawyk, N Garcia and P Souchu (1997). Variability in nitrate uptake kinetics of phytoplankton communities in a Mediterranean coastal lagoon. *Estuarine Coastal Shelf Sci.* 44: 369-375.

Conley DJ and SS Kilham (1989). Differences in silica content between marine and freshwater diatoms. *Limnol. Oceanog.* 34: 205-213.

Conway HL and PJ Harrison (1977). Marine diatoms grown in chemostats under silicate or ammonium limitations. IV. Transient response of *Chaetoceros debilis*, *Skeletonema costatum*, and *Thalassiosira gravida* to a single addition of the limiting nutrient. *Mar. Biol.* 43: 33-43.

Conway HL, PJ Harrison and CO Davis (1976). Marine diatoms grown in chemostats under silicate or ammonium limitation. II. Transient response of *Skeletonema costatum* to a single addition of the limiting nutrient. *Mar. Biol.* 35: 187-199.

Darley WM and BE Volcani (1969). Role of silicon in diatom metabolism: A silicon requirement for deoxyribonucleic acid synthesis in the diatom *Cylindrotheca fusiformis* Reimann and Lewin. *Exp. Cell Res.* 58: 334-342.

Del Amo Y and MA Brzezinski (1999). The chemical form of dissolved Si taken up by marine diatoms. *J. Phycol.* 35: 1162-1170.

Eppley RW, JN Rogers and JJ McCarthy (1969). Half-saturation constants for uptake of nitrate and ammonium by marine phytoplankton. *Limnol. Oceanog.* 14: 912-920.

Grachev MA, NN Denikina, SI Belikov, EV Likhoshvai, MV Usol'tseva, IV Tikhonova, RV Adel'shin, SA Kler and TA Sherbakova (2002). Elements of the active center of silicon transporters in diatoms. *Mol. Biol. (Moscow)* 36: 534-536.

Guillard RR and JH Ryther (1962). Studies of marine planktonic diatoms. I. *Cyclotella nana* Hustedt and *Detonula confervacea* Cleve. *Can. J. Microbiol.* 8: 229-239.

Guillard RRL (1975). Culture of phytoplankton for feed marine invertebrates *in* Culture of Marine Invertebrate Animals. WL Smith and MH Chanley. New York, N.Y., Plenum Press**:** 29-60.

Harrison PJ, JS Parslow and HL Conway (1989). Determination of nutrient uptake kinetic parameters: a comparison of methods. *Mar. Ecol. Prog. Ser.* 52: 301-312.

Hildebrand M, LG Frigeri and AK Davis (in press). Synchronized growth of *Thalassiosira pseudonana* (Bacillariophyceae) provides novel insights into cell wall synthesis processes in relation to the cell cycle. *J. Phycol.*

Hildebrand M (2000). Silicic acid transport and its control during cell wall silicification in diatoms *in* Biomineralization: From Biology to Biotechnology and Medical Applications. E Bäuerlein. Weinheim, Wiley-VCH**:** 171-188.

Hildebrand M, K Dahlin and BE Volcani (1998). Characterization of a silicon transporter gene family in *Cylindrotheca fusiformis*: Sequences, expression analysis, and identification of homologs in other diatoms. *Mol. Gen. Genet.* 260: 480-486.

Hildebrand M, BE Volcani, W Gassmann and JI Schroeder (1997). A gene family of silicon transporters. *Nature* 385: 688-689.

Hildebrand M and R Wetherbee (2003). Components and control of silicification in diatoms *in* Progress in Molecular and Subcellular Biology. WEG Muller. Berlin Heidelberg, Springer-Verlag. **33:** 11-57.

Hitomi Y, CE Outten and TV O'Halloran (2001). Extreme zinc-binding thermodynamics of the metal sensor/regulatory protein, ZntR. *J. Am. Chem. Soc.* 123: 8614-8615.

Iler RK (1979). The Chemistry of Silica: Solubility, Polymerization, Colloid and Surface Properties, and Biochemistry. New York, John Wiley & Sons.

Lewin JC (1957). Silicon metabolism in diatoms IV. Growth and frusule formation in *Navicula pelliculosa*. *Can. J. Microbiol.* 3: 427-433.

Leynaert A, E Bucciarelli, P Claquin, RC Dugdale, V Martin-Jézéquel, P Pondaven and O Ragueneau (2004). Effect of iron deficiency on diatom cell size and silicic acid uptake kinetics. *Limnol. Oceanog.* 49: 1134-1143.

Likhoshway YV, YA Masyukova, TA Sherbakova, DP Petrova and MA Grachev (2006). Detection of the gene responsible for silicic acid transport in Chyrsophycean algae. *Doklady Biological Sciences* 408: 256-260.

Lobban CS and PJ Harrison (1997). Seaweed Ecology and Physiology. Cambridge, UK, Cambridge University Press.

Lomas MW and PM Glibert (1999). Temperature regulation of nitrate uptake: a novel hypothesis about nitrate uptake and reduction in cool-water diatoms. *Limnol. Oceanog.* 44: 556-572.

Martin-Jézéquel V, M Hildebrand and MA Brzezinski (2000). Silicon metabolism in diatoms: Implications for growth. *J. Phycol.* 36: 821-840.

McCarthy JJ (1981). The kinetics of nutrient utilization. *Can. Bull. Fish. Aquat. Sci.* 210: 211-233.

Milligan A, DE Varela, MA Brzezinski and FMM Morel (2004). Dynamics of silicon metabolism and silicon isotopic discrimination in a marine diatom as a function of *p*CO2. *Limnol. Oceanog.* 49: 322-329.

Monod J, J Wyman and J-P Changeux (1965). On the nature of allosteric transitions: a plausible model. *J. Mol. Biol.* 12: 88-118.

Nelson DM and JJ Goering (1977). A stable isotope trace method to measure silicic acid uptake by marine phytoplankton. *Anal Biochem* 78: 139-147.

Nelson DM, JJ Goering, SS Kilham and RRL Guillard (1976). Kinetics of silicic acid uptake and rates of silica dissolution in the marine diatom *Thalassiosira pseudonana*. *J. Phycol.* 12: 246-252.

Paasche E (1973a). Silicon and the ecology of marine plankton diatoms. I. *Thalassiosira pseudonana* (*Cyclotella nana*) grown in a chemostat with silicate as limiting nutrient. *Marine Biology* 19: 117-126.

Paasche E (1973b). Silicon and the ecology of marine plankton diatoms. II. Silicate-uptake kinetics in five diatom species. *Marine Biology* 19: 262-269.

Paasche E (1980). Silicon *in* The Physiological Ecology of Phytoplankton. Studies in Ecology. I Morris. Berkeley, CA, University of California Press. **7:** 259-284.

Reed RH (1990). Solute accumulation and osmotic adjustment *in* The Biology of the Red Algae. KM Cole and RG Sheath. Cambridge, UK, Cambridge University Press**:** 147-170.

Reidel GF and DM Nelson (1985). Silicon uptake by algae with no known Si requirement. II. Strong pH dependence of uptake kinetic parameters in *Phaeodactylum tricornutum* (Bacillariophyceae). *J. Phycol.* 21: 168-171.

Reimann BEF, JC Lewin and BE Volcani (1966). Studies on the biochemistry and fine structure of silica shell formation in diatoms. II. The structure of the cell wall of *Navicula pelliculosa* (Breb.) Hilse. *J. Phycol.* 2: 74-84.

Rogerson A, ASW DeFreitas and AG McInnes (1986). Growth rates and ultrastructure of siliceous setae of *Chaetoceros gracilis* (Bacillariophyceae). *J. Phycol.* 22: 56-62.

Rogerson A, ASW deFreitas and AG McInnes (1987). Cytoplasmic silicon in the centric diatom *Thalassiosira pseudonana* by electron spectroscopic imaging. *Can. J. Microbiol.* 33: 128-131.

Rueter JG, Jr and FMM Morel (1981). The interaction between zinc deficiency and copper toxicity as it affects the silicic acid uptake mechanisms in *Thalassiosira pseudonana*. *Limnol. Oceanog.* 26: 67-73.

Schmid AMM and D Schulze (1979). Wall morphogenesis in diatoms: deposition of silica by cytoplasmic vesicles. *Protoplasma* 100: 267-288.

Sherbakova TA, Y Masyukova, T Safonova, D Petrova, A Vereshagin, T Minaeva, R Adelshin, T Triboy, I Stonik, N Aizdaitcher, M Kozlov, Y Likhoshway and M Grachev (2005). Conserved motif CMLD in silicic acid transport proteins of diatoms. *Mol. Biol. (Moscow)* 39: 269-280.

Strickland JDH and TR Parsons (1968). A practical handbook of sea water analysis. *Bull. Fish. Res. Board. Can.* 167: 1-311.

Sullivan CW (1976). Diatom mineralization of silicic-acid. I. $Si(OH)_4$ transport characteristics in *Navicula pelliculosa*. *J. Phycol.* 12: 390-396.

Sullivan CW (1977). Diatom mineralization of silicic acid. II. Regulation of $Si(OH)_4$ transport rates during the cell cycle of *Navicula pelliculosa*. *J. Phycol.* 13: 86-91.

Sullivan CW (1979). Diatom mineralization of silicic acid IV. Kinetics of soluble Si pool formation in exponentially growing synchronized cultures of *Navicula pelliculosa*. *J. Phycol.* 15: 210-216.

Taylor NJ (1985). Silica incorporation in the diatom *Coscinodiscus granii* as affected by light intensity. *Br. Phycol. J.* 20: 365-374.

Thamatrakoln K, AJ Alverson and M Hildebrand (2006). Comparative sequence analysis of diatom silicon transporters: towards a mechanistic model for silicon transport. *J. Phycol.* 42: 822-834.

Tréguer P, DM Nelson, AJ Van Bennekom, DJ DeMaster, A Leynaert and B Queguiner (1995). The silica balance in the world ocean: A reestimate. *Science* 268: 375-379.

Watt DA, AM Armory and CF Cresswell (1992). Effect of nitrogen supply on the kinetics and regulation of nitrate assimilation in *Chlamydomonas reihnardtii* Dangeard. *J. Exp. Bot.* 43: 605-615.

Wheeler PA, PM Glibert and JJ McCarthy (1982). Ammonium uptake and incorporation by Chesapeake Bay phytoplankton: short-term uptake kinetics. *Limnol. Oceanog.* 27: 1113-1128.

chapter V

Conclusions and future directions

In 1891, Julius Scheiner suggested silicon may serve as a suitable alternative to carbon as the basis for life (Scheiner 1891). Silicon's abundance and location directly below carbon in the periodic table of elements makes it one of the more obvious potential substitutes for carbon (Schulze-Makuch and Irwin 2004). Although it has been debated, silicon-based life is likely more science fiction than science fact, primarily due to silicon's affinity for oxygen. The oxidized form of silicon, silicon dioxide (SiO_2), is more commonly referred to as glass and were silicon to serve as a substitute for carbon, humans would find themselves needing a mechanism for respiring glass rather than CO_2. Regardless, silicon is an important element to nearly every living organism on Earth. But despite its importance, relatively little is known about biologically-based interactions with silicon. As one of the largest group of silicifying organisms on the planet, diatoms are an excellent model system for understanding how biology interacts with silicon. In addition, diatoms play a major role in silicon biogeochemistry and because they are estimated to contribute 40% of marine primary production (Nelson et al. 1995), diatoms create the link between the silicon and carbon cycles. Thus, understanding how a key aspect of diatom silicon biology influences their growth and productivity has widespread implications.

This dissertation has focused on the molecular and biochemical characterization of silicon transporters to understand their role in silicon transport. Specifically, this research has explored the following: 1) details of how SITs recognize and bind silicic acid through identification of evolutionarily conserved residues through comparative sequence analysis, 2) the role of individual SITs in silicon transport through molecular and biochemical characterization of the three SITs in *T.*

pseudonana, and 3) silicon uptake kinetics in diatoms and development of a model for the role of SITs in saturable and nonsaturable uptake kinetics.

Phylogenetic analysis of SIT sequences isolated from diverse diatom species showed SITs grouped according to species (Chapter II). Structural analysis of full-length SITs suggested SITs evolved through an internal gene duplication. In addition, SITs isolated from two pennate species were predicted to contain a C-terminal coiled-coil motif, while SITs from two centric species were not. Comparative sequence analysis revealed a conserved sequence motif, GXQ, located in four regions of the protein. Based on this motif, a model was developed for the uptake of silicic acid that is consistent with known aspects of silicon transport (Chapter II).

A peptide antibody was generated against SITs and used in Western blot analysis of whole cell protein lysates taken during synchronized cell division. SIT protein expression had two distinct peaks separated by a period of low SIT expression that was concurrent with the period of DNA synthesis. Quantitative PCR showed mRNA levels of each *SIT* peaked prior to valve synthesis, with *TpSIT1* having an additional peak prior to girdle band synthesis. However, a disconnect between RNA and protein levels suggested regulation of SIT expression appears to be primarily at the translational or post-translational level (Chapter III). In addition, circumstantial evidence suggested *TpSIT3* may act as a silicon sensor.

Previous work measuring silicon uptake kinetics in diatoms have reported both nonsaturable and saturable Michaelis-Menten type kinetics. However, nonsaturable kinetics were often discarded as artifacts and mechanistic explanations were not provided. To determine the conditions producing nonsaturable uptake and the extent to

which SITs controlled uptake kinetics, silicon uptake was measured in different diatom species (Chapter IV). A time-dependent transition from nonsaturable to saturable kinetics was observed in all diatoms species investigated. Anti-TpEL4 affected both nonsaturable and saturable uptake suggesting SITs are the predominant means of $Si(OH)_4$ transport into the cell. A model for $Si(OH)_4$ uptake in diatoms was developed based on the interaction between SITs, intracellular soluble silicon pools, and cell wall silica incorporation.

Future Directions

Likely the most important next step in SIT research is determining the 3-D crystal structure of SITs using x-ray crystallography, or comparable, techniques. Although challenging to accomplish, 3-D structures for several membrane-associated transport proteins have been resolved (Toyoshima et al. 2000; Murakami et al. 2002; Abramson et al. 2003; Huang et al. 2003). Determining the 3-D structure of SITs would greatly clarify the transport mechanism and result in a detailed understanding of the coordination between silicic acid and interacting amino acids.

Identification of proteins that interact with SITs and determining whether SITs oligomerize to form a functional transporter will not only provide insight into how SITs function, but will also provide initial information on possible signaling cascades that may enable diatoms to respond to silicon or regulate transport. SITs in *C. fusiformis* are predicted to form a coiled-coil motif, a structure known to play a role in protein-protein interactions. To maintain supersaturated levels of silicic acid in a soluble state, silicic acid must be bound by an intracellular binding component.

Coordinating the uptake of silicic acid with maintenance in a soluble form may require the interaction of this binding component with SITs. Although SITs in *T. pseudonana* are not predicted to contain a coiled-coil motif, studies determining the oligomerization state of functional transporters may still prove useful. Two approaches to answer these questions are the split-ubiquitin system and immunoprecipitation techniques. The split-ubiquitin system is a recently developed genetic assay similar to the yeast two-hybrid, but designed specifically for detecting membrane protein interactions (Johnsson and Varshavsky 1994; Stagljar et al. 1998; Leeds and Beckwith 2000; Stagljar 2003). In addition to identifying novel protein interactions, this approach can also be used to determine if SITs homo- or hetero- dimerize as has been reported for many other transporter proteins (Reinders et al. 2002; Ludewig et al. 2003). Immunoprecipitation provides an alternative technique for identifying SIT-interacting proteins and is now feasible with the availability of a SIT-specific antibody (Chapter III).

The initial development of a heterologous expression system in *Saccharomyces cerevisiae* (Chapter IV) is a first step towards determining the uptake kinetics of individual SITs. This is crucial information for understanding why diatoms contain multiple SITs and what the role of each is in silicon uptake.

Finally, localization studies on SITs will be needed to clarify their roles in cellular silicon transport. While SITs are clearly membrane-associated proteins, it is unclear if any of them are intracellular localized, for example, to the silica deposition vesicle. One method for determining this is to generate fluorescently tagged SITs. The recent development of a procedure to transform *T. pseudonana* (Poulsen et al. in

press), as well as a technique for synchronously growing cultures of *T. pseudonana* (Hildebrand et al. in press) will allow researchers to generate fusions between SITs and fluorescent proteins, such as green fluorescent protein (GFP) and introduce these fusions into the native diatom host. SIT-GFP fluorescence can then be monitored by fluorescent microscopy.

Implications of SIT research

Studies on SITs have been part of a larger project aimed at developing biologically-based methods for the synthesis of silicon-based nanodevices. The complex 3-D shapes that diatoms are capable of reproducibly forming under ambient conditions are coveted by materials scientists and nanotechnologists who have struggled to design 2-D microstructures. Understanding diatom structure formation requires basic knowledge on all aspects of diatom silicon metabolism, including uptake and transport into the cell. Because of the specificity of transport, understanding its molecular details could be of benefit for nanotechnology. A possible application in which research on SITs could benefit nanotechnology is through the potential use of SITs as silicic acid delivery tools across membranes. Incorporation of SITs into lipid bilayer membranes could enable the specific transport of silicic acid into micellar structures or across planar membranes. By understanding the detailed mechanism of transport, one could adjust conditions to specifically deliver desired amounts of silicic acid across a bilayer membrane.

As mentioned, SITs are the only proteins shown to directly and specifically interact with silicic acid without inducing silica polymerization (Hildebrand et al.

1997); thus they are a model system for understanding how proteins in general recognize and bind silicon. This information could be useful in biomimetic approaches to materials synthesis, both in terms of the coordination and binding of silicon, but also in possible mechanisms of enzyme catalysis involving silicon. A hallmark of biology is the specific interaction between proteins and their substrates. In the case of enzymes, such interactions stabilize transition states and lower activation energies, resulting in catalysis under ambient biological conditions. The specificity of these interactions is a result of the three dimensional arrangement of amino acids in a protein relative to the interacting substrate. The identification of the GXQ motifs proposed to coordinate silicic acid to SITs is the first step towards understanding this biological interaction with silicon and such information could be invaluable in devising schemes to lower reaction energies in *in vitro* syntheses.

REFERENCES

Abramson J, I Smirnova, V Kasho, G Verner, HR Kaback and S Iwata (2003). Structure and mechanism of the lactose permease of *Escherichia coli*. *Science* 301: 610-615.

Hildebrand M, LG Frigeri and AK Davis (in press). Synchronized growth of *Thalassiosira pseudonana* (Bacillariophyceae) provides novel insights into cell wall synthesis processes in relation to the cell cycle. *J. Phycol.*

Hildebrand M, BE Volcani, W Gassmann and JI Schroeder (1997). A gene family of silicon transporters. *Nature* 385: 688-689.

Huang Y, J Lemieux, J Song, M Auer and D-N Wang (2003). Structure and mechanism of the glycerol-3-phosphate transporter from *Escherichia coli*. *Science* 301: 616-620.

Johnsson N and A Varshavsky (1994). Split ubiquitin as a sensor of protein interactions in vivo. *Proc. Natl. Acad. Sci. U.S.A.* 91: 10340-10344.

Leeds JA and J Beckwith (2000). A gene fusion method for assaying interactions of protein transmembrane segments in vivo. *Methods Enzymol.* 327: 165-175.

Ludewig U, S Wilken, B Wu, W Jost, P Obrdlik, M El Bakkoury, A-M Marini, B Andre, T Hamacher, E Boles, N von Wiren and WB Frommer (2003). Homo- and Hetero-oligomerization of ammonium transporter-1 NH_4 uniporters. *J. Biol. Chem.* 278: 45603-45610.

Murakami S, R Nakashima, E Yamashita and A Yamaguchi (2002). Crystal structure of bacterial multidrug efflux transporter AcrB. *Nature* 419: 587-593.

Nelson DM, P Tréguer, MA Brzezinski and A Leynaert (1995). Production and dissolution of biogenic silica in the ocean: revised global estimates, comparison with regional data and relationship to biogenic sedimentation. *Global Biogeochemical Cycles* 9: 359-372.

Poulsen N, PM Chesley and N Kröger (in press). Molecular genetic manipulation of the diatom *Thalassiosira pseudonana* (Bacillariophyceae). *J. Phycol.*

Reinders A, W Schulze, S Thaminy, I Stagljar, WB Frommer and JM Ward (2002). Intra- and intermolecular interactions in sucrose transporters at the plasma membrane detected by the split-ubiquitin system and functional assays. *Structure (Cambridge)* 10: 763-772.

Scheiner J (1891). Astrophysicist at the University of Potsdam, considering life based on silicon in a scientific essay.

Schulze-Makuch D and LN Irwin (2004). Building blocks of life. *Advances in Astrobiology and Biogeophysics* 3: 77-100.

Stagljar I (2003). Finding partners: Emerging protein interaction technologies applied to signaling networks. *Science's STKE* 56.

Stagljar I, C Korostensky, N Johnsson and S te Heesen (1998). A genetic system based on split-ubiquitin for the analysis of interactions between membrane proteins in vivo. *Proc. Natl. Acad. Sci. U.S.A.* 95: 5187-5192.

Toyoshima C, M Nakasako, H Nomura and H Ogawa (2000). Crystal structure of the calcium pump of sarcoplasmic reticulum at 2.6 Å resolution. *Nature* 405: 647-655.